1993-09

A numerical study of airplanes flying in proximity

Porter, David B.

Monterey, California. Naval Postgraduate School

Approved for public release; distribution is unlimited.

A Numerical Study of Airplanes Flying in Proximity

by

David B. Porter
Lieutenant Commander, United States Navy
B.S.A.E., United States Naval Academy, 1980

Submitted in partial fulfillment of the requirements for
the degree of

MASTER OF SCIENCE IN AERONAUTICAL ENGINEERING

from the

NAVAL POSTGRADUATE SCHOOL
September, 1993

Jnclassified

:CURITY CLASSIFICATION OF THIS PAGE

REPORT DOCUMENTATION PAGE

. REPORT SECURITY CLASSIFICATION: Unclassified

1b. RESTRICTIVE MARKINGS

. SECURITY CLASSIFICATION AUTHORITY

3. DISTRIBUTION/ AVAILABILITY OF REPORT: Approved for public release; distribution is unlimited.

. DECLASSIFICATION/DOWNGRADING SCHEDULE

PERFORMING ORGANIZATION REPORT NUMBER(S)

5. MONITORING ORGANIZATION REPORT NUMBER(S)

. NAME OF PERFORMING ORGANIZATION: Naval Postgraduate School

6b. OFFICE SYMBOL *(If Applicable)*: AA

7a. NAME OF MONITORING ORGANIZATION: Naval Postgraduate School

. ADDRESS *(city, state, and ZIP code)*: Monterey, CA 93943-5000

7b. ADDRESS *(city, state, and ZIP code)*: Monterey, CA 93943-5000

ı. NAME OF FUNDING/SPONSORING ORGANIZATION

8b. OFFICE SYMBOL *(If Applicable)*

9. PROCUREMENT INSTRUMENT IDENTIFICATION NUMBER

. ADDRESS *(city, state, and ZIP code)*

10. SOURCE OF FUNDING NUMBERS

PROGRAM ELEMENT NO.	PROJECT NO.	TASK NO.	WORK UNIT ACCESSION NO.

. TITLE *(Include Security Classification)*: A NUMERICAL STUDY OF AIRPLANES FLYING IN PROXIMITY

. PERSONAL AUTHOR(S): Porter, David B.

a. TYPE OF REPORT: Master's Thesis

13b. TIME COVERED: FROM TO

14. DATE OF REPORT *(year, month,day)*: September 1993

15. PAGE COUNT: 140

. SUPPLEMENTARY NOTATION

The views expressed in this thesis are those of the author and do not reflect the official policy or position of the Department of Defense or the U.S. Government.

. COSATI CODES

FIELD	GROUP	SUBGROUP

18. SUBJECT TERMS *(continue on reverse if necessary and identify by block number)*: Formation Flying, Panel Method, Stability and Control

. ABSTRACT *(Continue on reverse if necessary and identify by block number)*

During an emergency such as an unsafe landing gear indication, a second aircraft is often used to perform an airborne visual inspection of the landing gear. The chase airplane may be quite dissimilar in size and wing loading and consequently experience unexpected aerodynamic forces and moments caused by the other airplane. A numerical study of the inherent danger involved with the aerodynamic interaction of aircraft flying in proximity was made using the low-order panel code PMARC (Panel Method Ames Research Center). PMARC validation was made by comparing wind tunnel and analytically-derived stability data for T-34 and F-14 models with PMARC results. A T-34 was then placed at various distances underneath an F-14 to determine changes in lift and pitching moments on the T-34. Color illustrations of pressure coefficients were used to highlight the changes in aerodynamic forces and moments as vertical separation between the two aircraft was decreased. PMARC showed that 4.5 deg. of elevator trim change were required as a T-34 approached to within its semispan of an F-14.

. DISTRIBUTION/AVAILABILITY OF ABSTRACT

X UNCLASSIFIED/UNLIMITED ☐ SAME AS RPT. ☐ DTIC USERS

21. ABSTRACT SECURITY CLASSIFICATION: Unclassified

a. NAME OF RESPONSIBLE INDIVIDUAL: Richard M. Howard

22b. TELEPHONE (Include Area Code): (408) 656-2870

22c. OFFICE SYMBOL: AA/HO

) FORM 1473, 84 MAR — 83 APR edition may be used until exhausted. All other editions are obsolete

SECURITY CLASSIFICATION OF THIS PAGE: Unclassified

ABSTRACT

During an emergency such as an unsafe landing gear indication, a second aircraft is often used to perform an airborne visual inspection of the landing gear. The chase airplane may be quite dissimilar in size and wing loading and consequently experience unexpected aerodynamic forces and moments caused by the other airplane. A numerical study of the inherent danger involved with the aerodynamic interaction of aircraft flying in proximity was made using the low-order panel code PMARC (Panel Method Ames Research Center). PMARC validation was made by comparing wind tunnel and analytically-derived stability data for T-34 and F-14 models with PMARC results. A T-34 was then placed at various distances underneath an F-14 to determine changes in lift and pitching moments on the T-34. Color illustrations of pressure coefficients were used to highlight the changes in aerodynamic forces and moments as vertical separation between the two aircraft was decreased. PMARC showed that 4.5 degrees of elevator trim change were required as a T-34 approached to within its semispan of an F-14.

TABLE OF CONTENTS

NOMENCLATURE

ac	aerodynamic center
a_t	tail lift curve slope
a_w	wing lift curve slope
AR	aspect ratio
$\bar{c}$	length of mean aerodynamic chord
cg	center of gravity
C_{l_α}	local section lift curve slope
$C_{l_{\alpha\ tail}}$	local section lift curve slope for the tail
$C_{l_{\delta e}}$	change in section lift coefficient due to elevator deflection
C_L	lift coefficient
C_{L_α}	change in lift coefficient with angle of attack (lift curve slope)
$C_{L_{\alpha\ tail}}$	tail lift curve slope
$C_{L_{\alpha wing}}$	wing lift curve slope
$C_{L_{\delta e}}$	change in lift coefficient due to elevator deflection
C_m	pitching moment coefficient
C_{m_α}	change in pitching moment coefficient with angle of attack
$C_{m_{\delta e}}$	change in pitching moment coefficient due to elevator deflection
$d\varepsilon/d\alpha$	change in downwash angle due to change in angle of attack
$\Delta_{\delta e}$	change in elevator deflection
ε_{1wing}	induced-angle span efficiency factor of wing
ε_{1tail}	induced-angle span efficiency factor of tail
h	cg position, in fraction of mac
$h_{ac_{wb}}$	position of aerodynamic center for wing-body, in fraction of mac

l_{tail}	length from cg to horizontal tail aerodynamic center
mac	mean aerodynamic chord
η_t	efficiency factor for tail, q_{tail}/q
ρ	air density
q	dynamic pressure ($1/2\rho V^2$)
q_{tail}	tail dynamic pressure ($1/2\rho V_t^2$)
V	free-stream velocity
S_W	wing area
S_t	horizontal tail area
V_H	horizontal tail volume coefficient
V_t	free-stream velocity at tail

ACKNOWLEDGMENTS

This study could not have been completed without the help and generosity of many people. Dan Lyon's initial instruction and guidance on PMARC fundamentals were instrumental in getting this project started. Stephen Bachner and Mark Byers of NAWC AD spent considerable time gathering and discussing F-14 and T-34 data. Steve Keith of Sterling Software was always available for help with GVS. He developed a truly great product in GVS and to him I give credit for the outstanding images in Appendix A. Matthew Koebbe's expertise in UNIX and the NPGS Visualization Lab was instrumental in the production of the video associated with this thesis.

I would especially like to thank Dr. Richard Howard, my thesis advisor, for all of his help and guidance. Finally, a very special recognition goes to Mr. Dale Ashby of NASA Ames. His unselfish dedication and technical expertise with PMARC kept the project on track.

I. INTRODUCTION

On 14 January 1992, an F-14A experienced an unsafe landing gear indication prior to recovery at a Naval air station. The F-14 air crew requested a chase aircraft to conduct a visual inspection of their landing gear in accordance with Naval Air Training and Operating Procedures Standardization Program (NATOPS) procedures. A T-34C with instructor and student pilot joined on the F-14 to inspect the landing gear. Shortly after notifying the F-14 crew that their gear looked good, the T-34 collided with the substantially larger aircraft. Significant damage to T-34 control surfaces resulted in uncontrolled flight and subsequent loss of the aircraft and its air crew. The F-14 received minor damage and returned to the Naval air station without further incident.

A study of Navy and Air Force mid-air collisions involving formation flying over the past ten years has shown that pilot error is the predominant common denominator. Task saturation; preoccupation with cockpit duties; and failures to judge closure rates and take sufficient, timely and appropriate action to avoid collision, are major factors in mishap findings [Refs. 1 and 2]. Mutual interference of the flow patterns around aircraft in proximity is rarely discussed in mishap findings or even flight training, yet may be a significant causal factor. Interference of airflow over lifting surfaces such as wings and tails can alter the aerodynamic characteristics of the aircraft. Unexpected changes in lift and pitching moments may occur that affect closure rate and task saturation of the unaware or uninformed pilot.

Very little information is available to military aviators concerning changes in aerodynamic forces and moments that result when airplanes fly close to each other. NAVAIR has subsequently tasked the Naval Postgraduate School to investigate mutual interference of aircraft flying in formation. The desires for better insight into the aerodynamic interactions between formation aircraft and a means to educate military aviators about them form the impetus for this study.

This study is a numerical investigation in aerodynamic trim changes of dissimilar aircraft flying in formation. The low-order panel code PMARC was used to determine aerodynamic pressures, forces and moments on various wings, wing-bodies and aircraft in proximity. Discussions include PMARC validation, numerical results, and limitations associated with the computer code for this type of study. Color illustrations and histograms are used to present the changes in pressure coefficients on a T-34 wing and tail as its vertical separation from an F-14 decreases. Subsequent changes in elevator trim position and lift are addressed to provide the aviator with a better understanding of the aerodynamic effects one airplane has on the other.

This study is offered as a supplement to existing formation flying literature and training aids. A video that graphically depicts the numerical results with narration oriented toward the student aviator has been produced as a training tool for aviation safety and formation flying education. Its purpose is to expose student pilots to changes in airplane trim and handling characteristics brought about by disturbances associated with formation flying. This research ultimately provides AIR-530 with an engineering approach to investigate the aerodynamics of formation flying.

II. BACKGROUND

A. NAVY FORMATION FLYING

Military pilots are instructed in the fundamentals of formation flying throughout their training syllabus. Ultimately, formation flying becomes standard operating procedure for most tactical aviators. Unfortunately the fundamentals are often limited to basic procedures and visual cues for flying in formation with similar type aircraft.

Student Naval aviators begin primary flight training in the T-34C. After solo and basic instrument instruction, the student is taught basic procedures for flying in formation with other T-34C airplanes. Classroom emphasis is placed on operating area familiarization, join-up, formation and breakup procedures with appropriate visual cues. Visual cues are used to judge closure rates, and to maintain proper separation and placement in level flight, turn and cross-under maneuvers. Classroom instruction does not include a thorough discussion of interference between airplanes in flight. Interference from lead aircraft prop wash and its effects on lateral-directional stability of airplanes in trail is addressed, however.[1] Aircraft in trail or performing cross-under maneuvers experience a weather-vane effect when flying in the lead aircraft's prop wash. This phenomenon is discussed with students and often demonstrated in flight.

Primary flight instructors come from diverse backgrounds. Most come from P-3, C-130, E-2 and helicopter communities where formation flying is not a

---

[1] Phone Conversation, 28 July 1993 between author and Lt. Freeman, VT-6, Milton NAS, FL

primary means of operation. This is not to say that these pilots do not make good formation pilots; but rather they have relatively little formation flying experience outside the basic principles they were taught during flight training and their more recent T-34 instructor under training (IUT) syllabus. Without vast experience in formation flying they rely heavily on "textbook" procedures and visual cues. The instructors may not be able to provide detailed information about potential changes in airplane aerodynamic characteristics caused by flying in proximity.

The latest revision of the T-34C Flight Training Instruction has a new sub-section addressing formation flight with dissimilar aircraft, specifically during landing gear inspections. This inclusion is attributed to the F-14 and T-34 mid-air collision and is evidence of the need for increased awareness of formation flying hazards. Adverse aerodynamic conditions that cause upward pitching moments and trim changes to maintain control of the aircraft are discussed. The instruction now stipulates [Ref. 3]:

> ...If the wing man does not anticipate this trim change, it could cause a significant controllability problem which could result in airborne collision. The magnitude of this flow interference is related to the configuration, speed, weight and distance between the two aircraft.
>
> The actual aerodynamic flow between a T-34C and a dissimilar aircraft will not normally be known. Because of the inherent danger involved when inspecting landing gear of dissimilar aircraft, the inspection pilot should be aware of the possible adverse flight conditions and avoid them.

Advanced flight training for tactical aviators is taught in the Navy's T-2, A-4 and T-45 aircraft. Formation training again places instructional emphasis on area and formation procedures and visual cues, with little formal instruction on mutual interference of flow patterns. Primary positions such as parade and line are discussed with video highlights. Hand signals, radio communications and maneuvers are also presented with video support. The new T-45 training program provides flight simulators to aid in formation flying instruction.

Simulators expose the student pilot to section take-off, TACAN rendezvous, breakup and rendezvous, turns, cross-under and acrobatic formation maneuvers. Formation flight instruction in the T-45 primarily emphasizes procedures and visual cues, but pilots are also exposed to changes in aircraft stability as T-45's get closer together. A T-45 flight instructor from VT-21 in Kingsville, Texas, indicated that formation pilots, lead and wing man, can feel the presence of each other's airplane through changes in trim conditions as they get closer.[2] Instructor pilots warn the students of the danger in flying too close and demonstrate how to maneuver back to the ideal position, but the aerodynamic cause and effect do not seem to be addressed at this level. Formation flying is limited to groups of similar aircraft as the students prepare for carrier qualifications and fleet aircraft selection.

Formation flying becomes routine in most fleet tactical squadrons as airplanes sortie together for low-level navigation, strikes, combat air patrol, in-flight refueling and escort operations. Procedures and visual cues remain primary instructional tools, but complexities and variations arise due to the diversity of carrier aircraft. Without a basic understanding of potential aerodynamic interferences between airplanes flying in formation, the inexperienced fleet aviator may have few resources to call upon when joining on a different type aircraft, especially for the first time.

The truth is that most formation flying instruction appears to be passed down from aviator to aviator. Procedural standards and techniques are presented to the students and fleet aviators for their type aircraft, but there is very little textbook information to supplement the mechanics of formation flying. Even the Blue

---

[2] Phone Conversation, 28 July 1993 between author and Lt. Renner USN, VT-21, Kingsville NAS, TX

Angels aerial demonstration team relies on basic techniques that are passed from one formation pilot to the next. A diamond formation pilot for the Blue Angels could not pinpoint any known literature used by the team to teach potential interference effects between airplanes in the formation.[3]

Aerodynamics For Naval Aviators, by H. H. Hurt, is the only Navy textbook found by the author that addresses disturbances in flow patterns caused by formation flying. Besides describing the phenomenon, Hurt points out [Ref. 4:p. 385]:

> A common collision problem is the case of an airplane with a malfunctioning landing gear. If another airplane is called to inspect the malfunctioning landing gear, great care must be taken to maintain adequate separation and preserve orientation. Many instances such as this have resulted in a collision when the pilot of the trailing airplane became disoriented and did not maintain adequate separation.

In-flight refueling and supersonic flight issues pertaining to formation flying are also addressed, though recommended procedures are lacking.

To maintain proficiency, combat readiness and safety, Naval aviators receive continuous training in the cockpit, simulator and classroom. To this end, a more thorough understanding of formation flying aerodynamics provided by this study can enhance pilot awareness and safety.

B. PREVIOUS FORMATION FLYING STUDIES

Many studies have been conducted involving formation flying. Topics include formation flight trainer evaluations, formation station keeping concepts, wakes at large distances (up to 250 chords) from wings, airplane formation flying qualities, and potential benefits of flying aircraft in formation on extended range

---

[3] Phone Conversation, 21 July 1993 between author and LCdr. Packer USN, Blue Angels Flight Demonstration Team, Pensacola NAS, FL

missions. Human factor and physiology issues have also been addressed. There seems to be very little information available, however, concerning the issue of aerodynamic interference between airplanes flying in formation. [Refs. 5-8]

Vortex lattice calculations have been used to study the benefits of formation flying. Maskew [Ref. 8] applied a quadrilateral vortex-lattice method to a formation of three wings. Force and moment data were used in estimating potential benefits to flying aircraft in formation on extended range missions. Only echelon and double row formations were presented, but Maskew did point out that trimming in roll was required for the echelon formation.

C. COMPUTER CODES

Computational fluid dynamics have become an integral part of aircraft design and analysis. Most recently, powerful computer systems and codes provide solutions to Navier-Stokes and Euler equations for simple three-dimensional wing-body configurations. Potential flow panel codes have been developed for the past 25 years to aid in the design and analysis of arbitrary three-dimensional wing-bodies. Today's engineer has the option to choose from an abundance of computational programs based on project scope, available computer resources and problem complexity.

The potential-flow panel code PMARC (Panel Method Ames Research Center) was used for this study. PMARC was designed to numerically predict flow fields around complex three-dimensional bodies. Adjustable size arrays permit tailoring of the code for the size problem being solved and the available computer hardware. The decision to use PMARC was also based on past success using the code at the Naval Postgraduate School to conduct aerodynamic studies of the Pioneer unmanned air vehicle and the Service Aircraft Instrumentation Package (SAIP) [Refs. 9 and 10].

PMARC data are displayed by GVS 3.1 (General Visualization System) software. Designed specifically for PMARC, the program is ideal for visual representations of aerodynamic data on complex geometries.

1. PMARC Background

a. PMARC Description

PMARC is a low-order, potential flow panel code that is patterned after Analytical Methods Inc. VSAERO (Vortex Separation Aerodynamics Program). Surface geometries are broken up into panels with constant strength source and doublet distributions over each panel. These singularities distributed with constant strength over each panel qualify PMARC as a low-order panel method. Higher-order methods allow the singularity strengths to vary linearly or quadratically over each panel. Better accuracy is obtained by the higher-order methods at the expense of code complexity and computation time [Ref. 11: p. 2]. Experience and research have shown, however, that low-order panel methods can provide nearly identical results as higher-order methods over a wide range of cases. PMARC's potential flow model theory can be found in Ref. 11.

PMARC version 11 is written in FORTRAN 77. Adjustable size arrays within the code permit simple to very complex geometries, wakes, off-body velocity scans and streamlines. Basic input data include body geometry and coordinate systems, free-stream conditions, angular position and rates, symmetry parameters and requests for off-body velocity scans and streamlines. Outputs consist of geometries, wakes, aerodynamic parameters, off-body velocities and off-body streamline data. Aerodynamic data provide doublet strength, velocity components, pressure coefficient, and local Mach number for each panel. Forces and moments for panel sections, components and entire geometries are summed and put in coefficient form. Force and moment coefficients are then expressed for wind, stability and body axes.

b. Operating Systems

PMARC is designed to run on computers ranging from personal computers (Macintosh II based) to the powerful Cray Y-MP. Disk space and memory requirements for operating the code are dependent on the size of the operator-selected arrays. This research used approximately 2,350 geometry panels. According to Ref. 11, the scratch disk space required to run PMARC is approximately 67 Mb for this application. Memory requirements for storing the executing instructions and output data are difficult to predict and are significantly effected by dimensioning the code.

The Naval Postgraduate School's Cray Y-MP EL 8/2048 was used to operate PMARC for this study. There was ample storage on the Cray with 2 Gigabytes of main memory and several 50-Gigabyte local disks. Eight vector processors provided a peak operation of 133-MFLOP (Million Floating point Operations) per processor [Ref. 12].

c. Coordinate Systems

Aircraft geometries are described in a body-fixed coordinate system. PMARC assumes that the body-fixed coordinate system is coincident with the origin of an inertial reference frame. Assembly and component coordinate systems are also provided for complex geometries and configurations. Separate component and assembly coordinate systems were used in this analysis to differentiate between the F-14 and T-34, for example.

Constant velocity vectors and constant angular rotation rates about the three coordinate axes are used to describe geometry motion. Normalized velocities with zero angular rotation rates were used throughout this analysis. The geometry incrementally moved through the prescribed motion in a series of time steps. Solutions were computed at each incremental time step that included updated surface source strengths. Instantaneous free-stream velocity vectors in the body-fixed reference frame were subsequently computed from the surface source strengths.

d. Geometry Modeling

PMARC geometries are modeled by a set of panels. Complex geometries such as aircraft, are subdivided into several pieces and modeled with sets of panels called patches. Patches are formed from two or more sections. A section is a set of points defining a cross-sectional area of the modeled object. Patches are usually four sided but fewer sides can exist for complex or intricate shapes. Wings, for example, are made by folding a patch over onto itself to form a common edge. [Ref. 11:p. 14]

Low-order panel methods do not demand exact matching between panels as higher-order methods do. This difference becomes important when trying to model from three-view drawings with little detail. Small gaps and panel mismatches that may arise due to modeling inaccuracies or ambiguities can be tolerated in PMARC without severe penalties in data accuracy.

The T-34 geometry sections were defined using the three-view drawing in Appendix A, Figure A1. Airfoil data were obtained from Ref. 13. The tailless F-14 model, Appendix A, Figure A2, was used by Naval Air Warfare Center, Weapon Division (NAWC WD), China Lake, to conduct stores separation analysis. Horizontal and vertical tails were added with small gaps between them and the fuselage to simplify the model and minimize deformities. F-14 tail airfoil data were obtained from Ref. 14. Half-plane models were used with the assumption that the airflow and geometry are symmetric around the XZ plane. PMARC automatically adds the influence of the mirror image when calculating the total force and moment coefficients.

e. Wake Modeling

Wakes are shed from user-specified separation lines on the surface geometry. PMARC has provisions for three wake options. A time-stepping wake model is developed that moves downstream with the local velocity field. This option requires significant processing, particularly with complex and high-density panel geometries. Alternatively, the user can specify an initial wake that allows analysis of the steady-state problem without going through several time steps to reach a steady-state condition. A no-wakes option is also available, but its use for this study's application was limited to geometry-only plotting.

Initial wakes were specified for the majority of data runs in this analysis. The decision to use initial-wake specifications vice time-stepping wakes was based on discussions with PMARC's principal programmer, Dale Ashby. Numerical results between the two wake options are generally within five to seven percent of each other as long as the wake is reasonably approximated. Part of the wake should separate at or near the wing trailing edge, for example. Verification data are presented in Chapter III.

Wake separation lines and initial specifications must be handled with great care because they affect numerical results. User-defined wake sections must all go in the same direction as the separation line [Ref. 11:p. 16]. Defining the wake separation line becomes an art as the user stitches it along wing and fuselage panel edges. If the separation line changes direction or is incomplete, due to input coding errors, inaccurate and often unrealistic data will result. Specified wakes must also carry downstream approximately 20 chord lengths in order to provide reliable data.[4]

2. GVS BACKGROUND

a. GVS Description

GVS is designed to display PMARC data in a variety of formats. One of two PMARC output files is used by GVS to display geometries, wakes, and on-body and off-body streamlines that are collectively called objects. PMARC phenomena such as component velocities, pressure coefficients, doublet strengths and Mach numbers are qualitatively displayed in color on the various objects. A quantitative association for the data is provided by a histogram that identifies a numerical value for each color displayed, depending upon the observed phenomenon. Displayed objects can be rotated, translated and scaled for ease in data analysis.

b. Operating Systems

GVS is designed to run on Silicon Graphics Incorporated (SGI) Iris™ computer graphics workstations. It is a computationally intensive program that requires a great deal of memory and disk resources. A minimum of 72 Megabytes of disk space is required [Ref. 15]. Main memory requirements are difficult to estimate. GVS was designed on a system with 24 Megabytes of RAM and a 20 MHz processor but has run on Naval Postgraduate School SGI Iris

[4] Conversations between author and Dale Ashby, NASA Ames Research Center, April - June 1993.

machines running at 16 MHz with 16 Megabytes of RAM. The graphics monitor must provide 24-bit color; otherwise the color display of phenomenon data will be distorted. The program is designed to compile and run using IRIX 3.0.x and IRIX 4.0.x system software.

A SGI 4D/380, model VGX, Iris™ workstation was used for GVS data analysis, display and reproduction. The Naval Postgraduate School's Visualization Lab SGI system operates at 36 MHz and provides 128 Megabytes of RAM and 4 Gigabytes of disk space [Ref. 12:p. 4]. Color graphics were provided by a Shinko color Postscript printer.

III. GROUNDWORK AND PMARC VALIDATION

A. ANALYTIC DERIVATION OF T-34 STABILITY DERIVATIVES

The Navy did not buy stability derivative data when the T-34C was procured.[5] Several derivatives were required for this analysis, however, in order to determine elevator trim changes and to compare with PMARC output data. Stability and control data were consequently estimated from Smetana [Ref. 16], and from Perkins and Hage [Ref. 17]. Stability derivatives were then compared with typical values for other airplanes. Table I contains aerodynamic parameters and assumptions used in calculating T-34 stability derivatives for the cruise configuration, defined as gear and flaps retracted.

1. T-34 Lift-Curve Slope, C_{L_α}

Equation (1) [Ref. 16:p. 57] was used to approximate the lift curve slope of the T-34C. The contribution of the fuselage was assumed to be negligible.

$$C_{L_\alpha} = C_{L_{\alpha\,\text{wing}}} + C_{L_{\alpha\,\text{fuselage}}} + C_{L_{\alpha\,\text{tail}}}\left(1 - \frac{d\varepsilon}{d\alpha}\right)\frac{S_{\text{tail}}}{S_{\text{wing}}}\eta_{\text{tail}} \qquad (1)$$

Substitution of data from Table I into equation (1) yielded: C_{L_α}= 0.0894/deg.

2. T-34 Change in Pitching Moment with Angle of Attack, C_{m_α}

The change in pitching moment coefficient with angle of attack has significant impact on an airplane's longitudinal stability. It determines the response of the airframe to elevator motions, gusts and other aerodynamic disturbances. C_{m_α} is estimated by equation (2) [Ref. 16:pp. 67-69].

---

[5] Phone conversation between author and Mr. Buck Buchannon, NAVAIRSYSCOM Detachment PMA(F)-227, T-34C Class Desk, 5 August 1993.

TABLE I T-34 STABILITY AND CONTROL DERIVATIVE DATA

Wing Airfoil Type (1)	NACA 23012
C_{l_α} (2)	0.107/deg.
S_W (1)	179.56 ft^2
Wing Aspect Ratio (1)	6.22
$C_{L_\alpha\ wing}$ (6)	0.0812/deg.
$\varepsilon_{1\ wing}$ (3)	0.99
$d\varepsilon/d\alpha$ (4)	0.45
Tail Airfoil Type (1)	NACA 0008.2
$C_{l_\alpha\ tail}$ (5)	0.10965/deg.
S_t (1)	37.15 ft^2
Tail Aspect Ratio (1)	3.99
V_H (1)	0.5628
l_{tail} (1)	14.74 ft
$\varepsilon_{1\ tail}$ (3)	0.97
$C_{L_\alpha\ tail}$ (6)	0.0723/deg.
η_t (7)	1.0

1. Ref. 13
2. Ref. 18
3. Ref. 16
4. Ref. 17
5. $2\pi / 57.3$
6. $C_{L_\alpha} = \dfrac{C_{l_\alpha}}{1 + C_{l_\alpha} \dfrac{57.3}{\pi \varepsilon_1 AR}}$ [Ref. 16:p. 58]
7. Assumed

$$C_{m_\alpha} = a_w\left[\left(h - h_{ac_{wb}}\right) - V_H \frac{a_t}{a_w}\left(1 - \frac{d\varepsilon}{d\alpha}\right)\right] \quad (2)$$

The aircraft cg was assumed to be at the aerodynamic center. C_{m_α} equals -0.0339/deg.

3. T-34 Change in Lift Coefficient with Elevator Deflection, C_{L_δ}

The change in lift coefficient due to elevator deflection is approximated by equation (3) [Ref. 16:p. 94].

$$C_{L_{\delta_e}} = 1.05 C_{l_{\delta_e}} \frac{C_{L_{\alpha_t}}}{C_{l_{\alpha_t}}} \frac{S_t}{S_w} \eta_t \quad (3)$$

A positive elevator deflection is defined as trailing-edge down. The derivative represents the change in overall lift from a change in tail camber caused by an elevator deflection. Everything else remains constant; therefore angle of attack and associated lift changes are not considered in this derivative. The derivative is normally positive and small for conventional aircraft. Substitution of data from Table I into (3) yields: $C_{L_{\delta_e}} = 0.00745$/deg.

4. T-34 Change in Pitching Moment with Elevator Deflection, C_{m_δ}

The change in pitching moment coefficient with change in elevator deflection is commonly referred to as "elevator power" or "elevator effectiveness." The sign is usually negative due to the way elevator deflection is defined. Therefore, a positive deflection provides a negative pitching moment, making elevator power negative. A numerical value for elevator power is obtained from equation (4) [Ref. 16:p.101].

$$C_{m_{\delta_e}} = -\frac{l_{tail}}{\bar{c}} C_{L_{\delta_e}} \quad (4)$$

Substituting (3) into (4) yields a $C_{m_{\delta e}}$ value of -0.02026/deg.

B. T-34 DERIVATIVE COMPARISON WITH SIMILAR AIRPLANES

Stability and control derivatives for three similar aircraft are presented in Table II for comparison to estimated T-34C derivatives. The approximations appear reasonable and fall within Smetana's typical values. Further validation will be made by comparing the derivatives to PMARC results in subsequent sections.

TABLE II STABILITY DERIVATIVES OF VARIOUS AIRPLANES (1)

Derivative	C-172 (2)	Navion (3)	Jet Trainer (4)	T-34C
C_{L_α}	0.0803	0.0775	0.0960	0.0894
C_{m_α}	-0.0155	-0.0119	-0.0042	-0.0339
$C_{L_{\delta_e}}$	0.0075	0.0062	0.0066	0.0075
$C_{m_{\delta_e}}$	-0.0223	-0.0161	-0.0154	-0.0203

1. All derivatives are per degree and for a cruise configuration.
2. Ref. 19:p. 592
3. Ref. 20:p. 252
4. Ref. 19:p. 609

C. PMARC AND MODELING VALIDATION

PMARC was evaluated first using a simple wing test case. PMARC data from the test case were compared with data derived from 2-D airfoil theory for validity. Data from computer-generated wake models were then compared with data associated with operator-defined wake models. Geometry models for the T-34 and the F-14 were also validated by comparing PMARC results with analytically-derived stability data or wind tunnel report data. Observations and conclusions from these evaluations constituted the groundwork for the more complex analysis of two airplanes in proximity presented in Chapter IV.

1. NACA 4415 Airfoil Evaluation

a. PMARC Data Versus 2-D Airfoil Data

A NACA 4415 wing with an aspect ratio of 15 was analyzed at various angles of attack. Appendix A, Figure A3 shows the 4415 wing and its initial wake. The wake was defined by the author and extended 20 chord lengths aft of the trailing edge. Figure 1 shows the lift curve slope generated from PMARC data and corresponding information derived from a 2-D NACA 4415 airfoil from Abbott and Doenhoff [Ref. 18:p. 490]. Data from Ref. 18 were corrected for aspect ratio using the equation in Table I, note 6. Figure 2 shows analogous data for pitching moment coefficient versus angle of attack.

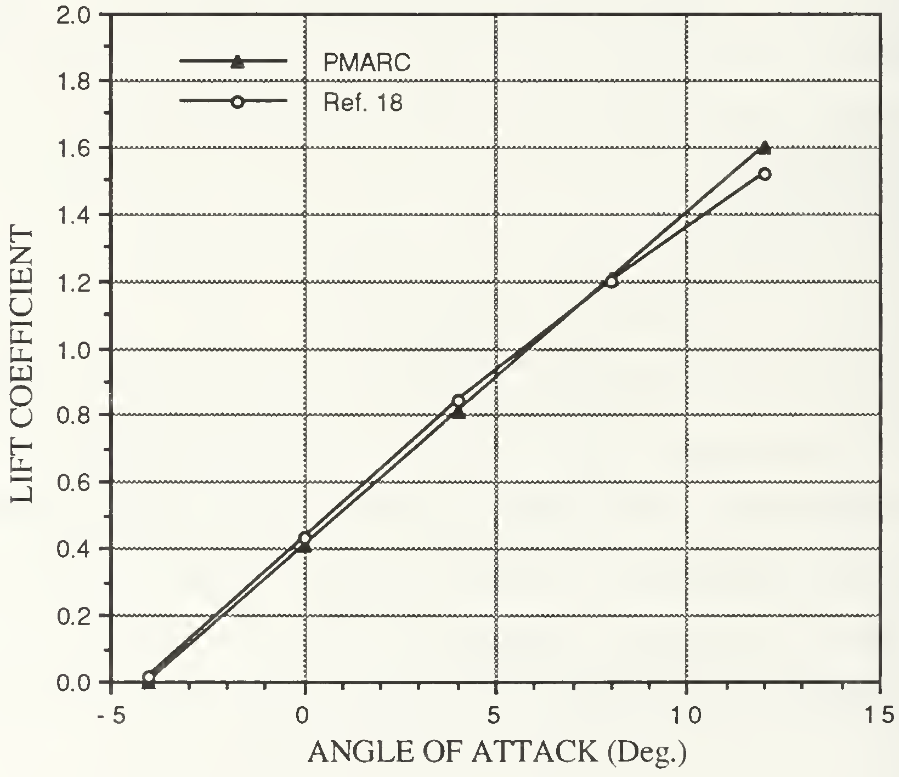

Figure 1. NACA 4415 Wing Lift Curve Slope

Upon inspection, PMARC results for a high-aspect-ratio wing correspond well with corrected 2-D data, especially at lower angles of attack.

Larger differences at higher angles of attack could be associated with the fact that the flow starts to separate, moving the effective aerodynamic center forward. A less negative pitching moment subsequently results. Indications of flow separation and subsequent stall are not predictable by panel codes. Within the scope of this analysis, however, PMARC results sufficiently agree with theoretical data.

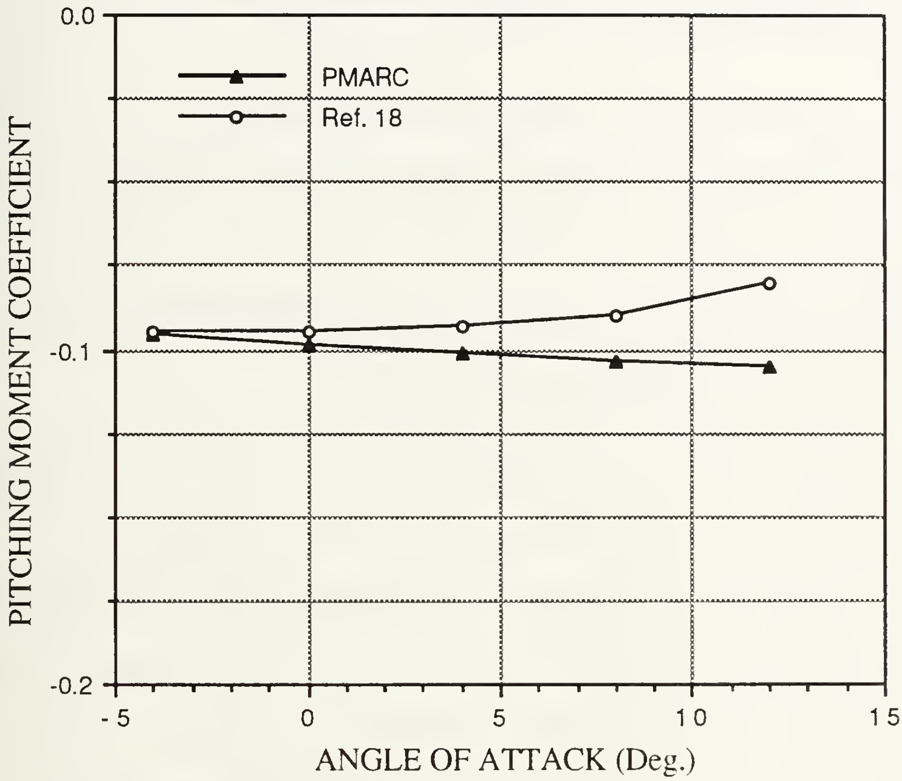

Figure 2. NACA 4415 Wing C_m (cg @ 0.25 mac) versus Angle of Attack

b. Computer-Generated Versus Operator-Defined Wakes

An experiment was made to determine the differences between PMARC results for geometries with user-defined wakes and those with computer-generated wakes. The motivation for this test was a reduction of high CPU times associated with computer-generated wakes without sacrificing data accuracy. Results indicate that data from a well-defined wake model are within two percent of the computer-generated wake model data as shown in Figures 3 and 4. An NACA 4415 wing and its computer-generated wake are found in Appendix A, Figure A4. Table III indicates the CPU times for each run. A three-fold saving in CPU time was made with very little sacrifice in data accuracy.

TABLE III CPU TIMES FOR PMARC WAKE MODELS

Wake Model	CPU Time (sec.)
User-defined	48
Computer-generated	170

It is important to emphasize that the CPU times in Table III are for a very simple geometry with 315 panels. The CPU times for test cases of the F-14 and T-34 together with operator-defined wakes were approximately 25 minutes. In contrast, a PMARC execution of a T-34 geometry with computer-generated wake experienced a CPU time-out after 2.5 hours.

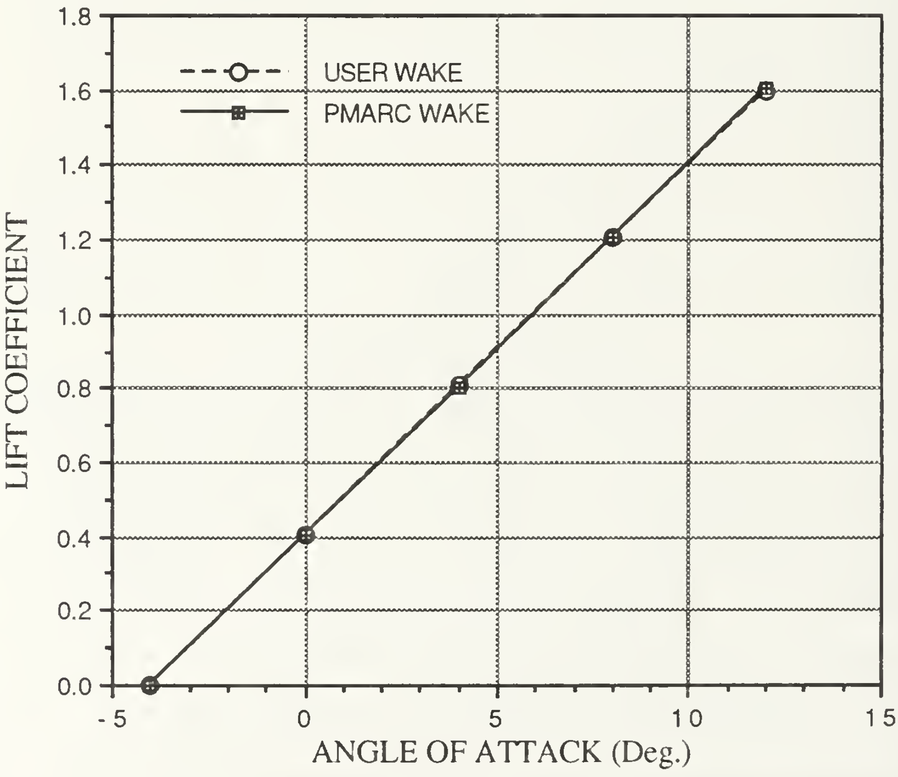

Figure 3. NACA 4415 Wing Lift Curve Slope

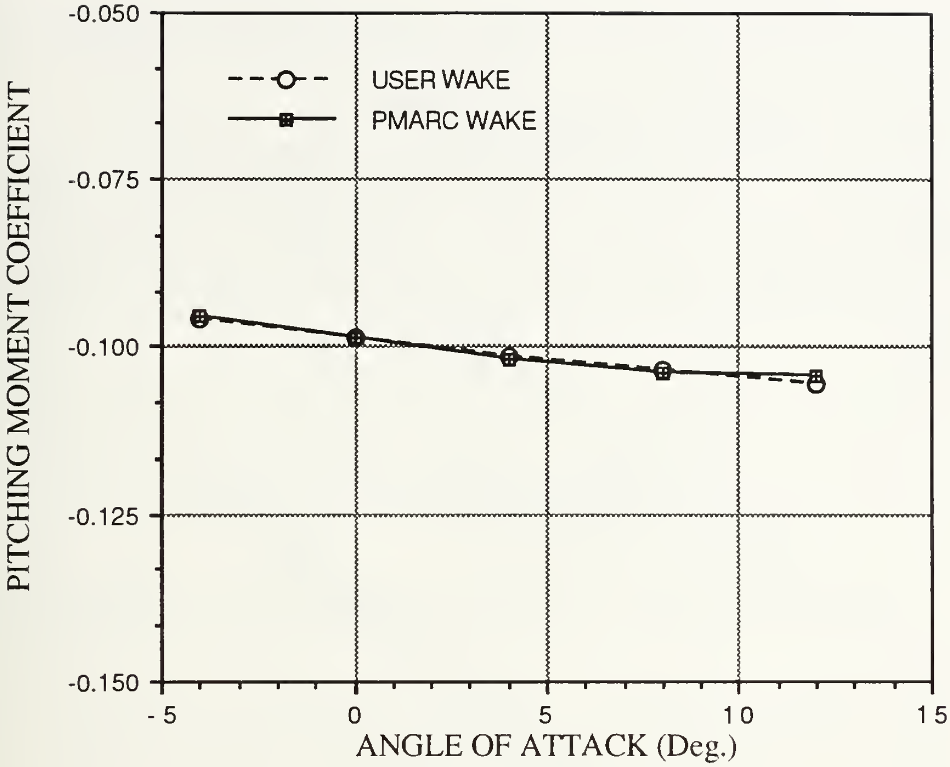

Figure 4. NACA 4415 Wing C_m (cg @ 0.25 mac) versus Angle of Attack

User-defined wakes were implemented for the remainder of the analysis based on the small differences in data sets between the computer-generated and user-defined wake geometries. The savings in CPU time permitted greater diversity of tests and test conditions within research time constraints.

2. T-34 Geometry Evaluation

A T-34 wing and tail were initially modeled to compare PMARC data with analytically-derived stability and control data described earlier. Appendix A, Figure A5 contains a T-34 wing and tail at five degrees angle of attack. Streamlines generated by PMARC are also included. Wakes on all remaining geometries are not shown to avoid clutter. A complete T-34 was then modeled with similar comparisons made. A T-34 model at one degree angle of attack is shown in Appendix A, Figure A6. Streamlines are moved outboard to observe the flow over the wing and tail vice the fuselage.

PMARC-generated lift and pitching moment coefficients are plotted against angle of attack in Figures 5 and 6 respectively. A cg location at 0.25 of the mean aerodynamic chord (mac) was assumed and used for all PMARC executions.

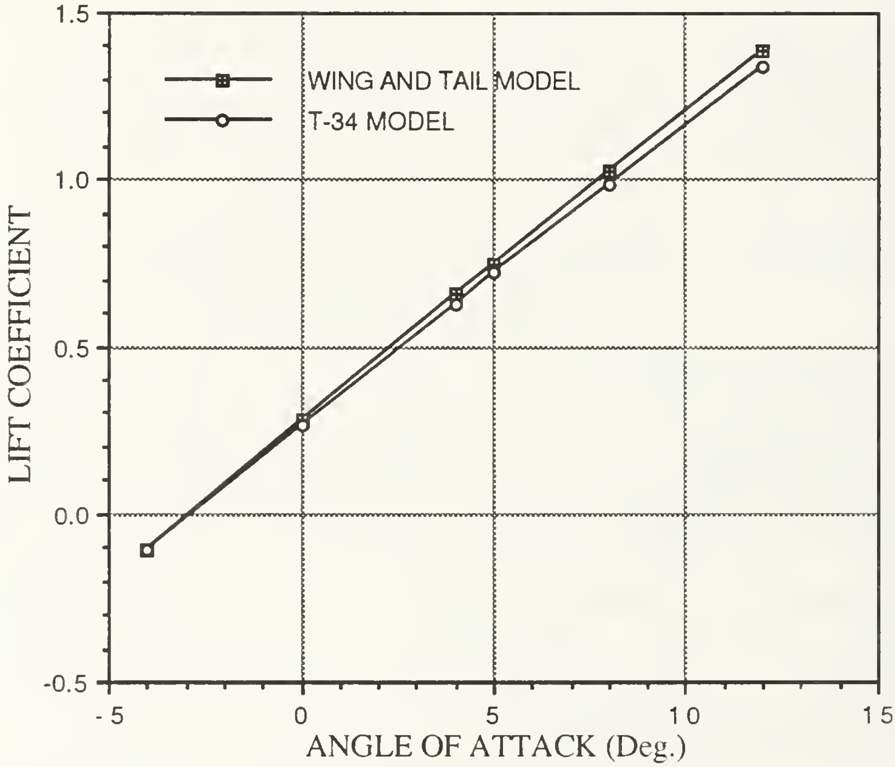

Figure 5. T-34 Geometry Lift Curve Slope

Lift curve slopes for each model were determined from Figure 5 by simple curve fits. The corresponding changes in pitching moment with angle of attack were obtained from curve fits of Figure 6. Stability derivatives are presented in Table IV for comparison with analytical results.

The lift curve slopes of each model are within five percent of analytical data. Pitching moment changes are within 34 percent of estimated data. The

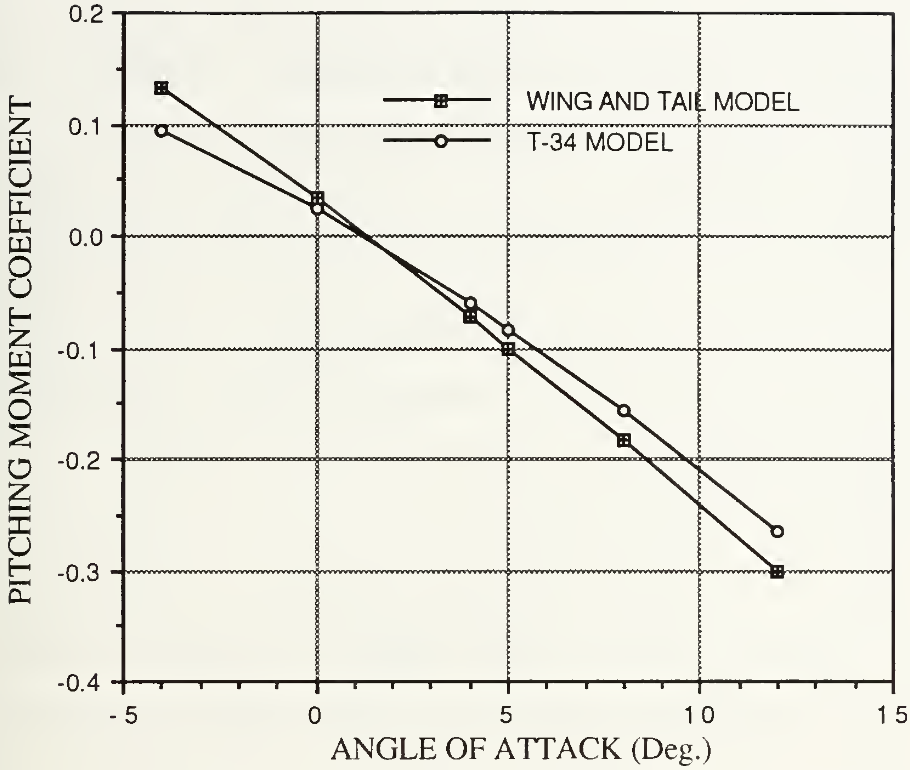

Figure 6. T-34 Geometry C_m (cg @ 0.25 mac) versus Angle of Attack

larger disparity in pitching moment data may be attributed to approximations for the geometric coordinates of the 0.25 mean aerodynamic chord location. PMARC uses these coordinates to compute forces and moments. Discrepancies

TABLE IV T-34 STABILITY DERIVATIVES

Derivative	T-34 Wing and Tail	T-34	Analytic Estimation
C_{L_α}	0.0933	0.0908	0.0894
C_{m_α}	-0.0271	-0.0224	-0.0339

between surface areas used in the analytical approximations and those generated from PMARC input geometries may also affect accuracy. Rounded T-34 wing and tail tips were truncated and modeled with little detail in order to keep the geometries as simple as possible.

It is important to emphasize that the analytic derivations used as reference standards for comparison were just estimates. A comparison of data in Tables II and IV shows that PMARC and analytic estimations are fairly close to expected values for the T-34's category of aircraft. The only exception is the estimate for the change in pitching moment with angle of attack. PMARC results appeared more consistent; therefore, the data were considered sufficiently accurate to conduct an investigation in the changes in trim conditions caused by airplanes flying in proximity.

3. F-14 Geometry Validation

A tailless F-14 model was obtained from NAWC WD, China Lake, CA. China Lake engineers used the model, written in VSAERO, to study stores separation characteristics. The code was converted to PMARC and used for this analysis. Thirty degrees of flaps were added to the model before conducting PMARC studies. Figures 7 and 8 show PMARC generated lift and moment coefficients versus angle of attack respectively. Geometry data from Ref. 14 were used to approximate a cg location at 0.25 of the wing's mean aerodynamic chord. The position was estimated by adding 0.25 of the mean geometric chord length to the longitudinal station coordinates of the mean geometric chord's leading edge. This center of gravity location was taken as noted with no verification by further analysis.

The tailless F-14's lift curve slope as a function of angle of attack was then determined by simple curve fit and is presented in Figure 9. Wind tunnel report data from Ref. 14 are included for comparison. The differences between PMARC and wind tunnel report data are attributed to variations in configuration

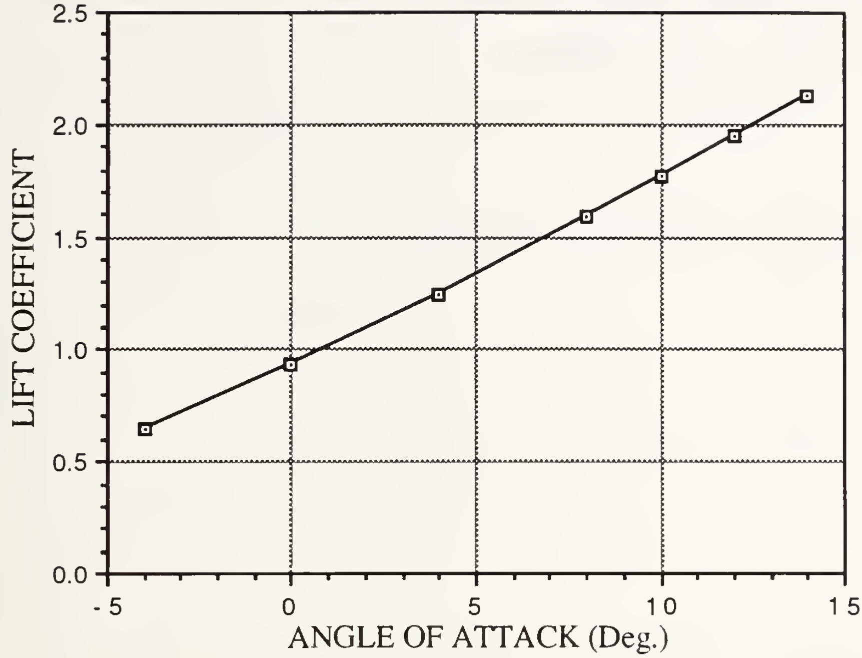

Figure 7. Tailless F-14 Lift Curve Slope

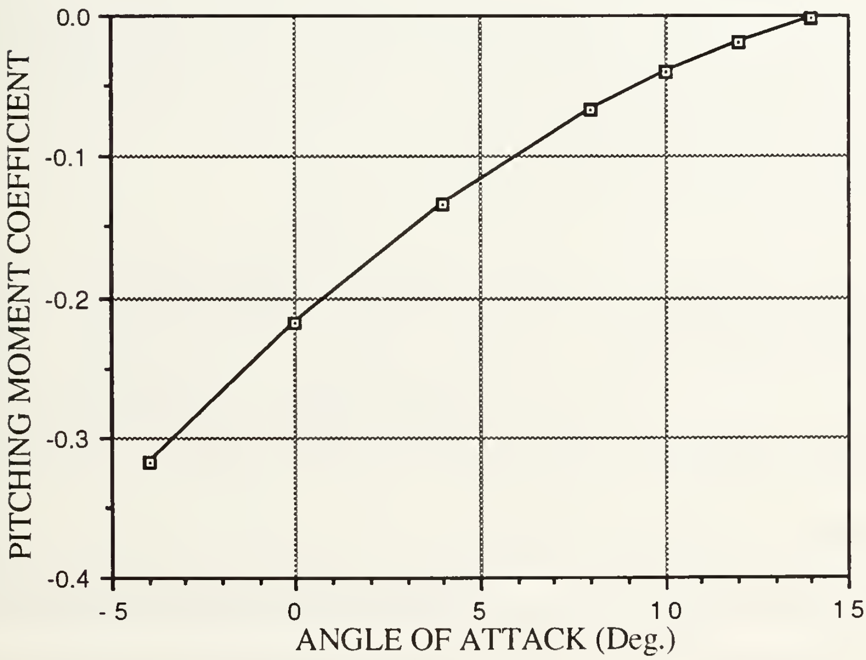

Figure 8. Tailless F-14 C_m (cg @ 0.25 mac) versus Angle of Attack

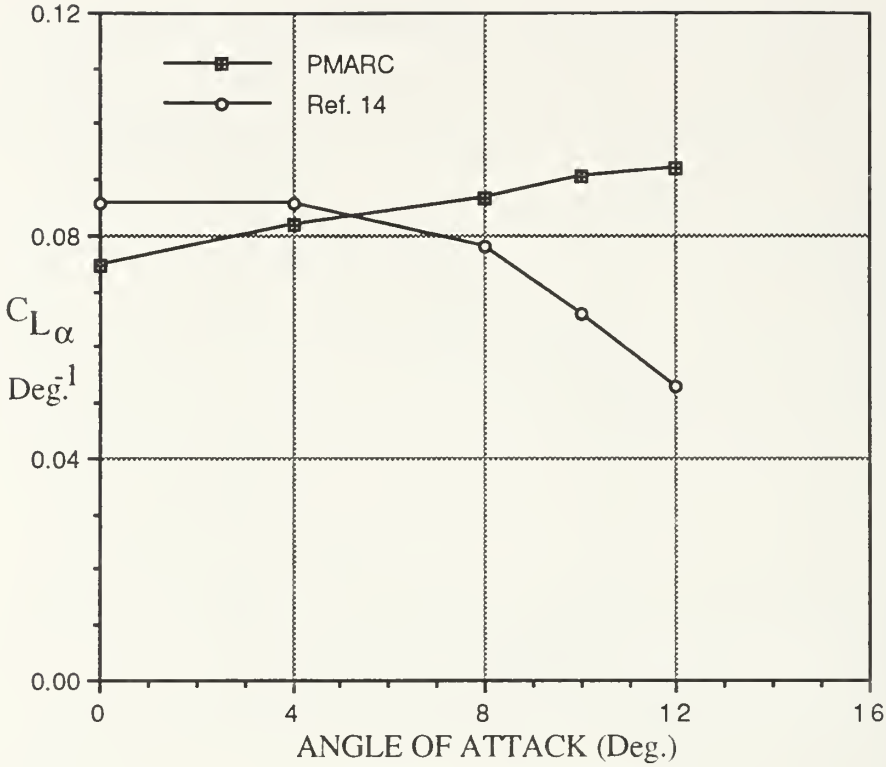

Figure 9. Tailless F-14 C_{L_α} versus Angle of Attack

for each test. Table V shows the configurations used for each data set. Flow separation effects at high angles of attack, mentioned earlier for the 4415 wing evaluation, could also account for contrasts in data.

TABLE V F-14 TEST CASE CONFIGURATIONS

Test Case	Landing Gear	Flaps	Slats	Speed Brake	Direct Lift Control
PMARC	Up	30°	Retracted	Retracted	Stowed
Ref. 14	Down	35°	Extended	Extended	Stowed

Tails were then modeled based on airfoil information obtained from Ref. 14. The tail patches did not join the original model but were placed as close as possible. Small gaps between patch surfaces remained but did not appear to corrupt output data. This approach simplified the model and provided an additional benefit of having moveable tail surfaces that were later used to trim the F-14. This modeling technique was not considered unrealistic, because the horizontal tail of the F-14 is an all moveable control surface attached to the airframe by a single pin.

The complete F-14 geometry used for this study is shown in Appendix A, Figure A7. PMARC-generated lift and pitching moment coefficients are plotted against angle of attack in Figures 10 and 11 respectively. A cg location at 0.25 mac was used for all PMARC applications. Computer simulation data from Ref. 21, are included for comparison. The simulation data were corrected to a cg location at 0.25 mac using equation (5) [Ref. 14:p. 1-3].

$$C_m = C_{m_{cg@0.162}} + C_L(h - 0.162) \quad (5)$$

The configurations were the same as those used for the tailless investigation presented in Table V. The horizontal tail used in the PMARC model was aligned with the body axis (zero relative angle of attack). The zero reference line for the F-14 tail angle of attack was not known, so data sets from several tail positions are presented in Figure 11. Differences between the PMARC body axes and the actual F-14 zero reference line could account for the PMARC data in Figure 11 lying between the +5 and 0 symmetric tail position data sets. Configuration differences mentioned in Table V and approximations for 0.25 mean aerodynamic chord location could also affect data.

The F-14 lift curve slope as a function of angle of attack was then determined by simple curve fit and is presented in Figure 12. Wind tunnel report data from Ref. 14 are included for comparison.

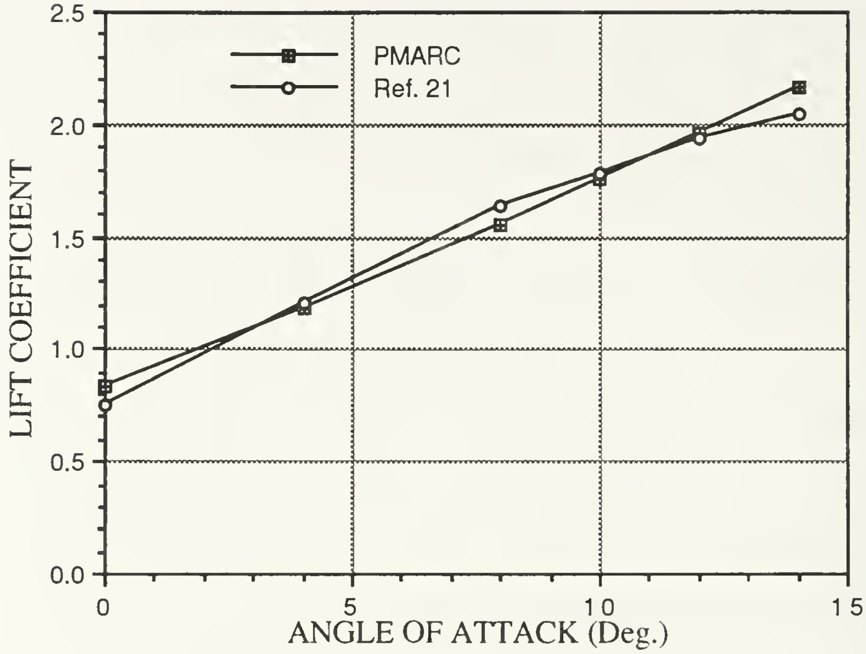

Figure 10. F-14 Lift Curve Slope

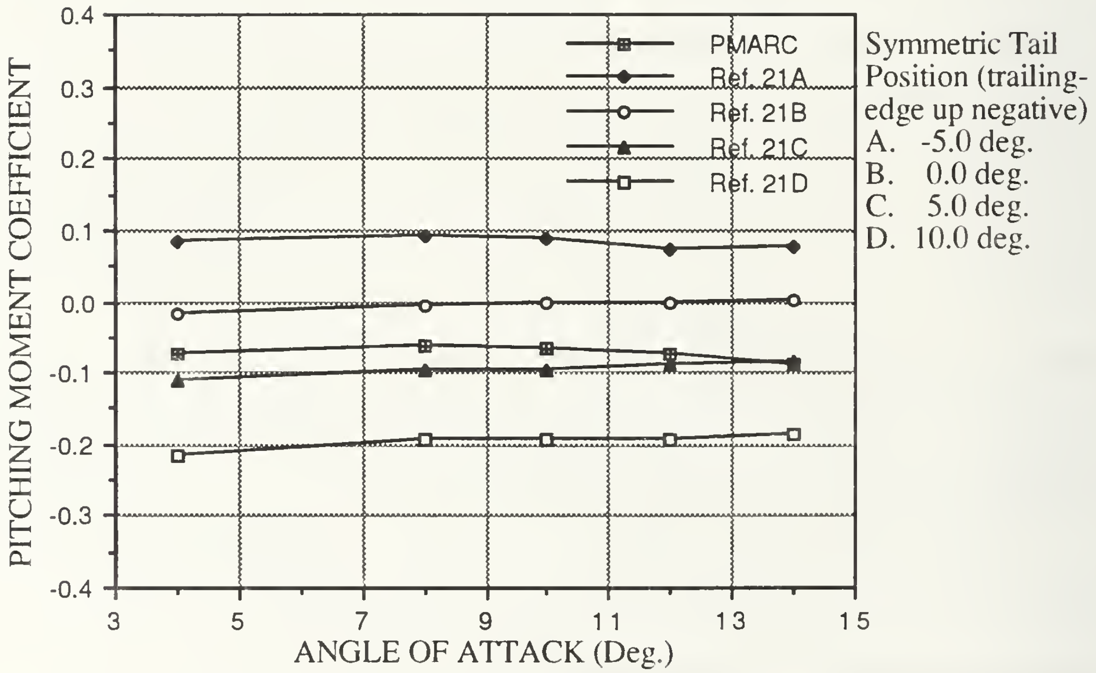

Figure 11. C_m (cg @ 0.25 mac) Versus Angle of Attack

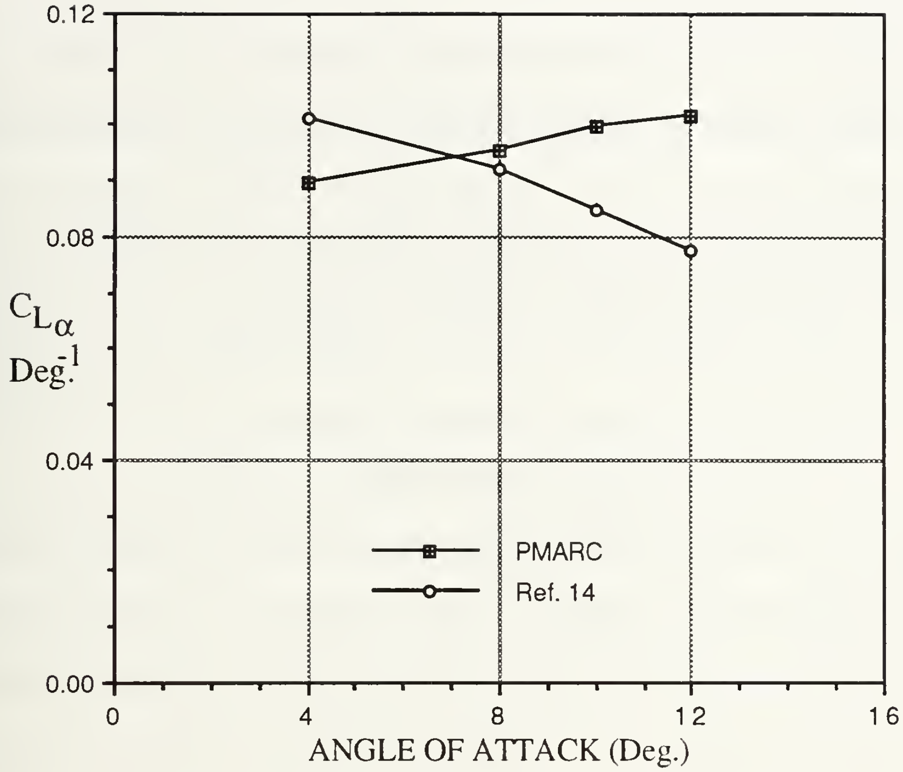

Figure 12. F-14 C_{L_α} Versus Angle of Attack

PMARC validation based on the results found in Figures 7 through 12 was not possible due to the configuration variations among the data sets. Data similarities in magnitudes and trends were deemed adequate for this study, however. The F-14 model was considered a good representation for further investigation of dissimilar airplanes flying in proximity.

The F-14 was then "trimmed" at 11 degrees angle of attack for the remainder of this study. This flight condition was based on a gross weight of 57,000 lbs. and an airspeed of 135 kts. Detailed test conditions are presented in Chapter IV. A horizontal elevator position of 4.9 degrees trailing-edge up was used to zero the pitching moment of the F-14 model. This trim setting was facilitated by the fact that the horizontal tail was modeled separately and was free to rotate independently.

IV. ANALYSIS OF AIRPLANES FLYING IN PROXIMITY

Several combinations of PMARC geometries were used to study the aerodynamic disturbances between airplanes in proximity. A T-34 wing and tail geometry was observed first as the configuration approached a much larger wing. Then, the T-34 model was looked at as it flew closer to an F-14. An additional study kept the vertical separation between two airplanes constant and varied their relative longitudinal positions fore and aft. Disturbances created by jet intakes were also briefly examined. Streamlines, lift coefficients, pitching moments and pressure coefficients were observed at incremental distances between PMARC geometries. Data were provided by PMARC output tables and displayed by GVS. Data reduction included changes in elevator deflection required to maintain longitudinal trim of the smaller geometry as it approached the larger configuration.

Geometry separations for all of the PMARC studies were constrained to the XZ plane of symmetry. This limitation was due to the half-plane models used, so PMARC could automatically add the influence of the mirror image when calculating the total force and moment coefficients. Investigations in other planes would require full geometry models, adding complexity and computational burden to the analysis, and were beyond the scope of the current study.

A. LARGE WING AND T-34 WING AND TAIL IN PROXIMITY

A large untapered wing and a T-34 wing and tail were modeled as shown in Appendix A, Figure A8. The two bodies were aligned in the XZ plane such that the T-34 wing's ac was directly under the larger wing's ac. Distances between the two geometries varied between 170.83 and 8.33 feet. In terms of T-34 wing spans, the distances varied between approximately 5.0 and 0.25. Test conditions and relative geometry sizes are presented in Table VI. Angles of attack for each geometry remained constant, as indicated in Table VI, throughout the PMARC executions. Variations in lift, moments and elevator trim requirements caused by aerodynamic interference could then be studied as a function of vertical separation only.

TABLE VI PMARC TEST CONDITIONS

Geometry	Airfoil	Span (ft)	Area (ft^2)	MAC (ft)	CG	AOA
Large Wing	4415	64.125	695.0	10.83	0.25 MAC	11 deg
T-34 Wing	23012	33.34	180.0	8.33	0.25 MAC	5 deg
T-34 Tail	0008	12.5	38.45	3.1	-----	-----

Figure 13 indicates a change in lift of the wing and tail as the vertical separation between modeled geometries decreases. The decrease in lift may be due to a reduction in local angle of attack caused by flow curvature under the larger wing or to increased ambient pressure due to the pressure side of the large wing. Figure 13 shows a 50 percent reduction in lift of the T-34 wing and tail when the model approaches the larger wing to within its own semi-span.

The pitching moment was also affected by changes in vertical separation as shown in Figure 14. At five degrees angle of attack, the T-34 configuration developed a nose-down pitching moment as expected. As the T-34 wing and tail approached the larger wing to within 12.5 feet, PMARC indicated that a nose-up pitching moment had developed. The nose-up pitching moment was approximately equal in magnitude to the nose-down moment obtained beyond the aerodynamic interference of the larger wing as shown in Figure 14.

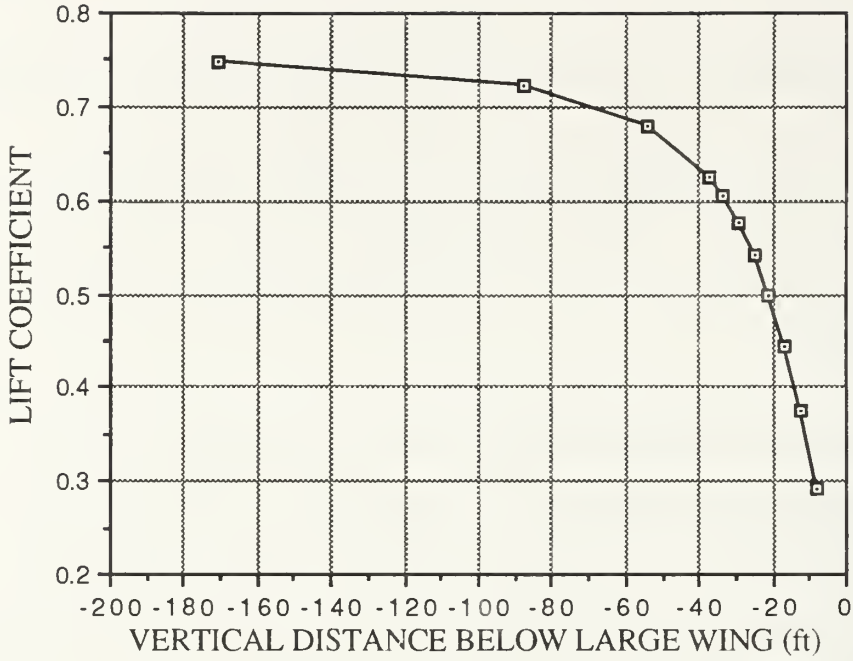

Figure 13. T-34 Wing and Tail Lift Coefficient Versus Vertical Separation

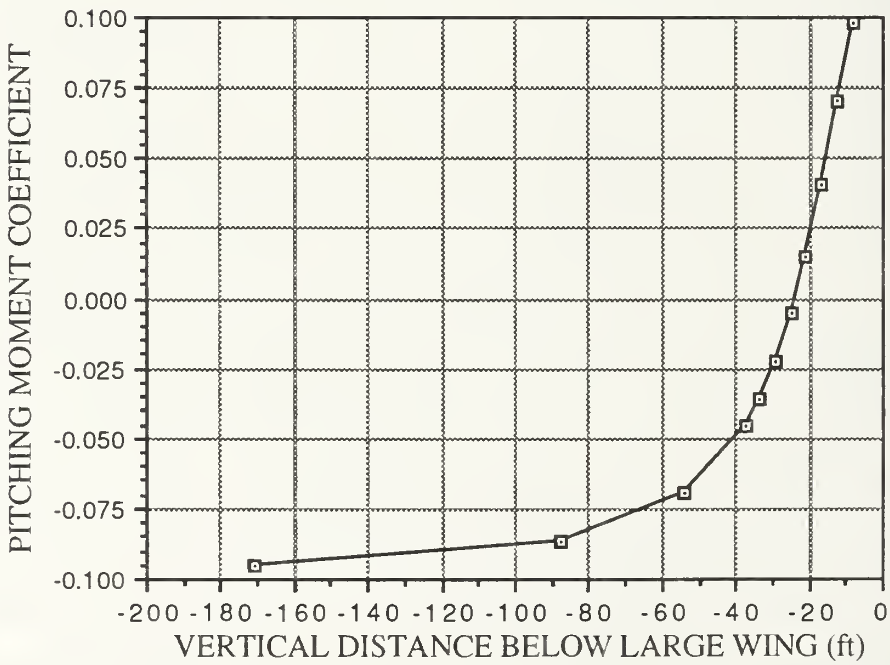

Figure 14. T-34 Wing and Tail C_m (cg @ 0.25 mac) Versus Vertical Separation

A baseline pitching moment coefficient of -0.10 was established for the T-34 wing and tail model at five degrees angle of attack, from Chapter III, Figure 6. The differences between the pitching moment coefficients for each vertical distance and the baseline were used to determine the changes in elevator deflection to maintain trim at five degrees angle of attack. The change in elevator deflection as a function of vertical separation was determined by equation (6).

$$C_{m_{baseline}} - C_{m_{interference}} = C_{m_{\delta_e}} \Delta\delta_e \tag{6}$$

Changes in elevator deflection data are presented in Figure 15. A positive change represents more trailing-edge down. PMARC data showed that a change

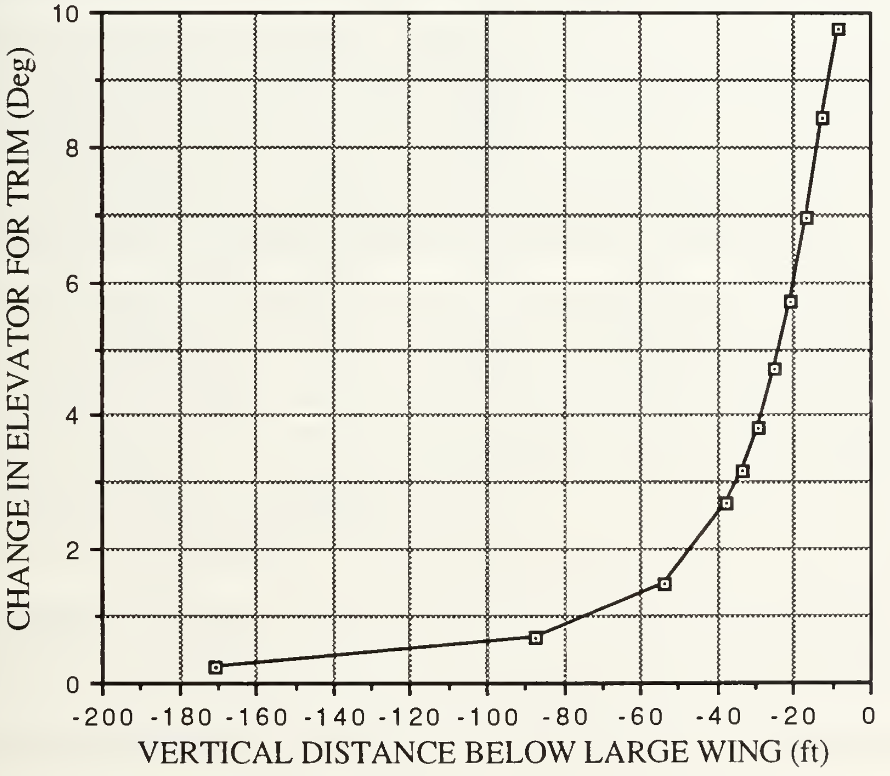

Figure 15. Change in Elevator Deflection Versus Vertical Separation

of 9.5 degrees in elevator deflection, more trailing-edge down, was required for trim as the T-34 wing and tail approached to within 8.33 feet of the large wing.

Streamlines plotted by GVS provided a qualitative analysis of the aerodynamic disturbances between the two configurations. Appendix A, Figure A9 shows just the T-34 wing and tail and associated streamlines. Appendix A, Figure A10 shows the streamlines when the T-34 wing and tail were 12.5 feet below the large wing. As the distance between the two models decreased, the streamlines were deflected slightly downward behind the large wing. This apparent downwash probably contributed to the positive pitching moment of the T-34 wing and tail. The downwash decreased the tail's relative angle of attack, decreasing positive lift and eventually producing lift in the downward direction.

The color display of pressure coefficients on the wing and tail also provided insights into the changes in pitching moment. Appendix A, Figure A11 shows the bottom of the T-34 tail when the wing and tail configuration was beyond any interference effects of other airplanes. The underside of the tail is predominantly yellow at the leading edge and blends to green toward the trailing edge. Free-stream conditions are represented by green. The histogram to the right of the figure indicates these pressures represent a small suction peak at the lower leading edge that tapers off to almost zero pressure coefficient, or free-stream pressure, at the trailing edge. Appendix A, Figure A12 shows the bottom of the tail when it is 8.33 feet from the large wing. A noticeable red band along the lower-surface leading edge has developed. A much stronger suction peak exists; therefore a greater downward force is acting on the tail. This downward force provided the positive pitching moment determined by PMARC and depicted in Figure 14.

B. F-14 AND T-34 IN PROXIMITY

1. Vertical Separation

An F-14 and T-34 were modeled as shown in Appendix A, Figure A13. The PMARC input code for this evaluation is presented in Appendix B. The two bodies were aligned in the XZ plane such that the T-34's cg was directly under the F-14's cg. Distances between the two geometries varied between 170.83 and 12.5 feet. In terms of T-34 wing spans, the distances varied between approximately 5.0 and 0.4. PMARC test conditions were determined from the data in Table VII. Angles of attack for each geometry remained constant, as indicated in Table VII, throughout the PMARC executions.

TABLE VII PMARC TEST CONDITIONS (F-14 AND T-34)

Configuration\A/C	T-34	F-14
Weight (lbs)	3760	57000
Velocity (kts)	135	135
Wing Area (ft^2)	180	565
C_L (1)	0.35	1.70
Angle of Attack	1°	11°
CG	0.25 MAC	0.25 MAC (2)

1. Standard day @ 1000 ft
2. Wing Mean Geometric Chord

Figure 16 shows a decrease in lift of the T-34 as it approaches the F-14. The T-34 loses approximately 55 percent of its lift when it is one wing span away from the larger aircraft and 91 percent of its lift when a semi-span away. Once again, the decrease in lift may be due to a decrease in the local angle of attack of the T-34 wing and the increased pressure felt by the upper wing surface due to its proximity to the pressure side of the F-14 wing. To the pilot, this loss of lift can correspond to a sensation of being pushed away by the F-14.

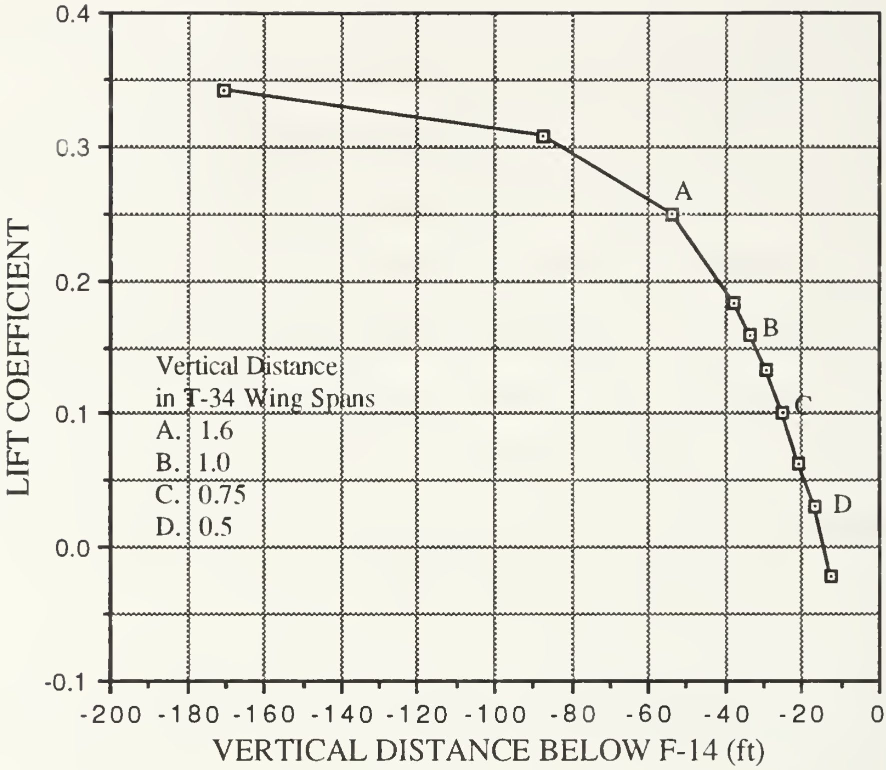

Figure 16. T-34 Lift Coefficient Versus Vertical Separation

The changes in lift on the T-34 are highlighted in Appendix A, Figures A14, A15 and A16. Figure A14 uses color to represent pressure coefficients on the T-34 wing and tail upper surfaces. The histogram to the right of the airplane geometry quantifies the representative colors. There is a large red band on the leading edge of the wing that represents a relatively strong suction peak. The colors transition to yellow, green, then dark blue at the trailing edge. Dark blue represents free-stream conditions for Figures A14, A15, and A16. Figure A15 displays the pressure coefficients on the T-34 when it is 37.5 feet or about a wing span beneath the F-14. The suction peak on the wing has decreased in magnitude and area as indicated by the smaller, narrower band of light red. Yellow has filled in for the red indicating less negative pressure coefficients. The lift coefficient at this flight condition was 0.183, indicating a loss of approximately 48 percent of the T-34 lift. Figure A16 represents the pressure coefficients on the T-34 when it was 25 feet from the F-14. Traces of red are very faint, while the wing's leading edge is predominately yellow. At 25 feet, the T-34 had lost 71 percent of its lift. The loss in T-34 lift is highlighted best by a comparison of the T-34 wing leading edge in Figures A14 and A16.

The T-34 pitching moment was also affected as the vertical separation between the two airplanes decreased. In the cruise configuration and at one degree angle of attack, the modeled T-34 had a small (0.004), positive pitching moment coefficient. Figure 17 shows that as the T-34 approached the F-14, the

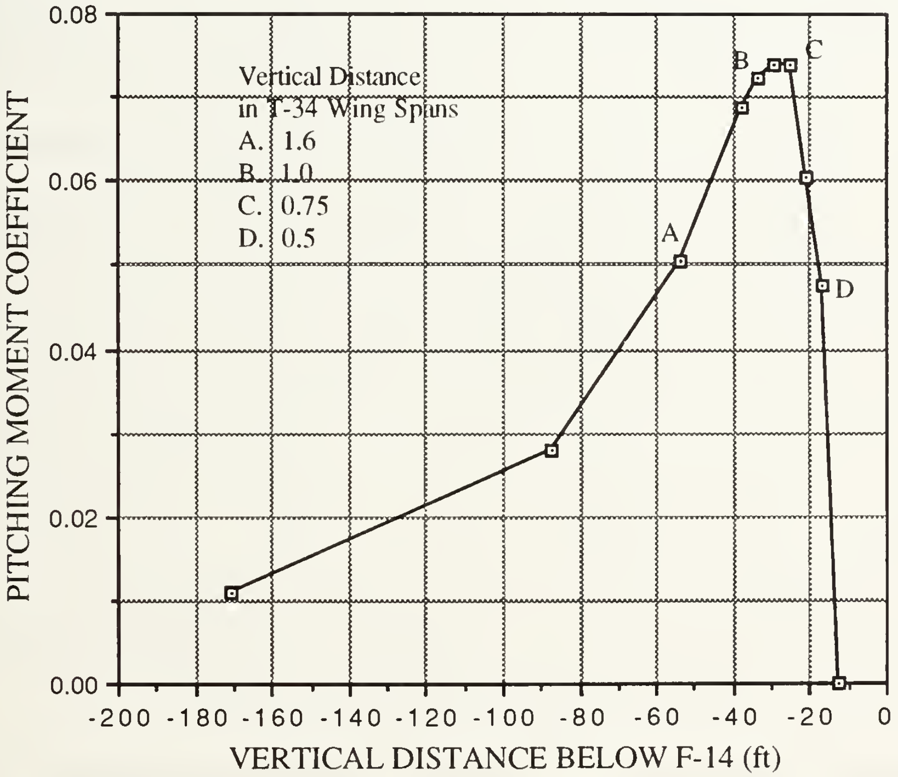

Figure 17. T-34 C_m (cg @ 0.25 mac) Versus Vertical Separation

T-34 pitching moment coefficient increased until the two airplanes were 25 feet, or 0.75 T-34 wing spans, away. The pitching moment coefficient then decreased with decreasing separation distance as shown in Figure 17. To the pilot, the increases in nose-up pitching moment will increase push-stick forces and will require nose-down trim to zero these forces. Nose-down trim will then have to be decreased if the distance between the two airplanes becomes less than 25 feet.

The decrease in pitching moment coefficient at separation distances of less than 25 feet is probably due to local pressure effects of the F-14 fuselage. The reader should be aware, however, that distances directly below another airplane of less than 20 feet are not considered pertinent to most practical applications of formation flying.

The color display of pressure coefficients on the bottom of the T-34 tail also provided insight into the changes in pitching moment. Appendix A, Figure 17 shows the bottom of the T-34 tail when the airplane was beyond interference effects of other aircraft. The underside of the tail is predominantly yellow at the leading edge and blends to green and then blue toward the trailing edge. The histogram to the right of the figure indicates these pressures represent a small suction peak at the leading edge that tapers off to free-stream conditions at the trailing edge. Free-stream conditions are represented by dark blue in the figure. Figure A17 represents the tail of the T-34 model with a pitching moment coefficient of 0.004. Appendix A, Figure 18 shows the bottom of the tail when the T-34 model is 37.5 feet below the F-14. F-14 panel edges are white while T-34 panel edges are colored. A noticeable red band has developed along the lower leading edge, indicating a much stronger suction peak exists. The tail is generating more lift in the downward direction providing the model with a greater nose-up pitching moment. The suction peak increased further when the airplanes closed to 25 feet as shown in Appendix A, Figure A19. The downward lift generated by the tail at this vertical distance produced the maximum nose-up pitching moment for the given test conditions as indicated in Figure 17.

A baseline pitching moment coefficient of 0.004 was established for the T-34 model at one degree angle of attack from Chapter III, Figure 6. As before, the differences between the pitching moment coefficients for each vertical distance and the baseline were used to determine the changes in elevator deflection to maintain trim at one degree angle of attack. Changes in elevator deflection for trim are presented in Figure 18. A positive change represents more

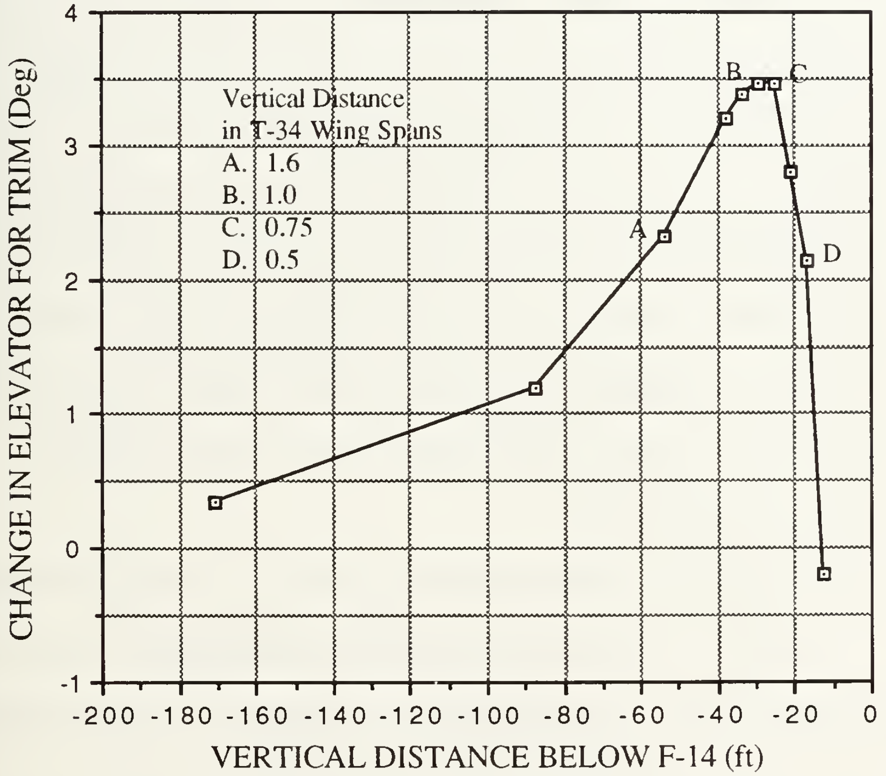

Figure 18. T-34 Change in Elevator Deflection Versus Vertical Separation

trailing-edge down. PMARC results indicated that a change of approximately 3.5 degrees in elevator deflection, more trailing-edge down, was required for trim as the T-34 approached to within 25 feet of the F-14. As the airplanes continued to close, the nose-down trim changes from the baseline decreased to zero as shown in Figure 18. The T-34 formation pilot will need to change the trim 3.5 degrees (nose-down) for approaches within 25 feet of the F-14. The required nose-down trim will then decrease if the airplanes close further.

Streamlines provided a qualitative analysis of the aerodynamic disturbances between the F-14 and T-34. Appendix A, Figure A20 shows the streamlines around the T-34 when it is 33.33 feet or a wing span beneath the F-14. Appendix A, Figure A21 depicts the streamlines when the two airplanes are 16.67 feet away from each other. Streamlines were spaced 10 inches apart. A comparison of Figures A20 and A21 shows that as the two airplanes approach each other, the streamlines are deflected downward. There are six streamlines above the tail in Figure A20 while there are only five above the tail in Figure A21. The sixth streamline from the top in Figure A21 flows below the horizontal tail. Unfortunately, PMARC did not provide quantitative streamline deflection angles. This apparent downwash depicted by the streamlines decreased the tail's relative angle of attack, thereby contributing to the nose-up pitching moment.

2. Horizontal Separation

An investigation was made to determine the changes in lift and moment coefficients as the T-34 maintained altitude below the F-14 but changed position in the horizontal direction. The intent was to simulate a T-34 approaching the F-14 from behind with a closure rate that was too high for a proper rendezvous. A 25-foot step-down position was chosen because the maximum pitching moment coefficient was found at that separation distance from the previous study. Horizontal distances were chosen along the F-14's longitudinal axis. A positive horizontal value represented the T-34 cg ahead of the F-14 cg, and a negative value behind.

The lift coefficient increased over a range of 0.3 as the T-34 position changed from 16.67 feet aft of the F-14 cg to a position 25 feet forward of the F-14 cg. Figure 19 shows the change in lift coefficient with horizontal distance from the F-14 cg. It is important to emphasize that the T-34 vertical separation

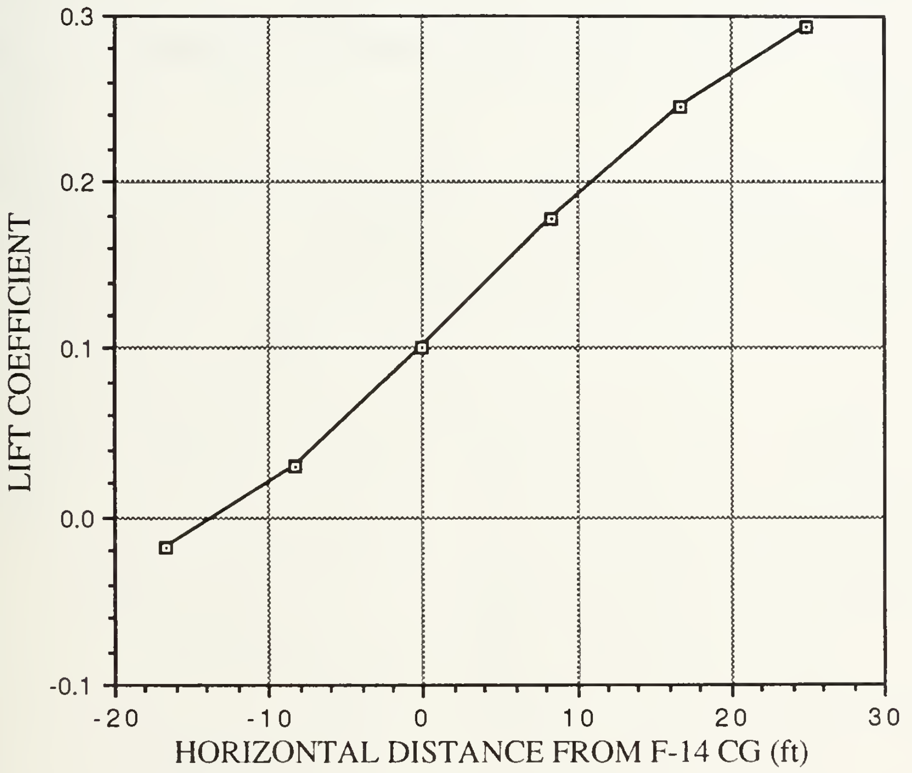

Figure 19. T-34 Lift Coefficient Versus Horizontal Distance from F-14 CG

from the F-14 remained fixed at 25 feet. This change in lift occurs from interference effects caused by the flow over the F-14. The flow is deflected downward as it comes off of the F-14's lifting surfaces. When the T-34 is aft of the F-14 cg, this downwash decreases the local angle of attack on the T-34 lifting surfaces, decreasing its overall lift. As the T-34 moves forward of the F-14 cg, it eventually experiences the upwash that occurs ahead of the F-14 wing and fuselage. The upwash increases the local angle of attack on the T-34, increasing its lift. Local ambient pressure changes due to the T-34's proximity to the high-pressure side of the F-14 wing complicate the analysis, but nonetheless, the changes in lift of the T-34 as it flies along the longitudinal axis of the F-14 are profound. The T-34 formation pilot should be acutely aware of these potential changes and how they might affect vertical closure rates. Unanticipated closure rates toward the F-14 as the T-34 develops more lift may increase the probability of a collision.

The T-34 pitching moment coefficient also changed with horizontal separation as shown in Figure 20. A maximum nose-up pitching moment coefficient occurred 8.33 feet ahead of the F-14 cg. The pilot experiences a

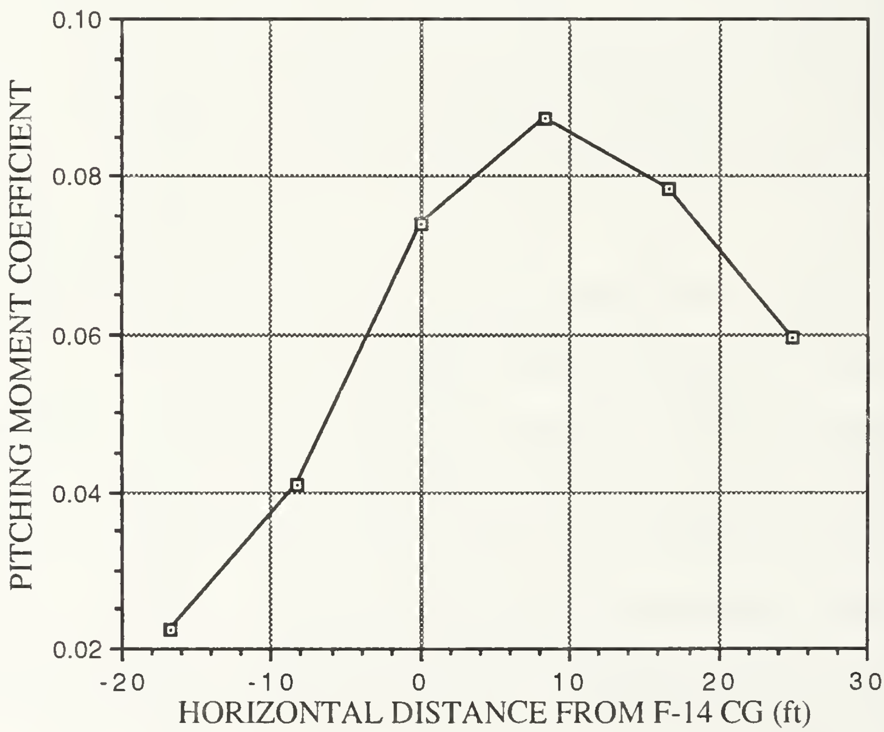

Figure 20. T-34 C_m (cg at 0.25 mac) Versus Horizontal Distance From F-14 CG

nose-up pitching moment throughout the longitudinal movement but the magnitude changes. The corresponding changes in elevator deflection for trim are presented in Figure 21. The data show that continuous elevator changes are required for trim and a maximum change of 4.12 deg. occurs at 8.33 feet forward of the F-14 cg position.

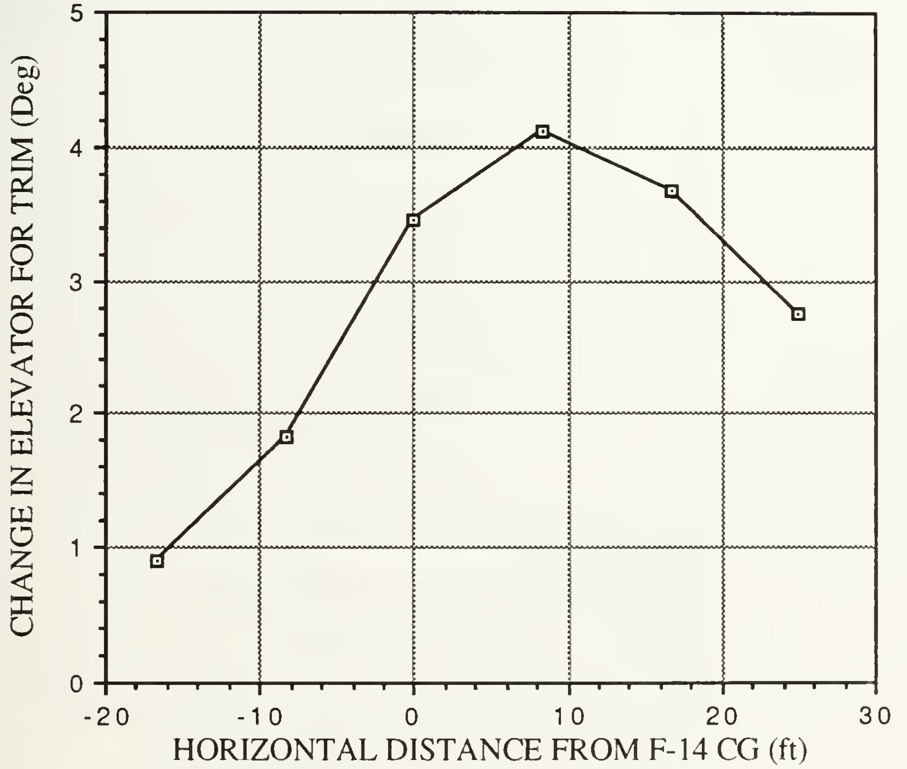

Figure 21. T-34 Change in Elevator Deflection Versus Horizontal Distance From F-14 CG

A follow-up study was conducted with the T-34 cg located 8.33 feet forward of the F-14 cg, where the maximum pitching moment coefficient discovered so far by the study was located. Vertical separation tests were performed to see if the T-34 pitching moment increased further. Lift and moment coefficient data are presented in Figures 22 and 23 respectively. The T-34 lift coefficient shown in Figure 22 does not decrease as appreciably as the lift coefficient shown in Figure 16. This is probably due to the upwash from the F-14 wing. When the T-34 is 8.33 feet forward of the original test position, it is exposed more to the upwash of the F-14 wing. The direction of flow in the upwash is more uniform; therefore the changes in local angle of attack with vertical separation changes are not as high. Under the F-14 cg, however, the flow experiences more bending and perturbations, consequently having a greater effect on the T-34's angle of attack and subsequent lift.

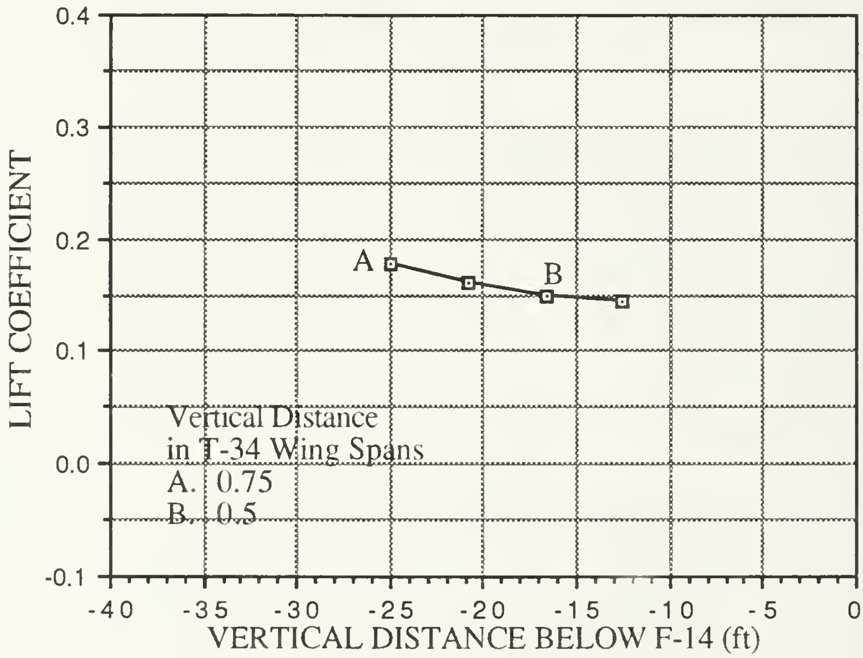

Figure 22. T-34 Lift Coefficient Versus Vertical Separation

A similar trend was noted with the T-34 pitching moment coefficient. The pitching moment did not decrease to zero as it had for the previous study. A new maximum pitching moment coefficient was obtained when the T-34 was 20.83 feet from the F-14 as shown in Figure 23. The change in elevator deflection required for trim was 4.47 degrees. It is important to emphasize that the scope of this study was limited and that a higher pitching moment may exist.

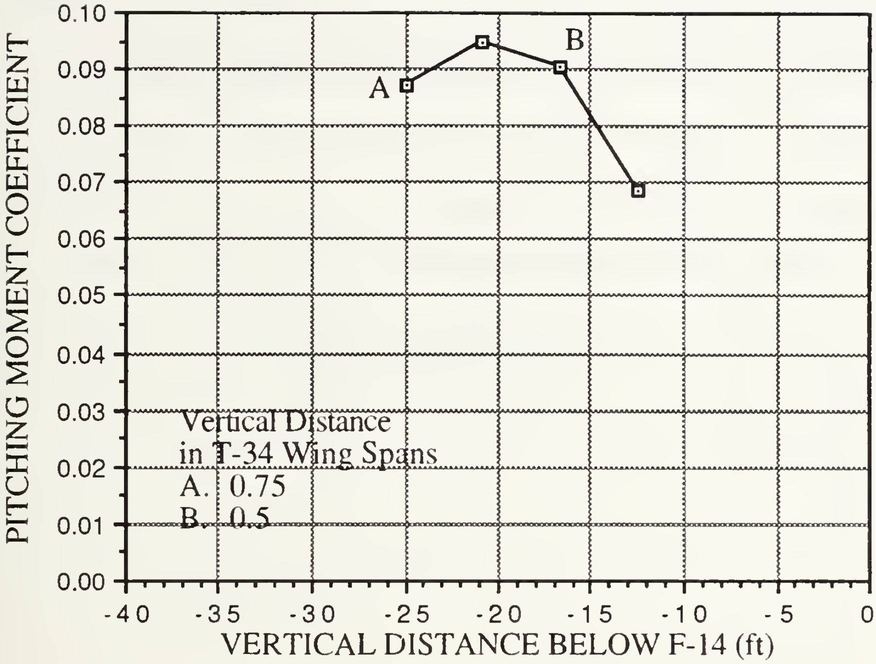

Figure 23. T-34 C_m (cg @ 0.25 mac) Versus Vertical Separation

3. F-14 Jet Intake Effects

PMARC provides a capability to prescribe normal velocities on groups of geometry panels. A brief investigation was conducted to see how the flow into the large F-14 jet intakes affected the lift and pitching moments on the T-34. A vertical separation study was conducted with the T-34 cg 8.33 feet forward of the F-14 cg. The location provided the maximum pitching moment discovered by this study and it placed the T-34 wing underneath the intakes. A flow velocity of Mach 0.3 was assumed at the face of the jet intakes. The changes in lift and pitching moment coefficients with vertical separation are shown in Figures 24 and 25 respectively. Data from Figures 22 and 23 are included to compare the effects with and with out jet intake considerations.

The data show that the flow into the jet intakes does influence the lift and pitching moment of the T-34. The influence is relatively small, however, as lift and pitching moments were increased by less than 5 percent. A new maximum pitching moment was determined, however, at 20.83 feet below the F-14 with the T-34 cg 8.33 feet forward of the F-14 cg. In the presence of jet intake effects, a pitching moment of 0.0956 was realized on the T-34. The change in elevator deflection required for trim was 4.5 degrees.

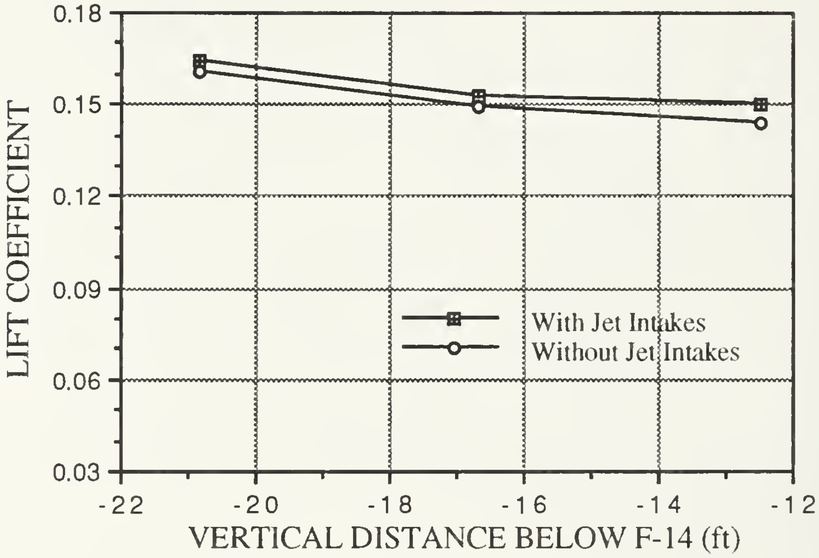

Figure 24. T-34 Lift Coefficient Versus Vertical Separation From Jet Intakes

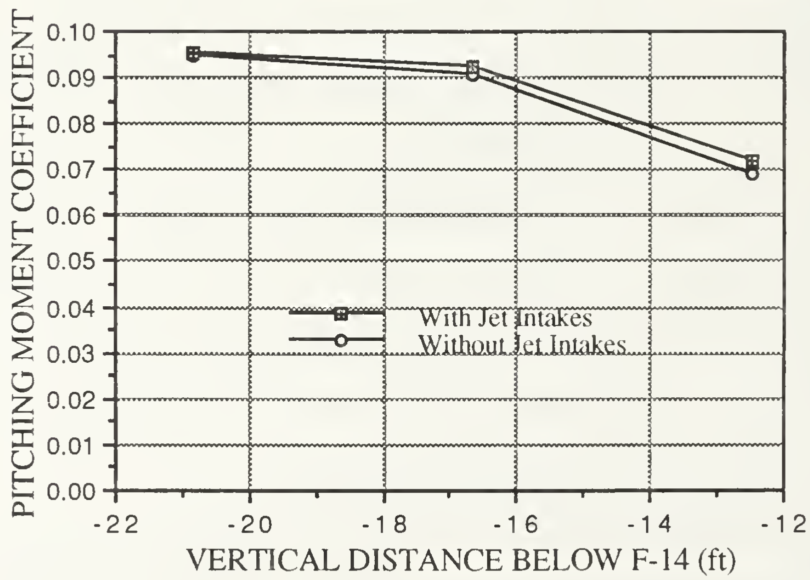

Figure 25. T-34 C_m (cg @ 0.25 mac) Versus Vertical Separation From Jet Intakes

V. CONCLUSIONS AND RECOMMENDATIONS

A. CONCLUSIONS

Airplanes flying in proximity to one another create mutual interference. PMARC studies have shown that this mutual interference affects the flow over each airplane, subsequently altering their aerodynamic characteristics. Significant changes in the lift and pitching moments of an airplane flying in formation underneath another were observed.

A T-34 flying beneath an F-14 will lose half of its lift as it closes to within one wing span. This loss of lift is accompanied by a nose-up pitching moment. The T-34 formation pilot is subsequently presented with confusing cues as he approaches the larger airplane. The loss of lift will correspond to a sensation of being pushed away by the F-14; yet as he gets closer, the T-34 will want to pitch up toward the F-14. This may cause the inexperienced or uninformed pilot to become disoriented. An appreciation of this mutual interference phenomenon combined with anticipated nose-down trim changes should help to avoid the possibility of a collision.

A T-34 will experience large changes in lift as it travels fore and aft underneath an F-14 with approximately one wing span of vertical separation. PMARC showed that as the T-34 moved from a point 25 feet aft of the F-14 cg to a point approximately 18 feet forward of the cg, the lift coefficient increased by 0.3. Combined with variations in nose-up pitching moments, unanticipated and possibly dangerous closure rates toward the F-14 may occur.

This study discovered that 9.5 degrees of elevator trim change were required as a T-34 wing and tail approached a large wing. A maximum of 4.5 degrees was required for a T-34 as it approached an F-14. There are several issues that account for the relative discrepancy. The test conditions were identical except the AOA of the T-34 wing and tail was arbitrarily chosen at five degrees while the T-34 model AOA was established at one degree. This AOA difference varied the baseline pitching moments used to compute changes in elevator deflection. A case was conducted with the T-34 model at 5 degrees that showed a maximum of 7.5 degrees of elevator trim change was required underneath the F-14. Additionally, the flow disturbances created by the large wing were probably more effective than the F-14 on the T-34 tail. Downwash from the entire span of the large wing could impinge upon the T-34 tail creating a greater nose-up pitching moment. The F-14 fuselage prevented a significant portion of the downwash from interfering with the tail at the given test conditions.

Dissimilar airplanes in formation may experience aerodynamic interference. This phenomenon requires an increased awareness of the pilot to anticipate necessary trim and lift changes. A more thorough understanding of the effect one airplane has on another will increase the safety of formation flying.

B. RECOMMENDATIONS

1. Conduct further studies with complete geometry models. This will enable investigations into the changes in lateral and directional aerodynamic characteristics of formation aircraft. Geometries will not be confined to the XZ plane of symmetry; therefore, typical fleet formations such as parade and inflight refueling can be examined. There may be areas under the F-14 that provide more adverse effects than those revealed in this study.

2. Conduct further studies that include wing loading considerations for each airplane in the formation. This study assumed an F-14 that was "trimmed" in a

modified approach configuration. AOA and loading variations for the F-14 and T-34 were not addressed.

APPENDIX A PMARC/GVS FIGURES

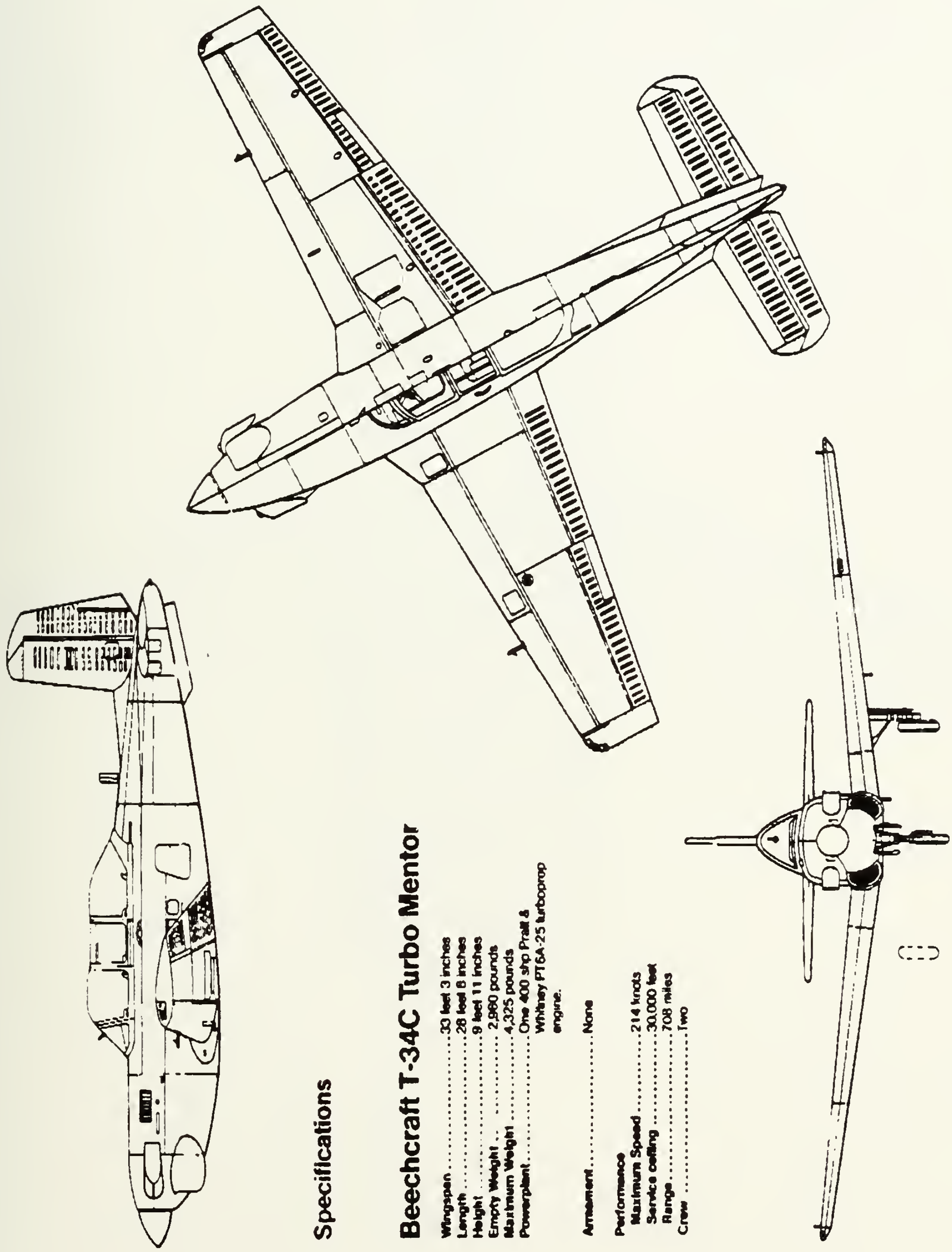

Figure A1 3-View Drawing of T-34

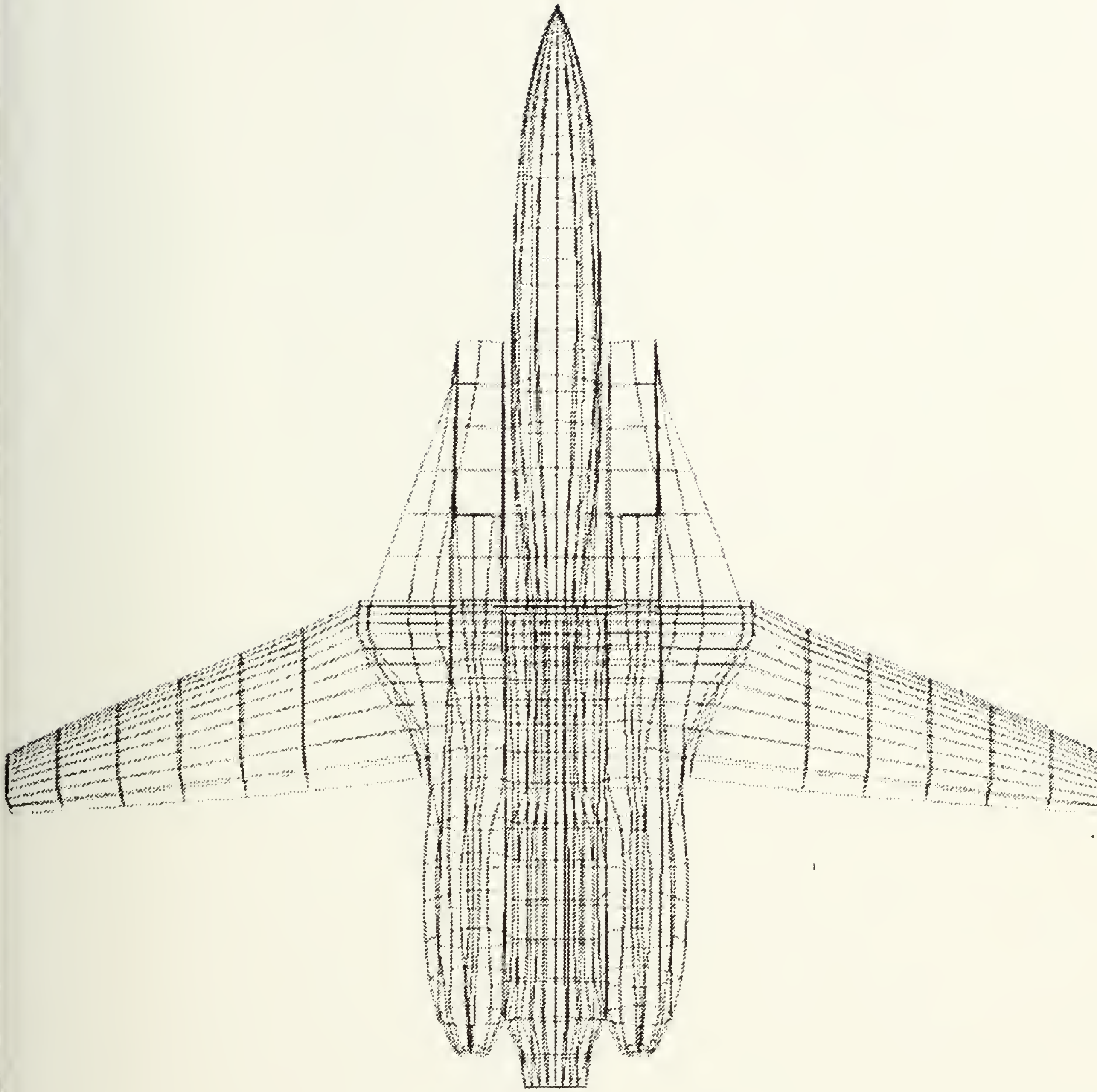

Figure A2 Tailless F-14 (Top View)

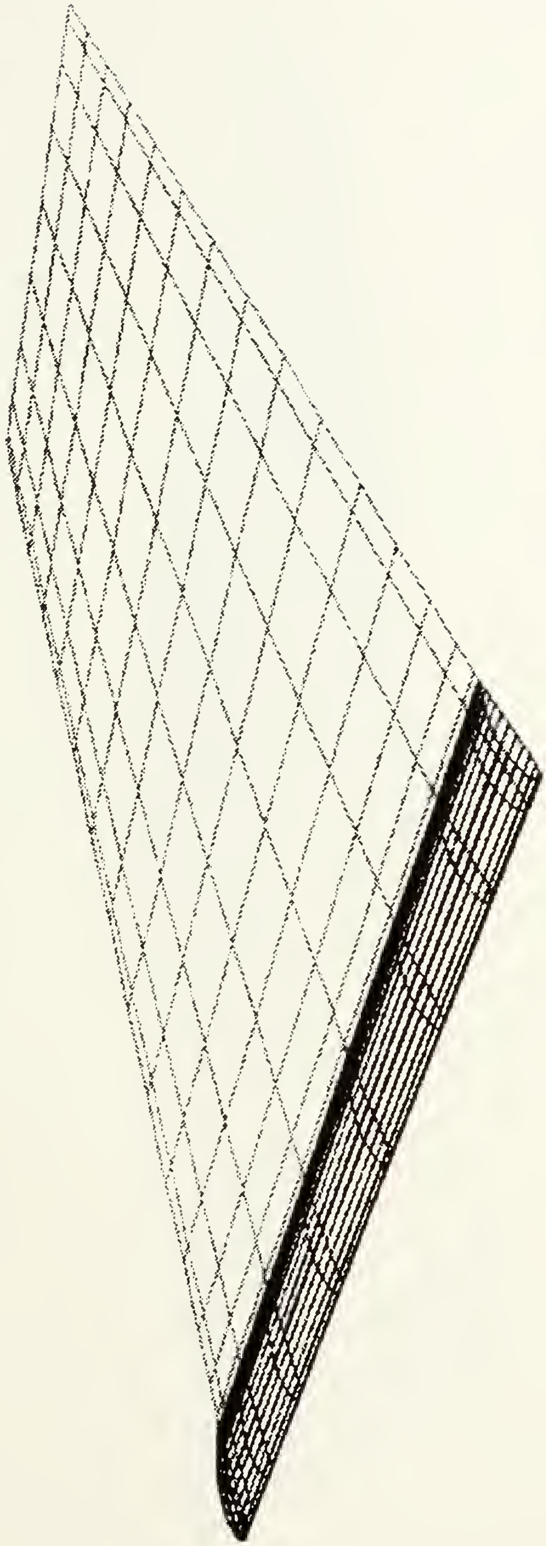

Figure A3 NACA 4415 Wing with Operator Defined Wake

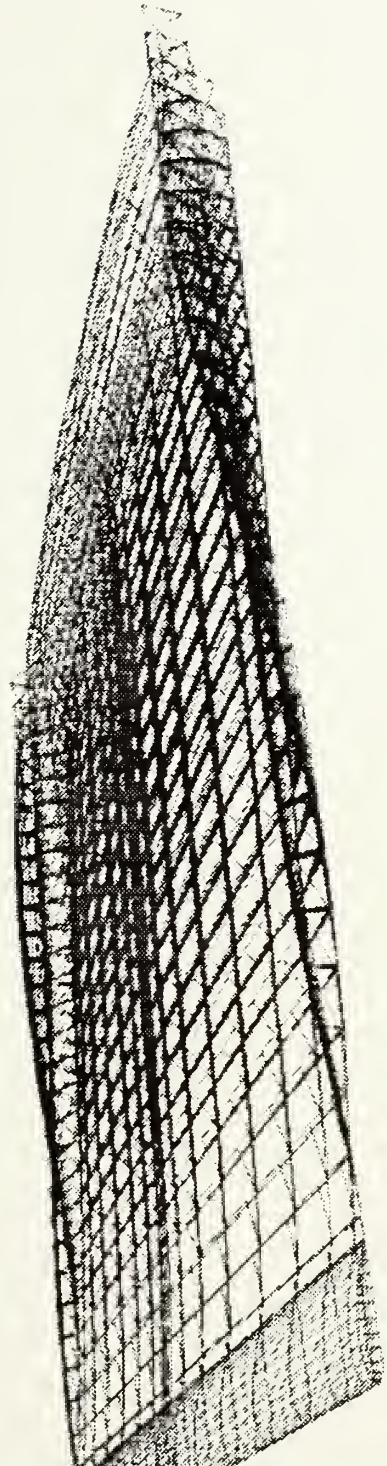

Figure A4 NACA 4415 Wing with PMARC Generated Wake

Figure A5 T-34 Wing and Tail with Streamlines at 5° AOA

Figure A6 T-34 at 1° AOA with Streamlines

Figure A7 F-14 at 11° AOA

Figure A8 Large NACA 4415 Wing with T-34 Wing and Tail

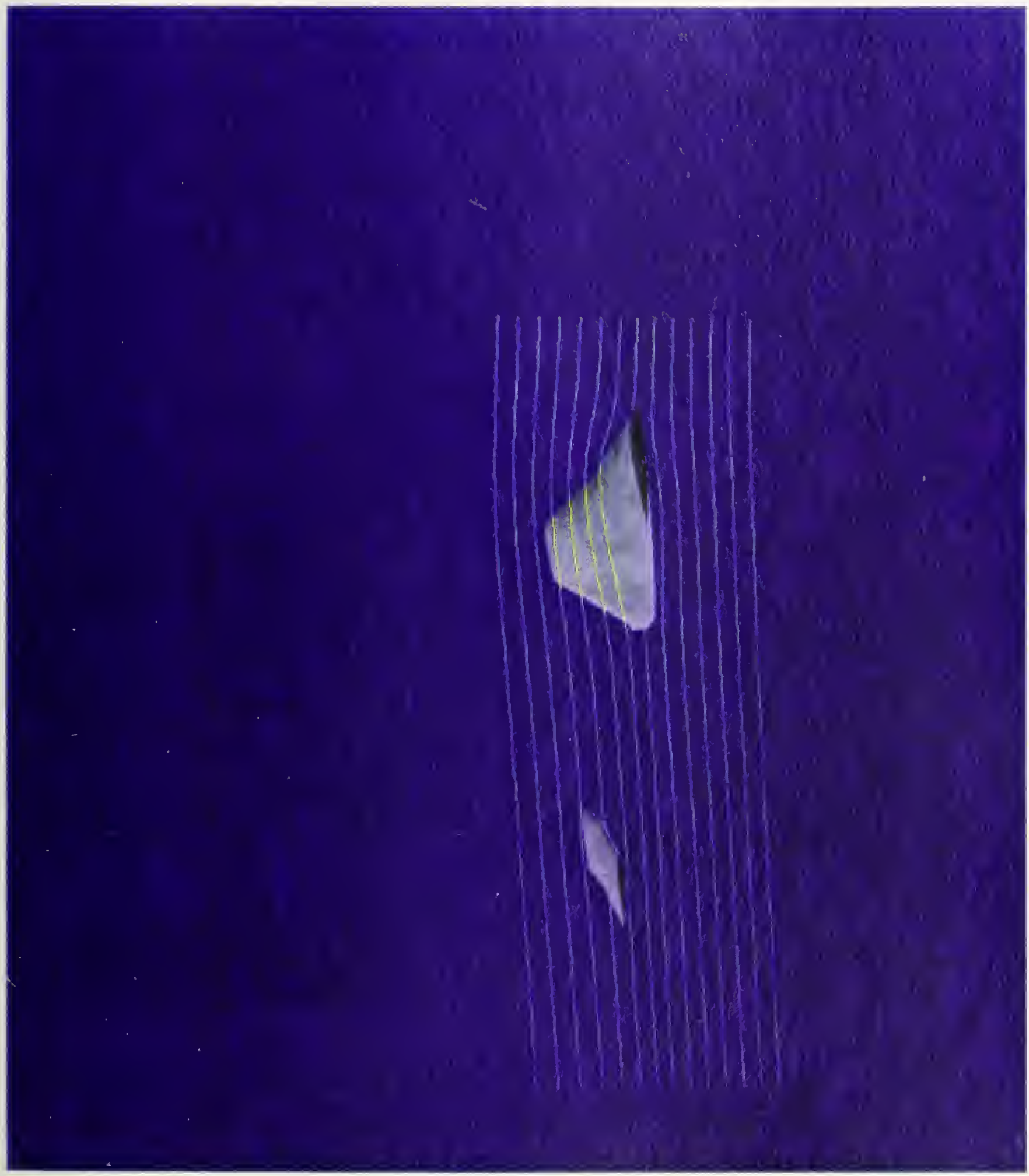

Figure A9 T-34 Wing and Tail Beyond Interference Effects

Figure A10 T-34 Wing and Tail 12.5 Feet Below Large Wing

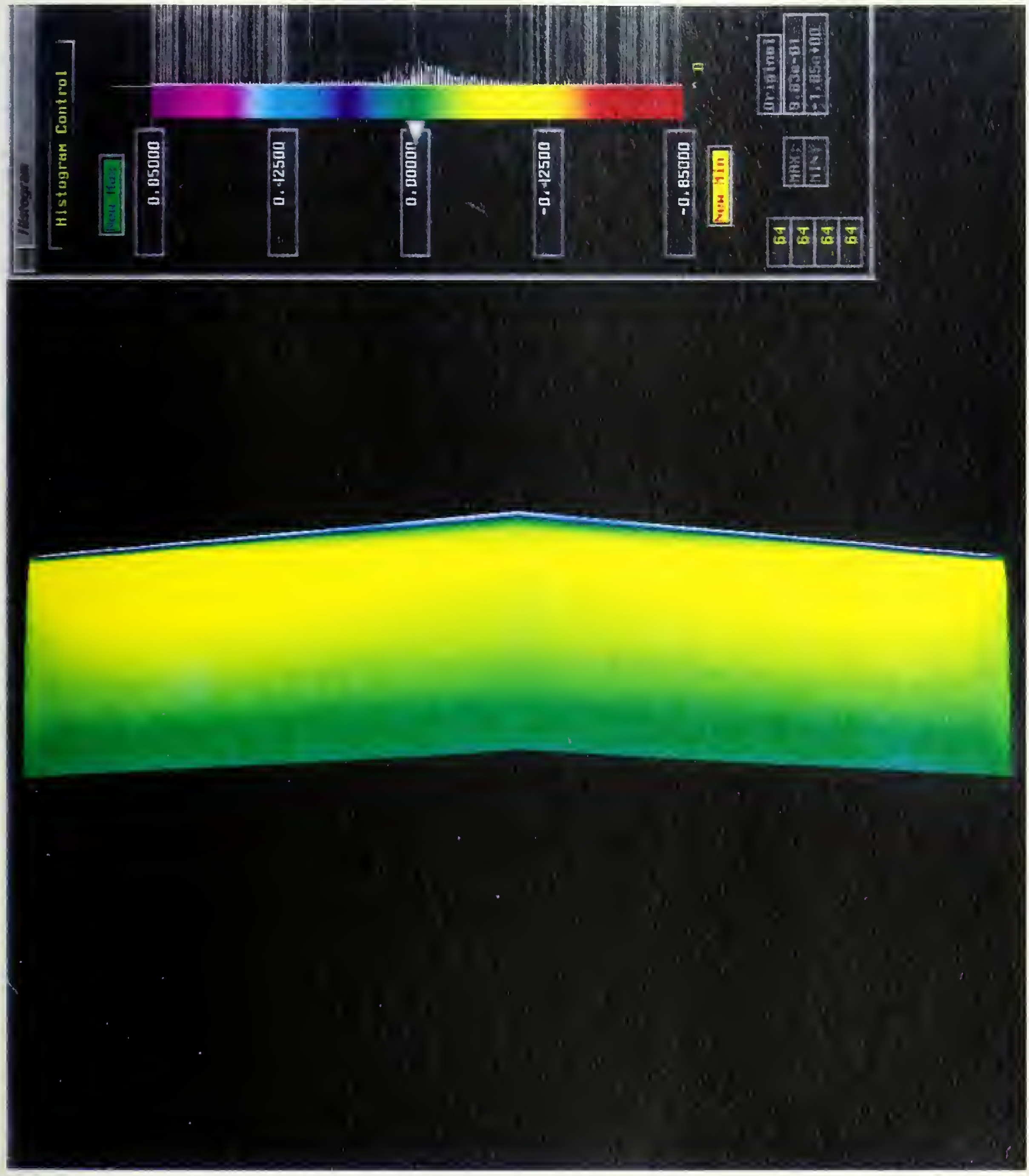

Figure A11 Pressure Coefficients on Bottom Surface of T-34 Tail When Beyond Interference Effects of Other Airplanes

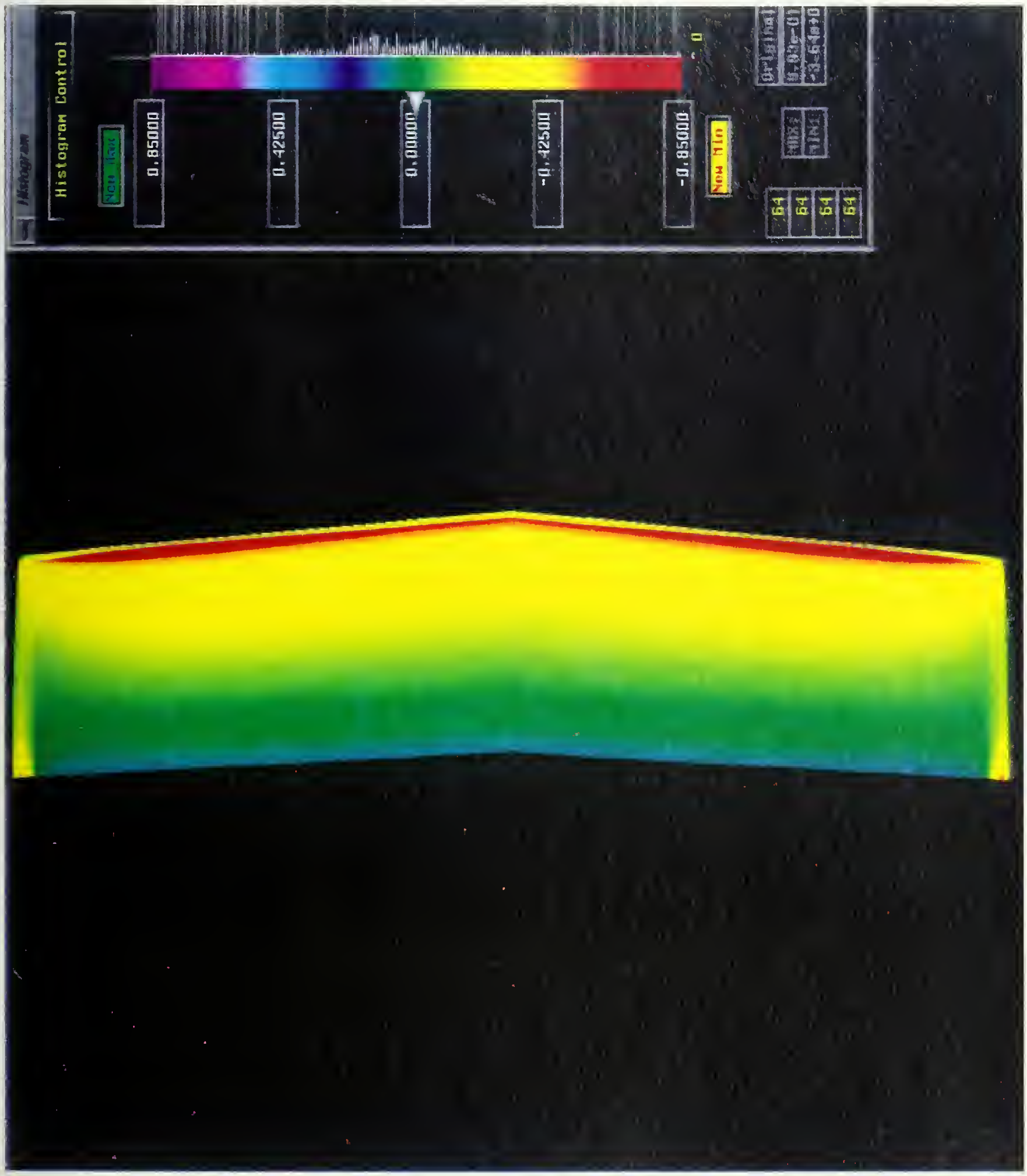

Figure A12 Pressure Coefficients on Bottom Surface of T-34 Tail When 8.33 Feet From Large Wing

Figure A13 F-14 and T-34 in Proximity Test Case

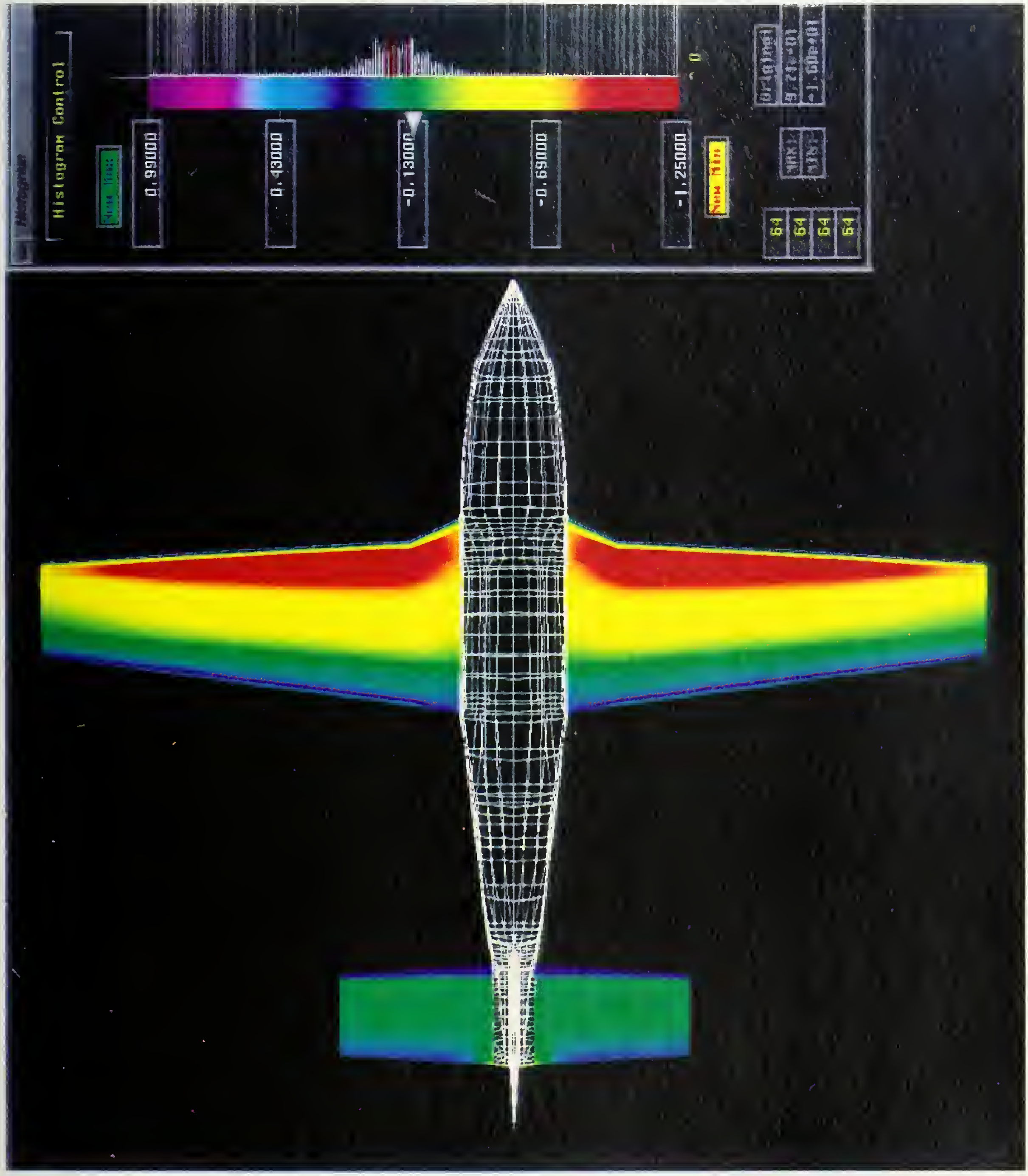

Figure A14 Pressure Coefficients on T-34 Wing and Tail When Beyond Interference Effects of Other Airplanes

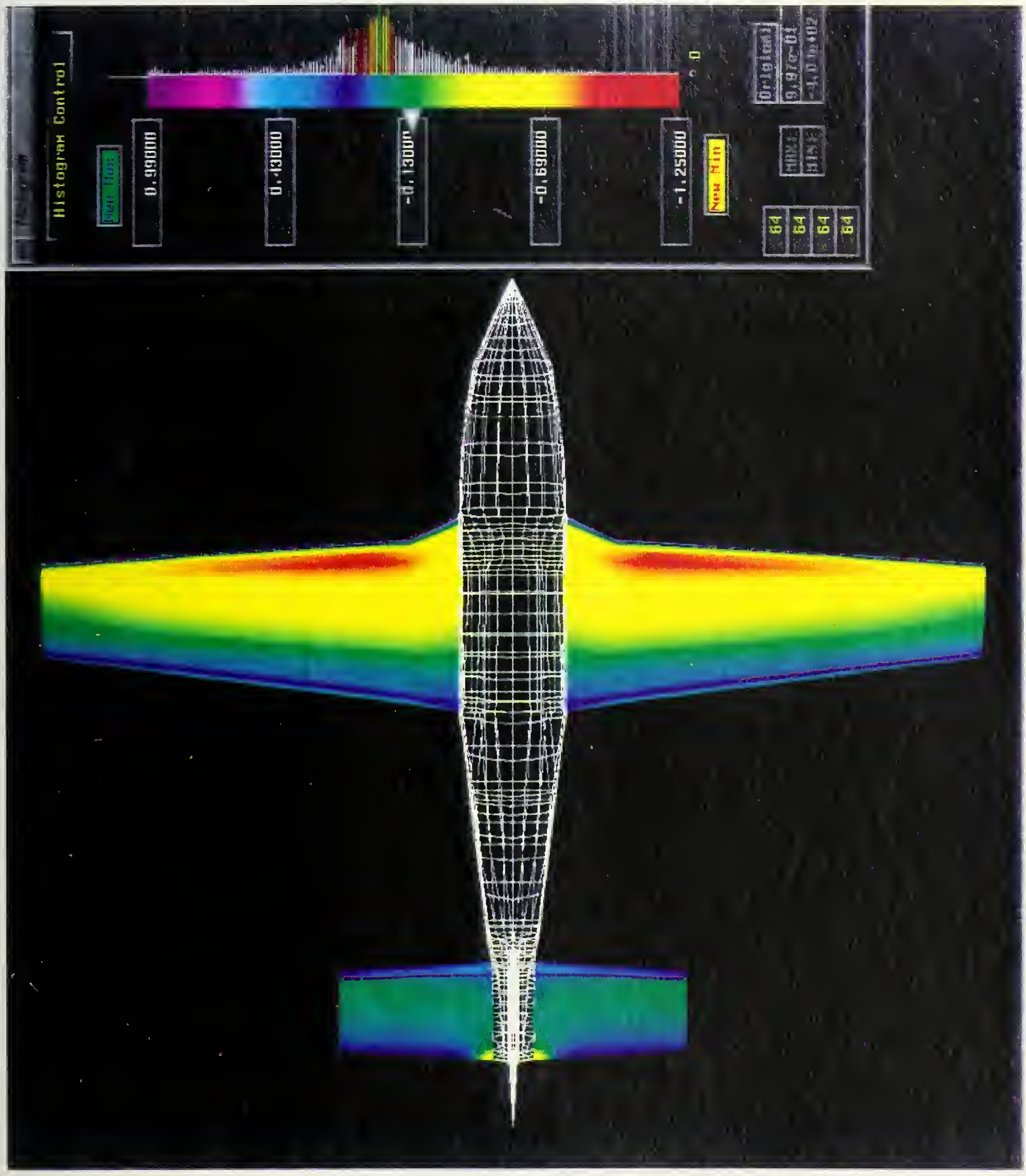

Figure A15 Pressure Coefficients on T-34 Wing and Tail When 37.5 Feet Beneath the F-14

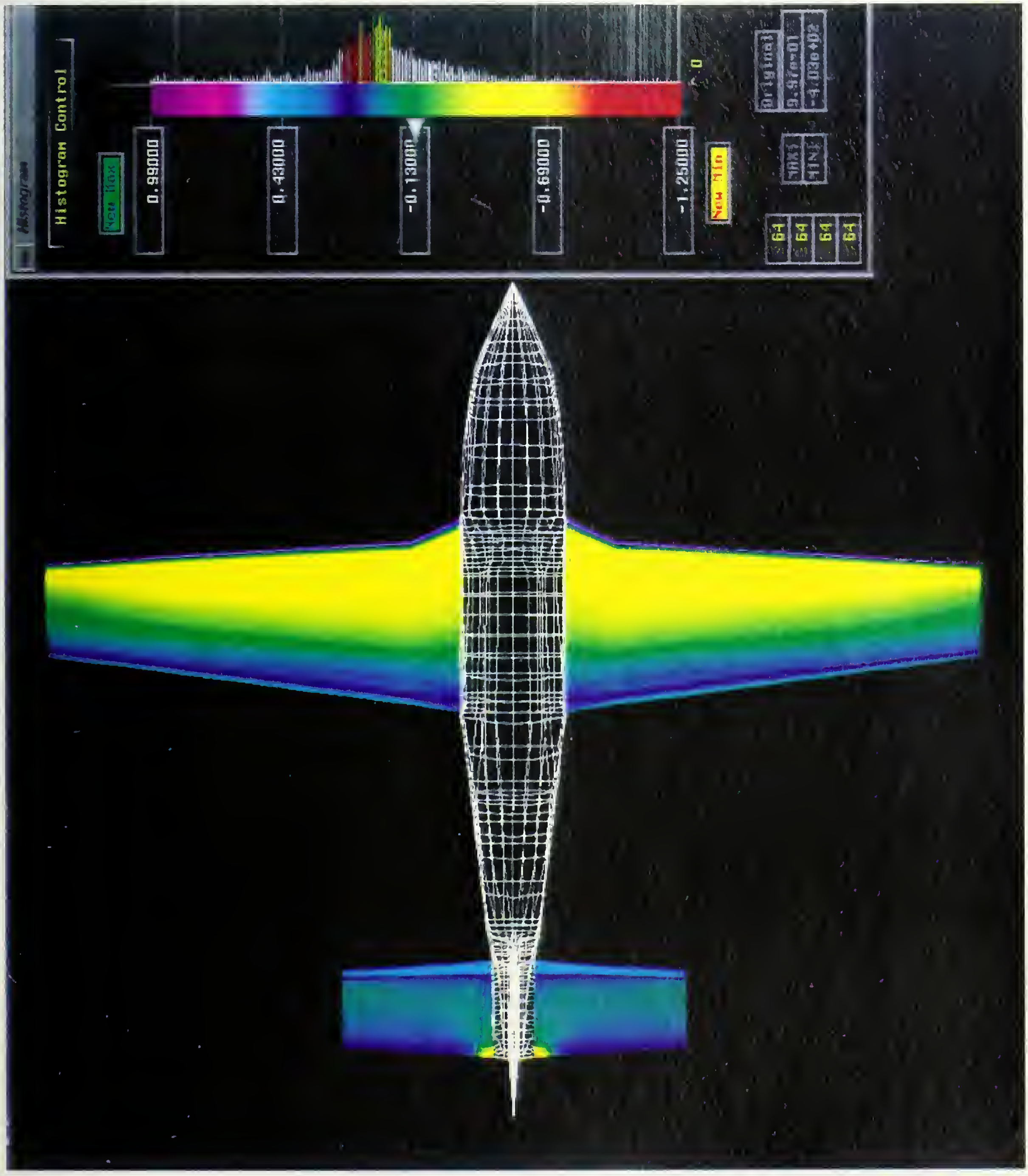

Figure A16 Pressure Coefficients on T-34 Wing and Tail When 25 Feet Beneath the F-14

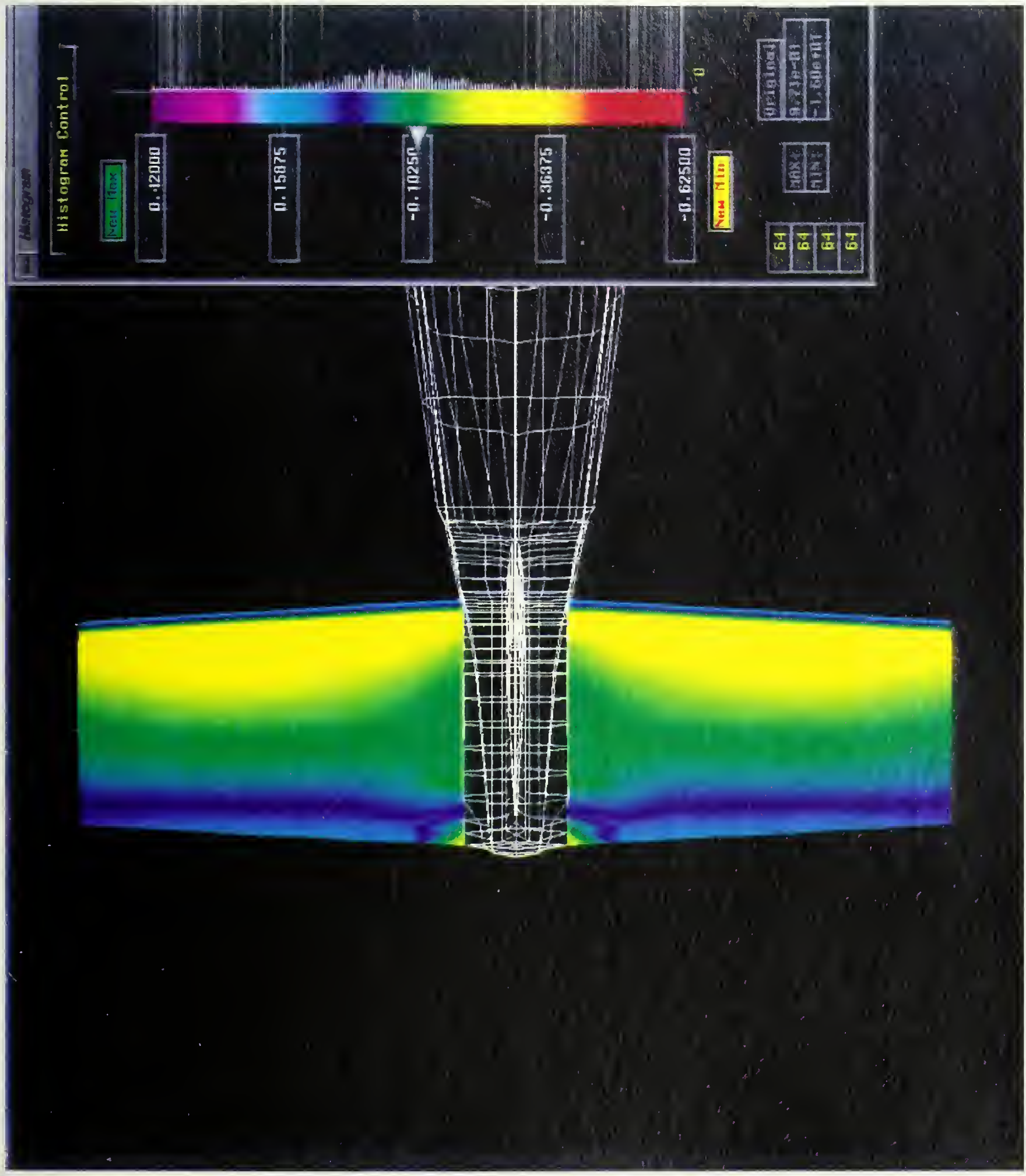

Figure A17 Pressure Coefficients on Bottom Surface of T-34 Tail When Beyond Interference Effects of Other Airplanes

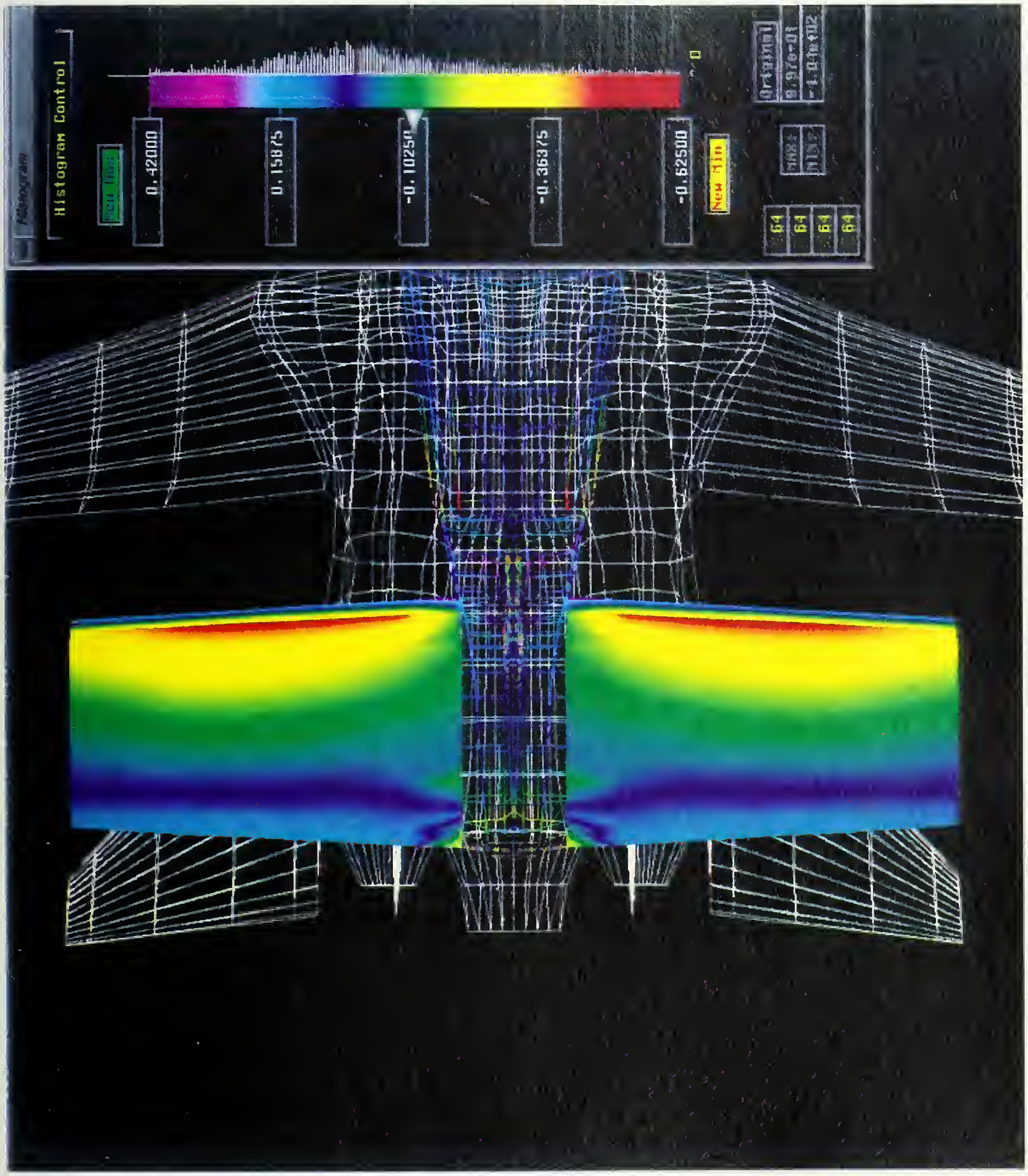

Figure A18 Pressure Coefficients on Bottom Surface of T-34 Tail When 37.5 Feet Beneath the F-14

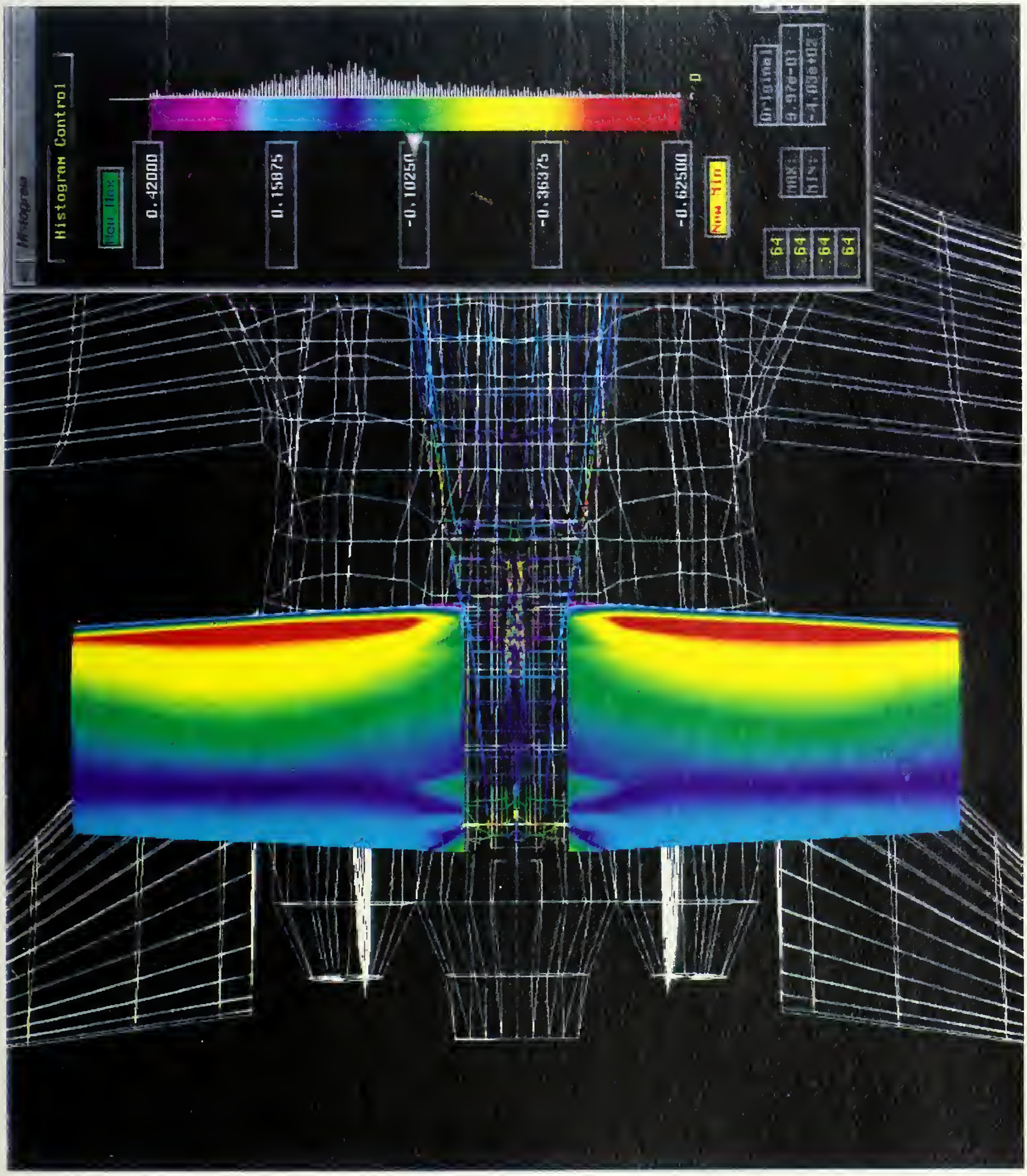

Figure A19 Pressure Coefficients on Bottom Surface of T-34 Tail When 25 Feet Beneath the F-14

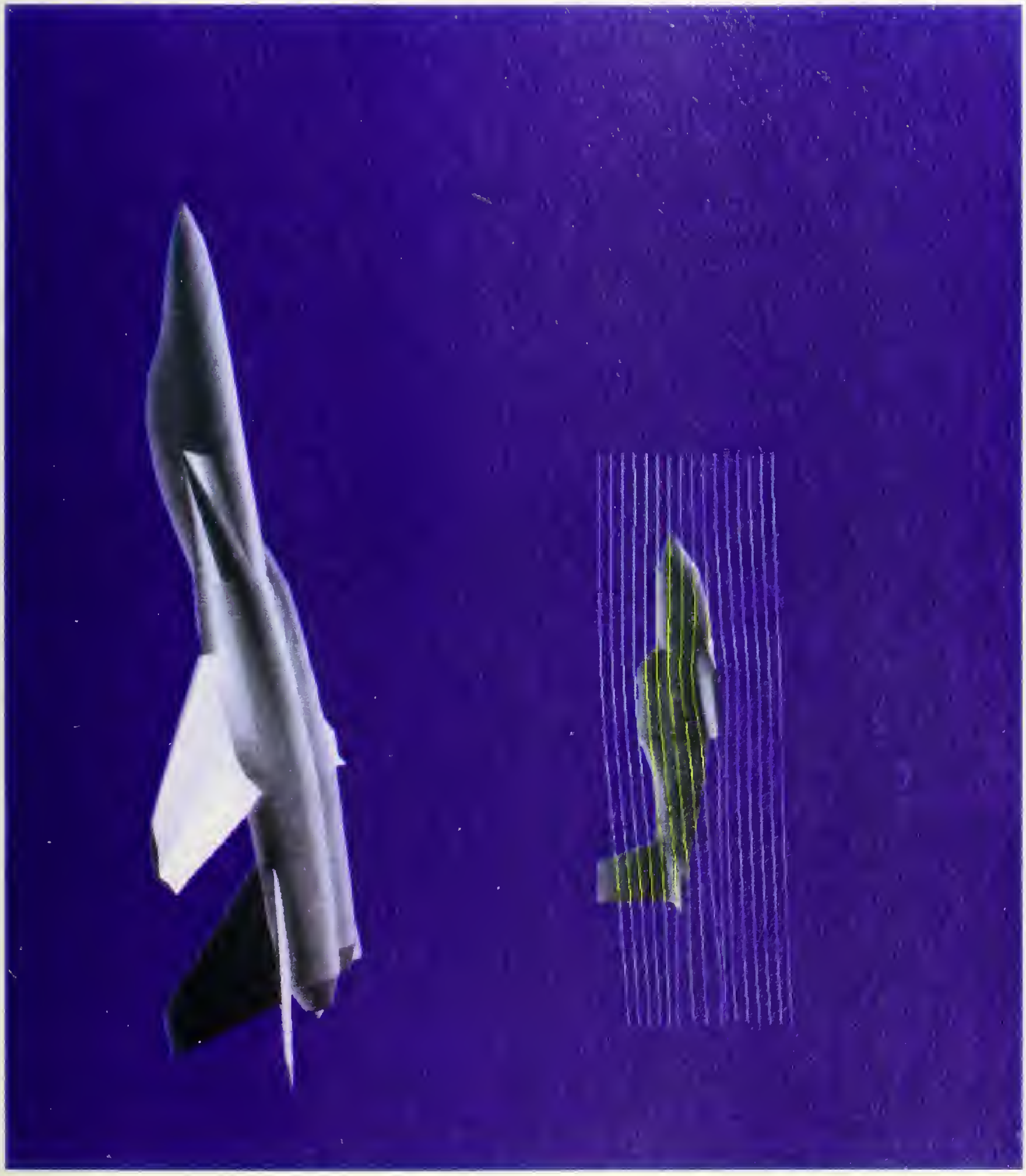

Figure A20 T-34 and Streamlines 33.33 Feet Beneath the F-14

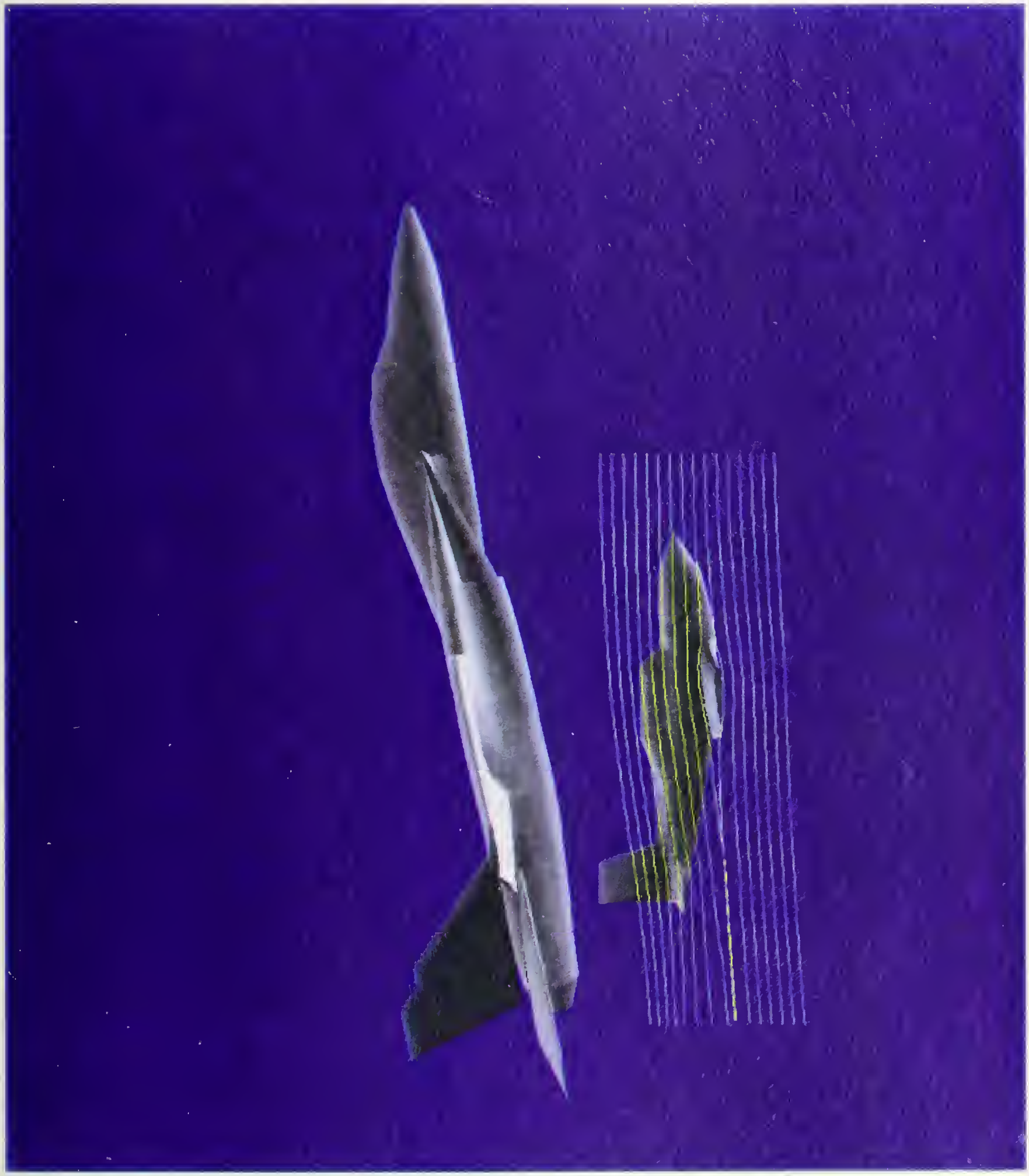

Figure A21 T-34 and Streamlines 16.67 Feet Beneath the F-14

APPENDIX B PMARC F-14/T-34 INPUT

```
F14 AND T34
&BINP2  LSTINP=2,   LSTOUT=1,  LSTFRQ=1,   LENRUN=0,                      &END
&BINP3  LSTGEO=1, LSTNAB=0, LSTWAK=3,  LSTCPV=0, LSTJET=0,                &END
&BINP4  MAXIT=250, SOLRES=0.0005,                                         &END
&BINP5  NTSTPS=1,  DTSTEP=0.5,                                            &END
&BINP6  RSYM=0.0,  RGPR=0.0,  RFF=5.0,  RCORE=0.05,                       &END
&BINP7  VINF=1.0,  VSOUND=1116.0,   UNIT=0,   COMPOP=0.0,                 &END
&BINP8  ALDEG=0.0, YAWDEG=0.0, THEDOT=0.0, PSIDOT=0.0,
        PHIDOT=0.0,                                                       &END
&BINP9   CBAR=65.028,  SREF=25862.4,  SSPAN=200.04,
        RMPX=26.20,   RMPY=0.00,    RMPZ=0.00,                            &END
&BINP10 NORSET=0,     NBCHGE=0,     NCZONE=0,
        NCZPAN=0,     CZDUB=0.0,    VREF=0.0,                             &END
&BINP11 NORPCH=0,     NORF=0,       NORL=0,
        NOCF=0,       NOCL=0,       VNORM=0,                              &END
&BINP12 KPAN=0,       KSIDE=0,      NEWNAB=0,   NEWSID=0,                 &END

&ASEM1  ASEMX=0.00,  ASEMY=0.00,  ASEMZ=0.00,
        ASCAL=1.00,  ATHET=1.00,  NODEA=0,                                &END
&ASEM2  APXX=0.0,    APYY=0.0,    APZZ=0.0,
        AHXX=0.0,    AHYY=1.0,    AHZZ=0.0,                               &END

&ASEM1  ASEMX=0.00,  ASEMY=0.00,  ASEMZ=0.00,
        ASCAL=1.00,  ATHET=1.00,  NODEA=0,                                &END
&ASEM2  APXX=0.0,    APYY=0.0,    APZZ=0.0,
        AHXX=0.0,    AHYY=1.0,    AHZZ=0.0,                               &END

&ASEM1  ASEMX=-511.00,  ASEMY=0.00,   ASEMZ=2004.00,
        ASCAL=1.00,     ATHET=11.00,  NODEA=0,                            &END
&ASEM2  APXX=0.0,       APYY=0.0,     APZZ=0.0,
        AHXX=0.0,       AHYY=1.0,     AHZZ=0.0,                           &END

&ASEM1  ASEMX=-511.00,  ASEMY=0.00,   ASEMZ=2004.00,
        ASCAL=1.00,     ATHET=11.00,  NODEA=5,                            &END
&ASEM2  APXX=0.0,       APYY=0.0,     APZZ=0.0,
        AHXX=0.0,       AHYY=1.0,     AHZZ=0.0,                           &END

&COMP1  COMPX=0.00,     COMPY=0.00,   COMPZ=0.00,
        CSCAL=1.00,     CTHET=0.0,    NODEC=0,                            &END
&COMP2  CPXX=0.0,       CPYY=0.0,     CPZZ=0.0,
        CHXX=0.0,       CHYY=1.0,     CHZZ=0.0,                           &END

&COMP1  COMPX=0.00,     COMPY=0.00,   COMPZ=0.00,
        CSCAL=1.00,     CTHET=0.0,    NODEC=5,                            &END
&COMP2  CPXX=0.0,       CPYY=0.0,     CPZZ=0.0,
        CHXX=0.0,       CHYY=1.0,     CHZZ=0.0,                           &END

&PATCH1 IREV=0,  IDPAT=2,  MAKE=0,  KCOMP=1,  KASS=1,                     &END
 T34 FUSELAGE FORWARD #1
```

```
&SECT1  STX=-99.38, STY=0.00, STZ=0.00, SCALE=1.0,
     ALF=0.0,  THETA=0.0,
     INMODE=4, TNODS=0, TNPS=0, TINTS=0,                    &END
     0.0   0.0   25.388
     0.0   0.0   25.388
     0.0   0.0   25.388
     0.0   0.0   25.388
     0.0   0.0   25.388
     0.0   0.0   25.388
     0.0   0.0   25.388
     0.0   0.0   25.388
     0.0   0.0   25.388
&BPNODE TNODE=3, TNPC=12, TINTC=3,                          &END
&SECT1  STX=-81.359, STY=0.00,  STZ=0.00,  SCALE=1.0,
     ALF=0.0,  THETA=0.00,
     INMODE=4, TNODS=2, TNPS=2, TINTS=0,                    &END
     0.0   0.0     16.926
     0.0   3.238   17.57
     0.0   5.98    19.404
     0.0   7.817   22.15
     0.0   8.462   25.388
     0.0   7.817   28.626
     0.0   5.98    31.371
     0.0   3.238   33.206
     0.0   0.0     33.85
&BPNODE TNODE=3, TNPC=12, TINTC=3,                          &END
&SECT1  STX=-61.7, STY=0.0,  STZ=0.0,   SCALE=1.0,
     ALF=0.0, THETA=0.0,
     INMODE=4, TNODS=2, TNPS=2, TINTS=0,                    &END
     0.0   0.0      5.46
     0.0   12.0     6.0
     0.0   15.8    10.0
     0.0   16.3    15.0
     0.0   16.926  21.84
     0.0   16.5    28.0
     0.0   15.0    34.3
     0.0   10.0    37.5
     0.0   0.0     38.22
&BPNODE TNODE=3, TNPC=12, TINTC=3,                          &END
&SECT1  STX=-44.23, STY=0.0, STZ=0.0,  SCALE=1.0,
     ALF=0.0, THETA=0.0,
     INMODE=4, TNODS=2, TNPS=2, TINTS=0,                    &END
     0.0   0.0      0.0
     0.0   6.0      0.25
     0.0   12.0     0.5
     0.0   17.5     4.0
     0.0   19.4     9.0
     0.0   19.5    14.0
     0.0   19.657  19.11
     0.0   19.4    25.0
     0.0   19.2    31.0
     0.0   17.5    36.4
     0.0   13.0    38.35
     0.0   6.5     38.46
```

```
      0.0    0.0     38.5
&BPNODE TNODE=3, TNPC=12, TINTC=3,                                    &END
&SECT1  STX=-10.375, STY=0.0,  STZ=0.0,  SCALE=1.0,
      ALF=0.0,  THETA=0.0,
      INMODE=4, TNODS=1, TNPS=2, TINTS=0,                             &END
      0.0     0.0     -5.714
      0.0     7.5     -5.1
      0.0     15.0    -4.5
      0.0     20.9     0.0
      0.0     21.9     6.0
      0.0     22.4    11.0
      0.0     22.8    16.38
      0.0     22.4    23.0
      0.0     22.0    30.0
      0.0     19.0    35.0
      0.0     14.5    38.5
      0.0     7.0     39.25
      0.0     0.0     39.77
&BPNODE TNODE=3, TNPC=12, TINTC=3,                                    &END
&SECT1  STX=0.0,  STY=0.0,  STZ=0.0,  SCALE=1.0,
      ALF=0.0,  THETA=0.0,
      INMODE=4, TNODS=3, TNPS=0, TINTS=0,                             &END
      0.0     0.0     -5.714
      0.0     5.5     -5.714
      0.0     10.92   -5.714
      0.0     15.0    -4.5
      0.0     22.93    0.0
      0.0     22.93    8.0
      0.0     22.8    16.38
      0.0     22.4    24.0
      0.0     22.0    30.0
      0.0     19.0    35.0
      0.0     14.5    38.5
      0.0     7.0     39.35
      0.0     0.0     39.77
&BPNODE TNODE=3, TNPC=12, TINTC=3,                                    &END

&PATCH1 IREV=0, IDPAT=1, MAKE=0, KCOMP=1, KASS=1,                     &END
   T34 WING #2
&SECT1  STX=0.0,  STY=22.93,  STZ=0.0,  SCALE=1.0,
      ALF=0.0,  THETA=0.0,
      INMODE=4, TNODS=0, TNPS=0,  TINTS=0,                            &END
      88.457   0.0    0.0
      84.03    0.0   -0.849
      79.61    0.0   -1.513
      70.766   0.0   -2.698
      61.92    0.0   -3.724
      53.07    0.0   -4.591
      44.229   0.0   -5.254
      35.383   0.0   -5.661
      26.537   0.0   -5.714
      22.114   0.0   -5.555
      17.69    0.0   -5.21
      13.269   0.0   -4.679
```

```
      8.846    0.0   -3.954
      6.634    0.0   -3.485
      4.423    0.0   -2.910
      2.21     0.0   -2.123
      1.105    0.0   -1.451
      0.0      0.0    0.0
&BPNODE TNODE=2, TNPC=15,  TINTC=0,                                  &END
      0.0      0.0    0.0
      1.105    0.0    3.176
      2.21     0.0    4.175
      4.423    0.0    5.511
      6.634    0.0    6.431
      8.846    0.0    7.112
      13.269   0.0    7.935
      17.69    0.0    8.315
      22.114   0.0    8.465
      26.537   0.0    8.448
      35.383   0.0    8.023
      44.229   0.0    7.236
      53.07    0.0    6.183
      61.92    0.0    4.918
      70.766   0.0    2.609
      79.61    0.0    1.911
      84.03    0.0    1.053
      88.457   0.0    0.0
&BPNODE TNODE=3, TNPC=15, TINTC=0,                                   &END
&SECT1  STX=10.92, STY=45.87, STZ=2.1, SCALE=.84
      ALF=4.0, THETA=0.0,
      INMODE=0, TNODS=2, TNPS=0, TINTS=3,                            &END
&SECT1  STX=21.84, STY=202.0, STZ=22.0, SCALE=1.0,
      ALF=1.0, THETA=0.0,
      INMODE=4, TNODS=3, TNPS=10, TINTS=3,                           &END
      41.0     0.0    0.0
      38.95    0.0   -0.287
      36.9     0.0   -0.5
      32.8     0.0   -0.886
      28.7     0.0   -1.23
      24.6     0.0   -1.505
      20.5     0.0   -1.71
      16.4     0.0   -1.837
      12.3     0.0   -1.83
      10.25    0.0   -1.755
      8.2      0.0   -1.63
      6.15     0.0   -1.44
      4.1      0.0   -1.197
      3.08     0.0   -1.07
      2.05     0.0   -0.93
      1.03     0.0   -0.70
      0.51     0.0   -0.50
      0.0      0.0    0.0
&BPNODE TNODE=2, TNPC=15,  TINTC=0,                                  &END
      0.0      0.0    0.0
      0.51     0.0    1.09
      1.03     0.0    1.48
```

```
        2.05   0.0   2.01
        3.08   0.0   2.38
        4.10   0.0   2.64
        6.15   0.0   2.95
        8.2    0.0   3.08
        10.25  0.0   3.116
        12.3   0.0   3.096
        16.4   0.0   2.93
        20.5   0.0   2.63
        24.6   0.0   2.24
        28.7   0.0   1.79
        32.8   0.0   1.26
        36.9   0.0   0.69
        38.95  0.0   0.38
        41.0   0.0   0.0
&BPNODE TNODE=3, TNPC=15, TINTC=0,                                    &END

&PATCH1 IREV=0, IDPAT=1, MAKE=2, KCOMP=1, KASS=2,                     &END
  T34 WING TIP #3
&PATCH2 ITYP=1, TNODS=3, TNPS=2, TINTS=0, NPTTIP=0,                   &END

&PATCH1 IREV=0, IDPAT=2, MAKE=0, KCOMP=1, KASS=1,                     &END
  T34 FUSELAGE UNDER WING #4
&SECT1 STX=0.0, STY=0.0, STZ=0.0, SCALE=1.0,
      ALF=0.0, THETA=0.0,
      INMODE=4, TNODS=0, TNPS=0, TINTS=0,                             &END
        0.0     0.0   -5.714
        0.0    10.92  -5.714
        0.0    15.0   -5.5
        0.0    22.93   0.0
&BPNODE TNODE=3, TNPC=0, TINTC=0,                                     &END
&SECT1 STX=0.0, STY=0.0, STZ=0.0, SCALE=1.0,
      ALF=0.0, THETA=0.0,
      INMODE=4, TNODS=0, TNPS=3, TINTS=0,                             &END
        6.634   0.0   -5.714
        6.634  10.92  -5.714
        6.634  18.57  -5.714
        6.634  22.93  -3.485
&BPNODE TNODE=3, TNPC=0, TINTC=0,                                     &END
&SECT1 STX=0.0, STY=0.0, STZ=0.0, SCALE=1.0,
      ALF=0.0, THETA=0.0,
      INMODE=4, TNODS=0, TNPS=0, TINTS=0,                             &END
        8.846   0.0   -5.714
        8.846  10.92  -5.714
        8.846  18.57  -5.714
        8.846  22.93  -3.954
&BPNODE TNODE=3, TNPC=0, TINTC=0,                                     &END
&SECT1 STX=0.0, STY=0.0, STZ=0.0, SCALE=1.0,
      ALF=0.0, THETA=0.0,
      INMODE=4, TNODS=0, TNPS=0, TINTS=0,                             &END
        13.269   0.0   -5.714
        13.269  10.92  -5.714
        13.269  18.57  -5.174
        13.269  22.93  -4.679
```

```
&BPNODE TNODE=3, TNPC=0, TINTC=0,                    &END
&SECT1 STX=0.0, STY=0.0, STZ=0.0, SCALE=1.0,
    ALF=0.0, THETA=0.0,
    INMODE=4, TNODS=0, TNPS=0, TINTS=0,              &END
    17.69    0.0   -5.714
    17.69   10.92  -5.714
    17.69   18.57  -5.714
    17.69   22.93  -5.21
&BPNODE TNODE=3, TNPC=0, TINTC=0,                    &END
&SECT1 STX=0.0, STY=0.0, STZ=0.0, SCALE=1.0,
    ALF=0.0, THETA=0.0,
    INMODE=4, TNODS=0, TNPS=0, TINTS=0,              &END
    22.114   0.0   -5.714
    22.114  10.92  -5.714
    22.114  18.57  -5.714
    22.114  22.93  -5.555
&BPNODE TNODE=3, TNPC=0, TINTC=0,                    &END
&SECT1 STX=0.0, STY=0.0, STZ=0.0, SCALE=1.0,
    ALF=0.0, THETA=0.0,
    INMODE=4, TNODS=0, TNPS=0, TINTS=0,              &END
    26.537   0.0   -5.714
    26.537  10.92  -5.714
    26.537  18.57  -5.714
    26.537  22.93  -5.714
&BPNODE TNODE=3, TNPC=0, TINTC=0,                    &END
&SECT1 STX=0.0, STY=0.0, STZ=0.0, SCALE=1.0,
    ALF=0.0, THETA=0.0,
    INMODE=4, TNODS=0, TNPS=0, TINTS=0,              &END
    35.383   0.0   -5.661
    35.383  10.92  -5.661
    35.383  18.57  -5.661
    35.383  22.93  -5.661
&BPNODE TNODE=3, TNPC=0, TINTC=0,                    &END
&SECT1 STX=0.0, STY=0.0, STZ=0.0, SCALE=1.0,
    ALF=0.0, THETA=0.0,
    INMODE=4, TNODS=0, TNPS=0, TINTS=0,              &END
    44.229   0.0   -5.254
    44.229  10.92  -5.254
    44.229  18.57  -5.254
    44.229  22.93  -5.254
&BPNODE TNODE=3, TNPC=0, TINTC=0,                    &END
&SECT1 STX=0.0, STY=0.0, STZ=0.0, SCALE=1.0,
    ALF=0.0, THETA=0.0,
    INMODE=4, TNODS=0, TNPS=0, TINTS=0,              &END
    53.07    0.0   -4.591
    53.07   10.92  -4.591
    53.07   18.57  -4.591
    53.07   22.93  -4.591
&BPNODE TNODE=3, TNPC=0, TINTC=0,                    &END
&SECT1 STX=0.0, STY=0.0, STZ=0.0, SCALE=1.0,
    ALF=0.0, THETA=0.0,
    INMODE=4, TNODS=0, TNPS=0, TINTS=0,              &END
    61.92    0.0   -3.724
    61.92   10.92  -3.724
```

```
     61.92    18.57  -3.724
     61.92    22.93  -3.724
&BPNODE TNODE=3, TNPC=0, TINTC=0,                                &END
&SECT1 STX=0.0, STY=0.0, STZ=0.0, SCALE=1.0,
     ALF=0.0, THETA=0.0,
     INMODE=4, TNODS=0, TNPS=0, TINTS=0,                         &END
     70.766    0.0   -2.698
     70.766   10.92  -2.698
     70.766   18.57  -2.698
     70.766   22.93  -2.698
&BPNODE TNODE=3, TNPC=0, TINTC=0,                                &END
&SECT1 STX=0.0, STY=0.0, STZ=0.0, SCALE=1.0,
     ALF=0.0, THETA=0.0,
     INMODE=4, TNODS=0, TNPS=0, TINTS=0,                         &END
     79.61     0.0   -1.513
     79.61    10.92  -1.513
     79.61    18.57  -1.513
     79.61    22.93  -1.513
&BPNODE TNODE=3, TNPC=0, TINTC=0,                                &END
&SECT1 STX=0.0, STY=0.0, STZ=0.0, SCALE=1.0,
     ALF=0.0, THETA=0.0,
     INMODE=4, TNODS=0, TNPS=0, TINTS=0,                         &END
     84.03     0.0   -0.849
     84.03    10.92  -0.849
     84.03    18.57  -0.849
     84.03    22.93  -0.849
&BPNODE TNODE=3, TNPC=0, TINTC=0,                                &END
&SECT1 STX=0.0, STY=0.0, STZ=0.0, SCALE=1.0,
     ALF=0.0, THETA=0.0,
     INMODE=4, TNODS=3, TNPS=0, TINTS=0,                         &END
     88.457    0.0    0.0
     88.457   10.92   0.0
     88.457   18.57   0.0
     88.457   22.93   0.0
&BPNODE TNODE=3, TNPC=0, TINTC=0,                                &END

&PATCH1 IREV=0, IDPAT=2, MAKE=0, KCOMP=1, KASS=1,                &END
 T34 UPPER MIDDLE FUSELAGE #5
&SECT1 STX=0.0, STY=0.0, STZ=0.0, SCALE=1.0,
     ALF=0.0, THETA=0.0,
     INMODE=4, TNODS=0, TNPS=0, TINTS=0,                         &END
      0.0     22.93   0.0
      0.0     22.93  13.1
      0.0     22.38  16.38
      0.0     22.0   30.0
      0.0     20.0   36.0
      0.0     14.5   39.0
      0.0      0.0   39.77
&BPNODE TNODE=3, TNPC=9, TINTC=3,                                &END
&SECT1 STX=0.0, STY=0.0, STZ=0.0, SCALE=1.0,
     ALF=0.0, THETA=0.0,
     INMODE=4, TNODS=0, TNPS=3, TINTS=0,                         &END
      6.634   22.93   6.431
      6.634   22.93  25.1
```

```
        6.634    21.00  32.22
        6.634     6.55  39.9
        6.634     4.0   40.0
        6.634     2.0   41.0
        6.634     0.0   41.498
 &BPNODE TNODE=3, TNPC=9, TINTC=3,                          &END
 &SECT1 STX=0.0, STY=0.0, STZ=0.0, SCALE=1.0,
       ALF=0.0, THETA=0.0,
       INMODE=4, TNODS=0, TNPS=0, TINTS=0,                  &END
        8.846    22.93  7.112
        8.846    22.93  25.1
        8.846    21.00  32.22
        8.846    11.47  36.58
        8.846     6.0   41.498
        8.846     2.0   43.136
        8.846     0.0   44.775
 &BPNODE TNODE=3, TNPC=9, TINTC=3,                          &END
 &SECT1 STX=0.0, STY=0.0, STZ=0.0, SCALE=1.0,
       ALF=0.0, THETA=0.0,
       INMODE=4, TNODS=0, TNPS=0, TINTS=0,                  &END
       13.269    22.93   7.935
       13.269    22.93  25.1
       13.269    21.00  32.22
       13.269    14.46  36.038
       13.269     6.0   43.68
       13.269     2.0   46.96
       13.269     0.0   49.416
 &BPNODE TNODE=3, TNPC=9, TINTC=3,                          &END
 &SECT1 STX=0.0, STY=0.0, STZ=0.0, SCALE=1.0,
       ALF=0.0, THETA=0.0,
       INMODE=4, TNODS=0, TNPS=0, TINTS=0,                  &END
       17.69     22.93   8.315
       17.69     22.93  25.1
       17.69     21.00  32.22
       17.69     15.28  36.038
       17.69      6.5   48.05
       17.69      2.0   51.6
       17.69      0.0   54.0
 &BPNODE TNODE=3, TNPC=9, TINTC=3,                          &END
 &SECT1 STX=0.0, STY=0.0, STZ=0.0, SCALE=1.0,
       ALF=0.0, THETA=0.0,
       INMODE=4, TNODS=0, TNPS=0, TINTS=0,                  &END
       22.114    22.93   8.465
       22.114    22.93  25.1
       22.114    21.00  32.22
       22.114    15.28  36.038
       22.114     7.0   49.69
       22.114     2.0   53.51
       22.114     0.0   56.79
 &BPNODE TNODE=3, TNPC=9, TINTC=3,                          &END
 &SECT1 STX=0.0, STY=0.0, STZ=0.0, SCALE=1.0,
       ALF=0.0, THETA=0.0,
       INMODE=4, TNODS=0, TNPS=0, TINTS=0,                  &END
       26.537    22.93   8.448
```

```
     26.537    22.93  25.1
     26.537    21.00  32.22
     26.537    15.28  36.038
     26.537     8.5   55.15
     26.537     2.0   57.33
     26.537     0.0   58.97
&BPNODE TNODE=3, TNPC=9, TINTC=3,                               &END
&SECT1 STX=0.0, STY=0.0, STZ=0.0, SCALE=1.0,
     ALF=0.0, THETA=0.0,
     INMODE=4, TNODS=0, TNPS=0, TINTS=0,                        &END
     35.383    22.93  8.023
     35.383    22.93  25.1
     35.383    21.00  32.22
     35.383    15.28  36.038
     35.383     9.0   55.15
     35.383     2.0   57.33
     35.383     0.0   58.97
&BPNODE TNODE=3, TNPC=9, TINTC=3,                               &END
&SECT1 STX=0.0, STY=0.0, STZ=0.0, SCALE=1.0,
     ALF=0.0, THETA=0.0,
     INMODE=4, TNODS=0, TNPS=0, TINTS=0,                        &END
     44.229    22.93  7.236
     44.229    22.93  25.1
     44.229    21.00  32.22
     44.229    15.28  36.038
     44.229     9.0   55.15
     44.229     2.0   57.33
     44.229     0.0   58.97
&BPNODE TNODE=3, TNPC=9, TINTC=3,                               &END
&SECT1 STX=0.0, STY=0.0, STZ=0.0, SCALE=1.0,
     ALF=0.0, THETA=0.0,
     INMODE=4, TNODS=0, TNPS=0, TINTS=0,                        &END
     53.07     22.93   6.183
     53.07     22.93  25.1
     53.07     21.00  32.22
     53.07     15.28  36.038
     53.07      9.0   55.15
     53.07      2.0   57.33
     53.07      0.0   58.97
&BPNODE TNODE=3, TNPC=9, TINTC=3,                               &END
&SECT1 STX=0.0, STY=0.0, STZ=0.0, SCALE=1.0,
     ALF=0.0, THETA=0.0,
     INMODE=4, TNODS=0, TNPS=0, TINTS=0,                        &END
     61.92     22.93  4.918
     61.92     22.93  25.1
     61.92     21.00  32.22
     61.92     15.28  36.038
     61.92      9.0   55.15
     61.92      2.0   57.33
     61.92      0.0   58.97
&BPNODE TNODE=3, TNPC=9, TINTC=3,                               &END
&SECT1 STX=0.0, STY=0.0, STZ=0.0, SCALE=1.0,
     ALF=0.0, THETA=0.0,
     INMODE=4, TNODS=0, TNPS=0, TINTS=0,                        &END
```

```
        70.766    22.93    2.609
        70.766    22.93   25.1
        70.766    21.00   32.22
        70.766    15.28   36.038
        70.766     9.0    55.15
        70.766     2.0    57.33
        70.766     0.0    58.97
&BPNODE TNODE=3, TNPC=9, TINTC=3,                               &END
&SECT1 STX=0.0, STY=0.0, STZ=0.0, SCALE=1.0,
        ALF=0.0, THETA=0.0,
        INMODE=4, TNODS=0, TNPS=0, TINTS=0,                     &END
        79.61    22.93    1.911
        79.61    22.93   25.1
        79.61    21.00   32.22
        79.61    15.28   36.038
        79.61     9.0    55.15
        79.61     2.0    57.33
        79.61     0.0    58.97
&BPNODE TNODE=3, TNPC=9, TINTC=3,                               &END
&SECT1 STX=0.0, STY=0.0, STZ=0.0, SCALE=1.0,
        ALF=0.0, THETA=0.0,
        INMODE=4, TNODS=0, TNPS=0, TINTS=0.                     &END
        84.03    22.93    1.053
        84.03    22.93   25.1
        84.03    21.00   32.22
        84.03    15.28   36.038
        84.03     9.0    55.15
        84.03     2.0    57.33
        84.03     0.0    58.97
&BPNODE TNODE=3, TNPC=9, TINTC=3.                               &END
&SECT1 STX=0.0, STY=0.0, STZ=0.0, SCALE=1.0,
        ALF=0.0, THETA=0.0,
        INMODE=4, TNODS=3, TNPS=0, TINTS=0,                     &END
        88.457    22.93    0.0
        88.457    22.93    5.0
        88.457    22.93   10.0
        88.457    22.93   15.0
        88.457    22.93   20.0
        88.457    22.93   25.1
        88.457    21.00   32.22
        88.457    15.28   36.038
        88.457     9.0    55.15
        88.457     2.0    57.33
        88.457     0.0    58.97
&BPNODE TNODE=3, TNPC=9, TINTC=3,                               &END

&PATCH1 IREV=0, IDPAT=2, MAKE=0, KCOMP=1, KASS=1,               &END
  T34 AFT FUESELAGE #6
&SECT1  STX=0.0, STY=0.0, STZ=0.0, SCALE=1.0,
        ALF=0.0, THETA=0.0,
        INMODE=4, TNODS=0, TNPS=0, TINTS=0,                     &END
        88.457     0.0     0.0
        88.457    10.92    0.0
        88.457    18.57    0.0
```

```
        88.457   22.93   0.0
        88.457   22.93   5.0
        88.457   22.93  10.0
        88.457   22.93  15.0
        88.547   22.93  20.0
        88.457   22.93  25.1
        88.457   18.0   34.0
        88.457   15.28  36.038
        88.457    9.0   55.15
        88.457    4.0   57.33
        88.457    0.0   58.97
&BPNODE TNODE=3, TNPC=12, TINTC=3,                          &END
&SECT1  STX=0.0, STY=0.0, STZ=0.0, SCALE=1.0,
        ALF=0.0, THETA=0.0,
        INMODE=4, TNODS=2, TNPS=2, TINTS=3,                 &END
       119.58     0.0    2.73
       119.58    10.92   2.73
       119.58    18.02   2.73
       119.58    18.02  21.30
       119.58    18.02  33.85
       119.58    14.74  39.31
       119.58    10.92  43.00
       119.58     0.0   48.05
&BPNODE TNODE=3, TNPC=12, TINTC=3,                          &END
&SECT1  STX=0.0, STY=0.0, STZ=0.0, SCALE=1.0,
        ALF=0.0, THETA=0.0,
        INMODE=4, TNODS=2, TNPS=2, TINTS=3,                 &END
       127.77     0.0   4.37
       127.77    10.92  4.37
       127.77    16.93  4.37
       127.77    16.93  21.3
       127.77    16.93  33.85
       127.77    14.74  39.31
       127.77    10.37  42.04
       127.77     0.0   45.87
&BPNODE TNODE=3, TNPC=12, TINTC=3,                          &END
&SECT1  STX=0.0, STY=0.0, STZ=0.0, SCALE=1.0,
        ALF=0.0, THETA=0.0,
        INMODE=4, TNODS=2, TNPS=2, TINTS=3,                 &END
       146.88     0.0   7.64
       146.88    10.92  7.64
       146.88    14.74  7.64
       146.88    14.74  21.3
       146.88    14.74  33.85
       146.88    13.00  38.5
       146.88     8.74  40.41
       146.88     0.0   44.22
&BPNODE TNODE=3, TNPC=12, TINTC=3,                          &END
&SECT1  STX=0.0, STY=0.0, STZ=0.0, SCALE=1.0,
        ALF=0.0, THETA=0.0,
        INMODE=4, TNODS=2, TNPS=2, TINTS=3,                 &END
       179.64     0.0   13.3
       179.64     3.0   13.3
       179.64     7.00  13.3
```

```
      179.64     10.0   13.3
      179.64     11.3   13.3
      179.64     11.3   21.3
      179.64     11.3   27.84
      179.64     11.3   32.21
      179.64      5.46  38.22
      179.64      2.27  40.41
      179.64      0.0   46.96
&BPNODE  TNODE=3,  TNPC=12,  TINTC=3,                                   &END
&SECT1   STX=0.0,  STY=0.0,  STZ=0.0,  SCALE=1.0,
       ALF=0.0,  THETA=0.0,
       INMODE=4, TNODS=3,  TNPS=0,  TINTS=3,                            &END
      181.83      0.0   13.65
      181.83      3.0   13.65
      181.83      7.00  13.65
      181.83      9.0   13.65
      181.83     10.0   13.65
      181.83     10.5   13.65
      181.83     10.92  13.65
      181.83     10.92  14.5
      181.83     10.92  16.0
      181.83     10.92  21.3
      181.83     10.92  27.84
      181.83     10.92  32.216
      181.83      5.00  37.17
      181.83      2.6   39.86
      181.83      0.0   47.50
&BPNODE  TNODE=3,  TNPC=12,  TINTC=3,                                   &END

&PATCH1  IREV=0,  IDPAT=1,  MAKE=0,  KCOMP=1,  KASS=1,                  &END
  T34 HORIZONTAL TAIL #7
&SECT1   STX=0.0,  STY=0.0,  STZ=0.0,  SCALE=1.0,
       ALF=0.0,  THETA=0.0,
       INMODE=4, TNODS=0,  TNPS=0,  TINTS=3,                            &END
      234.795     8.74  32.216
      230.645     8.74  31.816
      226.495     8.74  31.490
      222.345     8.74  31.202
      218.195     8.74  30.953
      214.045     8.74  30.751
      209.895     8.74  30.610
      205.745     8.74  30.556
      203.670     8.74  30.572
      201.595     8.74  30.629
      199.520     8.74  30.737
      197.445     8.74  30.921
      196.408     8.74  31.054
      195.370     8.74  31.233
      194.332     8.74  31.493
      193.814     8.74  31.692
      193.295     8.74  32.216
&BPNODE  TNODE=2,  TNPC=15,  TINTC=3,                                   &END
      193.295     8.74  32.216
      193.814     8.74  32.740
```

```
       194.332     8.74  32.939
       195.370     8.74  33.199
       196.408     8.74  33.378
       197.445     8.74  33.511
       199.520     8.74  33.695
       201.595     8.74  33.803
       203.670     8.74  33.860
       205.745     8.74  33.870
       209.895     8.74  33.822
       214.045     8.74  33.681
       218.195     8.74  33.479
       222.345     8.74  33.230
       226.495     8.74  32.942
       230.645     8.74  32.616
       234.795     8.74  32.216
&BPNODE  TNODE=3,  TNPC=15,  TINTC=3,                                    &END
&SECT1   STX=0.0,  STY=0.0,  STZ=0.0,  SCALE=1.0,
       ALF=0.0,  THETA=0.0,
       INMODE=4, TNODS=3,  TNPS=7,  TINTS=3,                              &END
       231.517    73.168  32.216
       229.797    73.168  32.031
       228.077    73.168  31.884
       224.637    73.168  31.614
       221.197    73.168  31.376
       217.757    73.168  31.169
       214.317    73.168  31.002
       210.877    73.168  30.885
       207.437    73.168  30.840
       205.717    73.168  30.853
       203.997    73.168  30.900
       202.277    73.168  30.990
       200.557    73.168  31.142
       199.697    73.168  31.253
       198.837    73.168  31.401
       197.977    73.168  31.616
       197.289    73.168  31.781
       197.117    73.168  32.216
&BPNODE  TNODE=2,  TNPC=15,  TINTC=3,                                    &END
       197.117    73.168  32.216
       197.289    73.168  32.650
       197.977    73.168  32.816
       198.837    73.168  33.031
       199.697    73.168  33.179
       200.557    73.168  33.290
       202.277    73.168  33.442
       203.997    73.168  33.532
       205.717    73.168  33.579
       207.437    73.168  33.592
       210.877    73.168  33.547
       214.317    73.168  33.430
       217.757    73.168  33.263
       221.197    73.168  33.056
       224.637    73.168  32.818
       228.077    73.168  32.548
```

```
        229.797     73.168  32.400
        231.517     73.168  32.216
&BPNODE TNODE=3,  TNPC=15,  TINTC=3,                                          &END

&PATCH1  IREV=0,  IDPAT=1,  MAKE=7,  KCOMP=1,  KASS=2,                        &END
  T34 HORIZONTAL TAIL TIP #8
&PATCH2  ITYP=1,  TNODS=3,  TNPS=2,  TINTS=0,  NPTTIP=0,                      &END

&PATCH1  IREV=0,  IDPAT=2,  MAKE=0,  KCOMP=1,  KASS=1,                        &END
  T34 FUSELAGE UNDER TAIL #9
&SECT1   STX=0.0,  STY=0.0,  STZ=0.0,  SCALE=1.0,
         ALF=0.0,  THETA=0.0,
         INMODE=4, TNODS=0,  TNPS=0,  TINTS=0,                                &END
        181.83       0.0    13.65
        181.83      10.92   13.65
        181.83      10.92   25.0
        181.83      10.92   27.84
        181.83      10.92   32.216
&BPNODE  TNODE=3,  TNPC=0,  TINTC=0,                                          &END
&SECT1   STX=0.0,  STY=0.0,  STZ=0.0,  SCALE=1.0,
         ALF=0.0,  THETA=0.0,
         INMODE=4, TNODS=2,  TNPS=6,  TINTS=0,                                &END
        193.295      0.0    15.83
        193.295      8.74   15.83
        193.295      8.74   25.0
        193.295      8.74   27.84
        193.295      8.74   32.216
&BPNODE  TNODE=3,  TNPC=0,  TINTC=0,                                          &END
&SECT1   STX=0.0,  STY=0.0,  STZ=0.0,  SCALE=1.0,
         ALF=0.0,  THETA=0.0,
         INMODE=4, TNODS=0,  TNPS=0,  TINTS=0,                                &END
        194.332      0.0    16.00
        194.332      8.14   16.00
        194.332      8.14   25.0
        194.332      8.74   27.84
        194.332      8.74   31.493
&BPNODE  TNODE=3,  TNPC=0,  TINTC=0,                                          &END
&SECT1   STX=0.0,  STY=0.0,  STZ=0.0,  SCALE=1.0,
         ALF=0.0,  THETA=0.0,
         INMODE=4, TNODS=0,  TNPS=0,  TINTS=0,                                &END
        195.370      0.0    16.10
        195.370      7.94   16.10
        195.370      7.94   25.0
        195.370      8.74   27.84
        195.370      8.74   31.233
&BPNODE  TNODE=3,  TNPC=0,  TINTC=0,                                          &END
&SECT1   STX=0.0,  STY=0.0,  STZ=0.0,  SCALE=1.0,
         ALF=0.0,  THETA=0.0,
         INMODE=4, TNODS=0,  TNPS=0,  TINTS=0,                                &END
        197.445      0.0    16.381
        197.445      7.34   16.381
        197.445      7.34   25.0
        197.445      8.74   27.84
        197.445      8.74   30.921
```

```
&BPNODE TNODE=3, TNPC=0, TINTC=0,                                    &END
&SECT1  STX=0.0, STY=0.0, STZ=0.0, SCALE=1.0,
      ALF=0.0, THETA=0.0,
      INMODE=4, TNODS=0, TNPS=0, TINTS=0,                            &END
      199.520    0.0   16.654
      199.520    7.04  16.654
      199.520    7.04  25.0
      199.520    8.74  27.84
      199.520    8.74  30.737
&BPNODE TNODE=3, TNPC=0, TINTC=0,                                    &END
&SECT1  STX=0.0, STY=0.0, STZ=0.0, SCALE=1.0,
      ALF=0.0, THETA=0.0,
      INMODE=4, TNODS=0, TNPS=0, TINTS=0,                            &END
      201.595    0.0   16.93
      201.595    6.74  16.93
      201.595    6.74  25.0
      201.595    8.74  27.84
      201.595    8.74  30.629
&BPNODE TNODE=3, TNPC=0, TINTC=0,                                    &END
&SECT1  STX=0.0, STY=0.0, STZ=0.0, SCALE=1.0,
      ALF=0.0, THETA=0.0,
      INMODE=4, TNODS=0, TNPS=0, TINTS=0,                            &END
      203.67     0.0   17.473
      203.67     6.44  17.473
      203.67     6.44  25.0
      203.67     8.74  27.84
      203.67     8.74  30.572
&BPNODE TNODE=3, TNPC=0, TINTC=0,                                    &END
&SECT1  STX=0.0, STY=0.0, STZ=0.0, SCALE=1.0,
      ALF=0.0, THETA=0.0,
      INMODE=4, TNODS=0, TNPS=0, TINTS=0,                            &END
      205.745    0.0   18.02
      205.745    6.14  18.02
      205.745    6.14  25.0
      205.745    8.74  27.84
      205.745    8.74  30.556
&BPNODE TNODE=3, TNPC=0, TINTC=0,                                    &END
&SECT1  STX=0.0, STY=0.0, STZ=0.0, SCALE=1.0,
      ALF=0.0, THETA=0.0,
      INMODE=4, TNODS=0, TNPS=0, TINTS=0,                            &END
      209.895    0.0   18.9
      209.895    5.84  18.9
      209.895    5.84  25.0
      209.895    8.74  27.84
      209.895    8.74  30.61
&BPNODE TNODE=3, TNPC=0, TINTC=0,                                    &END
&SECT1  STX=0.0, STY=0.0, STZ=0.0, SCALE=1.0,
      ALF=0.0, THETA=0.0,
      INMODE=4, TNODS=0, TNPS=0, TINTS=0,                            &END
      214.045    0.0   19.11
      214.045    5.54  19.11
      214.045    5.54  25.0
      214.045    8.74  27.84
      214.045    8.74  30.751
```

```
&BPNODE TNODE=3, TNPC=0, TINTC=0,                                    &END
&SECT1  STX=0.0, STY=0.0, STZ=0.0, SCALE=1.0,
    ALF=0.0, THETA=0.0,
    INMODE=4, TNODS=0, TNPS=0, TINTS=0,                              &END
    218.195    0.0   20.48
    218.195    5.24  20.48
    218.195    5.24  25.0
    218.195    8.74  27.84
    218.195    8.74  30.953
&BPNODE TNODE=3, TNPC=0, TINTC=0,                                    &END
&SECT1  STX=0.0, STY=0.0, STZ=0.0, SCALE=1.0,
    ALF=0.0, THETA=0.0,
    INMODE=4, TNODS=0, TNPS=0, TINTS=0,                              &END
    222.345    0.0   21.30
    222.345    4.94  21.30
    222.345    4.94  25.0
    222.345    8.74  27.84
    222.345    8.74  31.202
&BPNODE TNODE=3, TNPC=0, TINTC=0,                                    &END
&SECT1  STX=0.0, STY=0.0, STZ=0.0, SCALE=1.0,
    ALF=0.0, THETA=0.0,
    INMODE=4, TNODS=0, TNPS=0, TINTS=0,                              &END
    226.495    0.0   21.84
    226.495    4.64  21.84
    226.495    4.64  25.0
    226.495    8.74  27.84
    226.495    8.74  31.49
&BPNODE TNODE=3, TNPC=0, TINTC=0,                                    &END
&SECT1  STX=0.0, STY=0.0, STZ=0.0, SCALE=1.0,
    ALF=0.0, THETA=0.0,
    INMODE=4, TNODS=0, TNPS=0, TINTS=0,                              &END
    230.645    0.0   22.67
    230.645    4.34  22.67
    230.645    4.34  25.0
    230.645    5.74  27.84
    230.645    8.74  31.816
&BPNODE TNODE=3, TNPC=0, TINTC=0,                                    &END
&SECT1  STX=0.0, STY=0.0, STZ=0.0, SCALE=1.0,
    ALF=0.0, THETA=0.0,
    INMODE=4, TNODS=0, TNPS=0, TINTS=0,                              &END
    232.72     0.0   23.04
    232.72     4.04  23.04
    232.72     4.04  25.0
    232.72     5.74  27.84
    232.72     8.74  31.993
&BPNODE TNODE=3, TNPC=0, TINTC=0,                                    &END
&SECT1  STX=0.0, STY=0.0, STZ=0.0, SCALE=1.0,
    ALF=0.0, THETA=0.0,
    INMODE=4, TNODS=0, TNPS=0, TINTS=0,                              &END
    234.795    0.0   23.95
    234.795    3.74  23.95
    234.795    3.74  25.0
    234.795    4.74  27.84
    234.795    8.74  32.181
```

```
&BPNODE TNODE=3, TNPC=0, TINTC=0,                                     &END
&SECT1  STX=0.0, STY=0.0, STZ=0.0, SCALE=1.0,
     ALF=0.0, THETA=0.0,
     INMODE=4, TNODS=3, TNPS=0, TINTS=0,                              &END
     235.5     0.0   23.95
     235.5     0.0   24.1
     235.5     0.0   25.0
     235.5     0.0   27.84
     235.5     0.0   32.181
&BPNODE TNODE=3, TNPC=0, TINTC=0,                                     &END

&PATCH1 IREV=0, IDPAT=2, MAKE=0, KCOMP=1, KASS=1,                     &END
 T34 VERTICAL TAIL #10
&SECT1  STX=0.0, STY=0.0, STZ=0.0, SCALE=1.0,
     ALF=0.0, THETA=0.0,
     INMODE=4, TNODS=2, TNPS=0, TINTS=3,                              &END
     181.83     0.0    47.5
     198.76     0.0    98.83
     198.76     0.0    98.83
&BPNODE TNODE=3, TNPC=0, TINTC=3,                                     &END
&SECT1  STX=0.0, STY=0.0, STZ=0.0, SCALE=1.0,
     ALF=0.0, THETA=0.0,
     INMODE=4, TNODS=2, TNPS=0, TINTS=3,                              &END
     182.47     0.49   47.5
     199.22     0.35   98.83
     199.22     0.0    98.83
&BPNODE TNODE=3, TNPC=0, TINTC=3,                                     &END
&SECT1  STX=0.0, STY=0.0, STZ=0.0, SCALE=1.0,
     ALF=0.0, THETA=0.0,
     INMODE=4, TNODS=2, TNPS=0, TINTS=3,                              &END
     183.12     0.67   47.5
     199.69     0.48   98.83
     199.69     0.0    98.83
&BPNODE TNODE=3, TNPC=0, TINTC=3,                                     &END
&SECT1  STX=0.0, STY=0.0, STZ=0.0, SCALE=1.0,
     ALF=0.0, THETA=0.0,
     INMODE=4, TNODS=2, TNPS=0, TINTS=3.                              &END
     184.41     0.92   47.5
     200.62     0.66   98.83
     200.62     0.0    98.83
&BPNODE TNODE=3, TNPC=0, TINTC=3,                                     &END
&SECT1  STX=0.0, STY=0.0, STZ=0.0, SCALE=1.0,
     ALF=0.0, THETA=0.0,
     INMODE=4, TNODS=2, TNPS=0, TINTS=3,                              &END
     185.69     1.08   47.5
     201.54     0.78   98.83
     201.54     0.0    98.83
&BPNODE TNODE=3, TNPC=0, TINTC=3,                                     &END
&SECT1  STX=0.0, STY=0.0, STZ=0.0, SCALE=1.0,
     ALF=0.0, THETA=0.0,
     INMODE=4, TNODS=2, TNPS=0, TINTS=3,                              &END
     186.98     1.21   47.5
     202.47     0.87   98.83
     202.47     0.0    98.83
```

```
&BPNODE TNODE=3, TNPC=0, TINTC=3,                                   &END
&SECT1  STX=0.0, STY=0.0, STZ=0.0, SCALE=1.0,
    ALF=0.0, THETA=0.0,
    INMODE=4, TNODS=2, TNPS=0, TINTS=3,                             &END
    189.56     1.38    47.5
    204.33     0.99    98.83
    204.33     0.0     98.83
&BPNODE  TNODE=3, TNPC=0, TINTC=3,                                  &END
&SECT1  STX=0.0, STY=0.0, STZ=0.0, SCALE=1.0,
    ALF=0.0, THETA=0.0,
    INMODE=4, TNODS=2, TNPS=0, TINTS=3,                             &END
    192.13     1.48    47.5
    206.18     1.06    98.83
    206.18     0.0     98.83
&BPNODE TNODE=3, TNPC=0, TINTC=3,                                   &END
&SECT1  STX=0.0, STY=0.0, STZ=0.0, SCALE=1.0,
    ALF=0.0, THETA=0.0,
    INMODE=4, TNODS=2, TNPS=0, TINTS=3,                             &END
    194.71     1.53    47.5
    208.04     1.10    98.83
    208.04     0.0     98.83
&BPNODE TNODE=3, TNPC=0, TINTC=3,                                   &END
&SECT1  STX=0.0, STY=0.0, STZ=0.0, SCALE=1.0,
    ALF=0.0, THETA=0.0,
    INMODE=4, TNODS=2, TNPS=0, TINTS=3,                             &END
    197.28     1.55    47.5
    209.89     1.11    98.83
    209.89     0.0     98.83
&BPNODE TNODE=3, TNPC=0, TINTC=3,                                   &END
&SECT1  STX=0.0, STY=0.0, STZ=0.0, SCALE=1.0,
    ALF=0.0, THETA=0.0,
    INMODE=4, TNODS=2, TNPS=0, TINTS=3,                             &END
    202.43     1.49    47.5
    213.60     1.08    98.83
    213.60     0.0     98.83
&BPNODE TNODE=3, TNPC=0, TINTC=3,                                   &END
&SECT1  STX=0.0, STY=0.0, STZ=0.0, SCALE=1.0,
    ALF=0.0, THETA=0.0,
    INMODE=4, TNODS=2, TNPS=0, TINTS=3,                             &END
    207.58     1.36    47.5
    217.31     0.98    98.83
    217.31     0.0     98.83
&BPNODE TNODE=3, TNPC=0, TINTC=3,                                   &END
&SECT1  STX=0.0, STY=0.0, STZ=0.0, SCALE=1.0,
    ALF=0.0, THETA=0.0,
    INMODE=4, TNODS=2, TNPS=0, TINTS=3,                             &END
    212.73     1.18    47.5
    221.02     0.85    98.83
    221.02     0.0     98.83
&BPNODE TNODE=3, TNPC=0, TINTC=3,                                   &END
&SECT1  STX=0.0, STY=0.0, STZ=0.0, SCALE=1.0,
    ALF=0.0, THETA=0.0,
    INMODE=4, TNODS=2, TNPS=0, TINTS=3,                             &END
    217.88     0.94    47.5
```

```
     224.73     0.68   98.83
     224.73     0.0    98.83
&BPNODE  TNODE=3,  TNPC=0,  TINTC=3,                                   &END
&SECT1   STX=0.0,  STY=0.0,  STZ=0.0,  SCALE=1.0,
       ALF=0.0,  THETA=0.0,
       INMODE=4, TNODS=2,  TNPS=0,  TINTS=3,                           &END
     223.03     0.68   47.5
     228.44     0.49   98.83
     228.44     0.0    98.83
&BPNODE  TNODE=3,  TNPC=0,  TINTC=3,                                   &END
&SECT1   STX=0.0,  STY=0.0,  STZ=0.0,  SCALE=1.0,
       ALF=0.0,  THETA=0.0,
       INMODE=4, TNODS=2,  TNPS=0,  TINTS=3,                           &END
     228.18     0.37   47.5
     232.15     0.27   98.83
     232.15     0.0    98.83
&BPNODE  TNODE=3,  TNPC=0,  TINTC=3,                                   &END
&SECT1   STX=0.0,  STY=0.0,  STZ=0.0,  SCALE=1.0,
       ALF=0.0,  THETA=0.0,
       INMODE=4, TNODS=2,  TNPS=0,  TINTS=3,                           &END
     230.76     0.21   47.5
     234.01     0.15   98.83
     234.01     0.0    98.83
&BPNODE  TNODE=3,  TNPC=0,  TINTC=3,                                   &END
&SECT1   STX=0.0,  STY=0.0,  STZ=0.0,  SCALE=1.0,
       ALF=0.0,  THETA=0.0,
       INMODE=4, TNODS=3,  TNPS=0,  TINTS=3,                           &END
     233.33     0.0    47.5
     235.86     0.0    98.83
     235.86     0.0    98.83
&BPNODE  TNODE=3,  TNPC=0,  TINTC=3,                                   &END

&PATCH1  IREV=0,  IDPAT=2,  MAKE=0,  KCOMP=1,  KASS=1,                 &END
  T34 FUS BTWN HOR AND VERT TAIL 1HV #11
&SECT1   STX=0.0,  STY=0.0,  STZ=0.0,  SCALE=1.0,
       ALF=0.0,  THETA=0.0,
       INMODE=4, TNODS=0,  TNPS=0,  TINTS=0,                           &END
     181.83     10.92   32.216
     181.83     5.00    37.17
     181.83     2.6     39.86
     181.83     0.0     47.5
&BPNODE  TNODE=3,  TNPC=0,  TINTC=0,                                   &END
&SECT1   STX=0.0,  STY=0.0,  STZ=0.0,  SCALE=1.0,
       ALF=0.0,  THETA=0.0,
       INMODE=4, TNODS=0,  TNPS=0,  TINTS=0,                           &END
     182.47     10.68   32.216
     182.47      5.0    37.07
     182.47      2.55   39.44
     182.47      0.49   47.5
&BPNODE  TNODE=3,  TNPC=0,  TINTC=0,                                   &END
&SECT1   STX=0.0,  STY=0.0,  STZ=0.0,  SCALE=1.0,
       ALF=0.0,  THETA=0.0,
       INMODE=4, TNODS=0,  TNPS=0,  TINTS=0,                           &END
     183.12     10.44   32.216
```

```
     183.12      5.0    36.97
     183.12      2.50   39.02
     183.12      0.67   47.5
&BPNODE  TNODE=3,  TNPC=0,  TINTC=0,                              &END
&SECT1   STX=0.0,  STY=0.0,  STZ=0.0,  SCALE=1.0,
      ALF=0.0,  THETA=0.0,
      INMODE=4, TNODS=0,  TNPS=0,  TINTS=0,                       &END
     184.41     10.20   32.216
     184.41      5.0    36.87
     184.41      2.45   38.6
     184.41      0.92   47.5
&BPNODE  TNODE=3,  TNPC=0,  TINTC=0,                              &END
&SECT1   STX=0.0,  STY=0.0,  STZ=0.0,  SCALE=1.0,
      ALF=0.0,  THETA=0.0,
      INMODE=4, TNODS=0,  TNPS=0,  TINTS=0,                       &END
     185.69      9.96   32.216
     185.69      5.0    36.77
     185.69      2.40   38.4
     185.69      1.08   47.5
&BPNODE  TNODE=3,  TNPC=0,  TINTC=0,                              &END
&SECT1   STX=0.0,  STY=0.0,  STZ=0.0,  SCALE=1.0,
      ALF=0.0,  THETA=0.0,
      INMODE=4, TNODS=0,  TNPS=0,  TINTS=0,                       &END
     186.98      9.72   32.216
     186.98      5.0    36.67
     186.98      2.38   38.18
     186.98      1.21   47.5
&BPNODE  TNODE=3,  TNPC=0,  TINTC=0,                              &END
&SECT1   STX=0.0,  STY=0.0,  STZ=0.0,  SCALE=1.0,
      ALF=0.0,  THETA=0.0,
      INMODE=4, TNODS=0,  TNPS=0,  TINTS=0,                       &END
     189.56     9.48    32.216
     189.56     5.0     36.57
     189.56     2.35    37.76
     189.56     1.38    47.5
&BPNODE  TNODE=3,  TNPC=0,  TINTC=0,                              &END
&SECT1   STX=0.0,  STY=0.0,  STZ=0.0,  SCALE=1.0,
      ALF=0.0,  THETA=0.0,
      INMODE=4, TNODS=0,  TNPS=0,  TINTS=0,                       &END
     192.13     9.24    32.216
     192.13     4.5     36.37
     192.13     2.32    37.34
     192.13     1.48    47.5
&BPNODE  TNODE=3,  TNPC=0,  TINTC=0,                              &END
&SECT1   STX=0.0,  STY=0.0,  STZ=0.0,  SCALE=1.0,
      ALF=0.0,  THETA=0.0,
      INMODE=4, TNODS=3,  TNPS=0,  TINTS=0,                       &END
     193.295     8.74   32.216
     193.295     4.00   36.17
     193.295     2.3    36.92
     193.295     1.5    47.5
&BPNODE  TNODE=3,  TNPC=0,  TINTC=0,                              &END

&PATCH1  IREV=0,  IDPAT=2,  MAKE=0,  KCOMP=1,  KASS=1,            &END
```

```
 T34 FUS BTWN HOR AND VERT TAIL 2H #12
&SECT1  STX=0.0,  STY=0.0,  STZ=0.0,  SCALE=1.0,
      ALF=0.0,  THETA=0.0,
      INMODE=4, TNODS=0,  TNPS=0,  TINTS=0,                    &END
      193.295    8.74   32.216
      193.295    4.0    36.17
      193.295    2.3    36.92
      193.295    1.6    38.0
&BPNODE  TNODE=3,  TNPC=0,  TINTC=0,                            &END
&SECT1  STX=0.0,  STY=0.0,  STZ=0.0,  SCALE=1.0,
      ALF=0.0,  THETA=0.0,
      INMODE=4, TNODS=0,  TNPS=0,  TINTS=0,                    &END
      193.814   8.74    32.74
      193.814   4.0     36.0
      193.814   2.3     36.82
      193.814   1.6     38.0
&BPNODE  TNODE=3,  TNPC=0,  TINTC=0,                            &END
&SECT1  STX=0.0,  STY=0.0,  STZ=0.0,  SCALE=1.0,
      ALF=0.0,  THETA=0.0,
      INMODE=4, TNODS=0,  TNPS=0,  TINTS=0,                    &END
      194.332   8.74    32.939
      194.332   4.0     35.9
      194.332   2.3     36.72
      194.332   1.6     38.0
&BPNODE  TNODE=3,  TNPC=0,  TINTC=0,                            &END
&SECT1  STX=0.0,  STY=0.0,  STZ=0.0,  SCALE=1.0,
      ALF=0.0,  THETA=0.0,
      INMODE=4, TNODS=0,  TNPS=0,  TINTS=0,                    &END
      195.37    8.74    33.199
      195.37    4.0     35.8
      195.37    2.3     36.62
      195.37    1.6     38.0
&BPNODE  TNODE=3,  TNPC=0,  TINTC=0,                            &END
&SECT1  STX=0.0,  STY=0.0,  STZ=0.0,  SCALE=1.0,
      ALF=0.0,  THETA=0.0,
      INMODE=4, TNODS=0,  TNPS=0,  TINTS=0,                    &END
      196.408   8.74    33.378
      196.408   4.0     35.7
      196.408   2.3     36.52
      196.408   1.6     38.0
&BPNODE  TNODE=3,  TNPC=0,  TINTC=0,                            &END
&SECT1  STX=0.0,  STY=0.0,  STZ=0.0,  SCALE=1.0,
      ALF=0.0,  THETA=0.0,
      INMODE=4, TNODS=0,  TNPS=0,  TINTS=0,                    &END
      197.445   8.74    33.511
      197.445   4.0     35.6
      197.445   2.3     36.42
      197.445   1.6     38.0
&BPNODE  TNODE=3,  TNPC=0,  TINTC=0,                            &END
&SECT1  STX=0.0,  STY=0.0,  STZ=0.0,  SCALE=1.0,
      ALF=0.0,  THETA=0.0,
      INMODE=4, TNODS=0,  TNPS=0,  TINTS=0,                    &END
      199.520   8.74    33.695
      199.52    4.0     35.5
```

```
     199.52    2.3      36.32
     199.52    1.6      38.0
&BPNODE TNODE=3, TNPC=0, TINTC=0,                        &END
&SECT1  STX=0.0, STY=0.0, STZ=0.0, SCALE=1.0,
      ALF=0.0, THETA=0.0,
      INMODE=4, TNODS=0, TNPS=0, TINTS=0,                &END
     201.595   8.74     33.803
     201.595   4.0      35.4
     201.595   2.3      36.22
     201.595   1.6      38.0
&BPNODE TNODE=3, TNPC=0, TINTC=0,                        &END
&SECT1  STX=0.0, STY=0.0, STZ=0.0, SCALE=1.0,
      ALF=0.0, THETA=0.0,
      INMODE=4, TNODS=0, TNPS=0, TINTS=0,                &END
     203.67    8.74     33.86
     203.67    4.0      35.3
     203.67    2.3      36.12
     203.67    1.6      38.0
&BPNODE TNODE=3, TNPC=0, TINTC=0,                        &END
&SECT1  STX=0.0, STY=0.0, STZ=0.0, SCALE=1.0,
      ALF=0.0, THETA=0.0,
      INMODE=4, TNODS=0, TNPS=0, TINTS=0,                &END
     205.745   8.74     33.87
     205.745   4.0      35.2
     205.745   2.3      36.02
     205.745   1.6      38.0
&BPNODE TNODE=3, TNPC=0, TINTC=0,                        &END
&SECT1  STX=0.0, STY=0.0, STZ=0.0, SCALE=1.0,
      ALF=0.0, THETA=0.0,
      INMODE=4, TNODS=0, TNPS=0, TINTS=0,                &END
     209.895   8.74     33.822
     209.895   4.0      35.1
     209.895   2.3      35.92
     209.895   1.6      38.0
&BPNODE TNODE=3, TNPC=0, TINTC=0,                        &END
&SECT1  STX=0.0, STY=0.0, STZ=0.0, SCALE=1.0,
      ALF=0.0, THETA=0.0,
      INMODE=4, TNODS=0, TNPS=0, TINTS=0,                &END
     214.045   8.74     33.681
     214.045   4.0      35.0
     214.045   2.3      35.82
     214.045   1.6      38.0
&BPNODE TNODE=3, TNPC=0, TINTC=0,                        &END
&SECT1  STX=0.0, STY=0.0, STZ=0.0, SCALE=1.0,
      ALF=0.0, THETA=0.0,
      INMODE=4, TNODS=0, TNPS=0, TINTS=0,                &END
     218.195   8.74     33.479
     218.195   4.0      34.9
     218.195   2.3      35.72
     218.195   1.6      38.0
&BPNODE TNODE=3, TNPC=0, TINTC=0,                        &END
&SECT1  STX=0.0, STY=0.0, STZ=0.0, SCALE=1.0,
      ALF=0.0, THETA=0.0,
      INMODE=4, TNODS=0, TNPS=0, TINTS=0,                &END
```

```
     222.345    8.74     33.23
     222.345    4.0      34.8
     222.345    2.3      35.62
     222.345    1.6      38.0
&BPNODE TNODE=3, TNPC=0, TINTC=0,                                    &END
&SECT1  STX=0.0, STY=0.0, STZ=0.0, SCALE=1.0,
      ALF=0.0, THETA=0.0,
      INMODE=4, TNODS=0, TNPS=0, TINTS=0,                            &END
     226.495    8.74     32.942
     226.495    4.0      34.7
     226.495    2.3      35.52
     226.495    1.6      38.0
&BPNODE TNODE=3, TNPC=0, TINTC=0,                                    &END
&SECT1  STX=0.0, STY=0.0, STZ=0.0, SCALE=1.0,
      ALF=0.0, THETA=0.0,
      INMODE=4, TNODS=0, TNPS=0, TINTS=0,                            &END
     230.645    8.74     32.616
     230.645    4.0      34.6
     230.645    2.3      35.42
     230.645    1.6      38.0
&BPNODE TNODE=3, TNPC=0, TINTC=0,                                    &END
&SECT1  STX=0.0, STY=0.0, STZ=0.0, SCALE=1.0,
      ALF=0.0, THETA=0.0,
      INMODE=4, TNODS=0, TNPS=0, TINTS=0,                            &END
     232.72    8.74     32.439
     232.72    4.0      34.5
     232.72    2.3      35.32
     232.72    1.6      38.0
&BPNODE TNODE=3, TNPC=0, TINTC=0,                                    &END
&SECT1  STX=0.0, STY=0.0, STZ=0.0, SCALE=1.0,
      ALF=0.0, THETA=0.0,
      INMODE=4, TNODS=0, TNPS=0, TINTS=0,                            &END
     234.795    8.74     32.216
     234.795    4.0      34.4
     234.795    2.3      35.22
     234.795    1.6      38.0
&BPNODE TNODE=3, TNPC=0, TINTC=0,                                    &END
&SECT1  STX=0.0, STY=0.0, STZ=0.0, SCALE=1.0,
      ALF=0.0, THETA=0.0,
      INMODE=4, TNODS=3, TNPS=0, TINTS=0,                            &END
     235.2     0.0     32.216
     235.2     0.0     34.4
     235.2     0.0     35.12
     234.0     0.0     38.0
&BPNODE TNODE=3, TNPC=0, TINTC=0,                                    &END

&PATCH1 IREV=0, IDPAT=2, MAKE=0, KCOMP=1, KASS=1,                    &END
  T34 FUS BTWN HOR AND VERT TAIL 3V #13
&SECT1  STX=0.0, STY=0.0, STZ=0.0, SCALE=1.0,
      ALF=0.0, THETA=0.0,
      INMODE=4, TNODS=0, TNPS=0, TINTS=0,                            &END
     193.295    1.6      38.0
     193.295    1.5      47.5
&BPNODE TNODE=3, TNPC=0, TINTC=0,                                    &END
```

```
&SECT1  STX=0.0,  STY=0.0,  STZ=0.0,  SCALE=1.0,
      ALF=0.0,  THETA=0.0,
      INMODE=4, TNODS=0,  TNPS=0,  TINTS=0,                          &END
      194.71     1.6     38.0
      194.71     1.53    47.5
&BPNODE  TNODE=3,  TNPC=0,  TINTC=0,                                 &END
&SECT1  STX=0.0,  STY=0.0,  STZ=0.0,  SCALE=1.0,
      ALF=0.0,  THETA=0.0,
      INMODE=4, TNODS=0,  TNPS=0,  TINTS=0,                          &END
      197.28     1.6     38.0
      197.28     1.55    47.5
&BPNODE  TNODE=3,  TNPC=0,  TINTC=0,                                 &END
&SECT1  STX=0.0,  STY=0.0,  STZ=0.0,  SCALE=1.0,
      ALF=0.0,  THETA=0.0,
      INMODE=4, TNODS=0,  TNPS=0,  TINTS=0,                          &END
      202.43     1.6     38.0
      202.43     1.49    47.5
&BPNODE  TNODE=3,  TNPC=0,  TINTC=0,                                 &END
&SECT1  STX=0.0,  STY=0.0,  STZ=0.0,  SCALE=1.0,
      ALF=0.0,  THETA=0.0,
      INMODE=4, TNODS=0,  TNPS=0,  TINTS=0,                          &END
      207.58     1.6     38.0
      207.58     1.36    47.5
&BPNODE  TNODE=3,  TNPC=0,  TINTC=0,                                 &END
&SECT1  STX=0.0,  STY=0.0,  STZ=0.0,  SCALE=1.0,
      ALF=0.0,  THETA=0.0,
      INMODE=4, TNODS=0,  TNPS=0,  TINTS=0,                          &END
      212.73     1.6     38.0
      212.73     1.18    47.5
&BPNODE  TNODE=3,  TNPC=0,  TINTC=0,                                 &END
&SECT1  STX=0.0,  STY=0.0,  STZ=0.0,  SCALE=1.0,
      ALF=0.0,  THETA=0.0,
      INMODE=4, TNODS=0,  TNPS=0,  TINTS=0,                          &END
      217.88     1.6     38.0
      217.88     0.94    47.5
&BPNODE  TNODE=3,  TNPC=0,  TINTC=0,                                 &END
&SECT1  STX=0.0,  STY=0.0,  STZ=0.0,  SCALE=1.0,
      ALF=0.0,  THETA=0.0,
      INMODE=4, TNODS=0,  TNPS=0,  TINTS=0,                          &END
      223.03     1.6     38.0
      223.03     0.68    47.5
&BPNODE  TNODE=3,  TNPC=0,  TINTC=0,                                 &END
&SECT1  STX=0.0,  STY=0.0,  STZ=0.0,  SCALE=1.0,
      ALF=0.0,  THETA=0.0,
      INMODE=4, TNODS=0,  TNPS=0,  TINTS=0,                          &END
      228.18     1.6     38.0
      228.18     0.37    47.5
&BPNODE  TNODE=3,  TNPC=0,  TINTC=0,                                 &END
&SECT1  STX=0.0,  STY=0.0,  STZ=0.0,  SCALE=1.0,
      ALF=0.0,  THETA=0.0,
      INMODE=4, TNODS=0,  TNPS=0,  TINTS=0,                          &END
      230.76     1.6     38.0
      230.76     0.21    47.5
&BPNODE  TNODE=3, TNPC=0,  TINTC=0,                                  &END
```

```
&SECT1  STX=0.0,  STY=0.0,  STZ=0.0,  SCALE=1.0,
     ALF=0.0,  THETA=0.0,
     INMODE=4, TNODS=0,  TNPS=0,  TINTS=0,                          &END
    233.33    1.6     38.0
    233.33    0.0     47.5
&BPNODE  TNODE=3,  TNPC=0,  TINTC=0,                                &END
&SECT1  STX=0.0,  STY=0.0,  STZ=0.0,  SCALE=1.0,
     ALF=0.0,  THETA=0.0,
     INMODE=4, TNODS=3,  TNPS=0,  TINTS=0,                          &END
    234.0     0.0     38.0
    234.0     0.0     47.5
&BPNODE  TNODE=3,  TNPC=0,  TINTC=0,                                &END


&PATCH1  IREV= 0,  IDPAT=  2,  MAKE=  0,  KCOMP=  2,  KASS=  3,     &END
 F14 NOSE CONE #14
&SECT1  STX=   0.0000, STY=   0.0000, STZ=   0.0000, SCALE=   1.0000,
     ALF=     0.0, THETA=    0.0,
     INMODE=    4, TNODS=      0, TNPS=       0, TINTS=       0,    &END
      93.00000     0.00000   131.50000
      93.00000     0.00000   131.50000
      93.00000     0.00000   131.50000
      93.00000     0.00000   131.50000
      93.00000     0.00000   131.50000
      93.00000     0.00000   131.50000
      93.00000     0.00000   131.50000
      93.00000     0.00000   131.50000
      93.00000     0.00000   131.50000
&BPNODE  TNODE=      3, TNPC=       0, TINTC=      0,               &END
&SECT1  STX=   0.0000, STY=   0.0000, STZ=   0.0000, SCALE=   1.0000,
     ALF=     0.0, THETA=    0.0,
     INMODE=    4, TNODS=      0, TNPS=       0, TINTS=       0,    &END
     103.00000     0.00000   127.41701
     103.00000     2.13000   127.99400
     103.00000     3.87900   129.38200
     103.00000     4.68200   131.45700
     103.00000     4.63300   133.66901
     103.00000     4.04400   135.14101
     103.00000     2.96900   136.28101
     103.00000     1.57700   136.91800
     103.00000     0.00000   137.08299
&BPNODE  TNODE=      3, TNPC=       0, TINTC=      0,               &END
&SECT1  STX=   0.0000, STY=   0.0000, STZ=   0.0000, SCALE=   1.0000,
     ALF=     0.0, THETA=    0.0,
     INMODE=    4, TNODS=      0, TNPS=       0, TINTS=       0,    &END
     116.23801     0.00000   123.50900
     116.23801     4.28500   124.68500
     116.23801     7.77400   127.46800
     116.23801     9.54400   131.54401
     116.23801     9.51700   135.97501
     116.23801     8.28300   138.98700
     116.23801     6.04300   141.30400
     116.23801     3.21400   142.77800
```

```
      116.23801    0.00000   143.25700
&BPNODE TNODE=      3, TNPC=       0, TINTC=      0,                    &END
&SECT1  STX=   0.0000, STY=   0.0000, STZ=   0.0000, SCALE=   1.0000,
      ALF=      0.0, THETA=    0.0,
      INMODE=     4, TNODS=       0, TNPS=       0, TINTS=       0,     &END
      133.02400    0.00000   120.12601
      133.02400    6.51000   121.62900
      133.02400   11.79000   125.72900
      133.02400   14.50300   131.82800
      133.02400   14.48400   138.50101
      133.02400   12.63100   143.14600
      133.02400    9.20500   146.74001
      133.02400    4.91000   149.18500
      133.02400    0.00000   150.00800
&BPNODE TNODE=      3, TNPC=       0, TINTC=      0,                    &END
&SECT1  STX=   0.0000, STY=   0.0000, STZ=   0.0000, SCALE=   1.0000,
      ALF=      0.0, THETA=    0.0,
      INMODE=     4, TNODS=       0, TNPS=       0, TINTS=       0,     &END
      153.68600    0.00000   117.67900
      153.68600    8.73900   119.05800
      153.68600   15.82700   124.28101
      153.68600   19.35200   132.37300
      153.68600   19.28300   141.22099
      153.68600   16.89700   147.56000
      153.68600   12.34600   152.53600
      153.68600    6.61300   156.03900
      153.68600    0.00000   157.18800
&BPNODE TNODE=      3, TNPC=       0, TINTC=      0,                    &END
&SECT1  STX=   0.0000, STY=   0.0000, STZ=   0.0000, SCALE=   1.0000,
      ALF=      0.0, THETA=    0.0,
      INMODE=     4, TNODS=       0, TNPS=       0, TINTS=       0,     &END
      178.57300    0.00000   117.08900
      178.57300   10.37500   118.23801
      178.57300   19.10200   123.87100
      178.57300   23.54800   133.21300
      178.57300   23.30400   143.62100
      178.57300   20.45399   151.51801
      178.57300   15.28600   158.09599
      178.57300    8.22000   162.42900
      178.57300    0.00000   163.96500
&BPNODE TNODE=      3, TNPC=       0, TINTC=      0,                    &END
&SECT1  STX=   0.0000, STY=   0.0000, STZ=   0.0000, SCALE=   1.0000,
      ALF=      0.0, THETA=    0.0,
      INMODE=     4, TNODS=       0, TNPS=       0, TINTS=       0,     &END
      208.05000    0.00000   118.00000
      208.05000   11.66900   118.07700
      208.05000   21.59200   123.72800
      208.05000   26.31100   134.23700
      208.05000   26.10600   145.88000
      208.05000   23.01401   155.58600
      208.05000   17.26601   163.95900
      208.05000    9.82200   170.55701
      208.05000    0.00000   172.95399
&BPNODE TNODE=      3, TNPC=       0, TINTC=      0,                    &END
```

```
&SECT1   STX=   0.0000, STY=   0.0000, STZ=   0.0000, SCALE=   1.0000,
     ALF=      0.0, THETA=    0.0,
     INMODE=     4, TNODS=      0, TNPS=       0, TINTS=        0,           &END
     242.50500     0.00000   118.53799
     242.50500    12.89300   118.53799
     242.50500    24.25000   124.16200
     242.50500    29.02000   135.87700
     242.50500    27.78101   148.71400
     242.50500    23.29300   161.87100
     242.50500    16.32100   173.58900
     242.50500    12.03400   186.30701
     242.50500     0.00000   192.42900
&BPNODE  TNODE=      3, TNPC=      0, TINTC=      0,                          &END
&SECT1   STX=   0.0000, STY=   0.0000, STZ=   0.0000, SCALE=   1.0000,
     ALF=      0.0, THETA=    0.0,
     INMODE=     4, TNODS=      0, TNPS=       0, TINTS=        0,           &END
     282.34595     0.00000   119.48500
     282.34595    14.21600   119.48500
     282.34595    26.76700   124.61500
     282.34595    30.03900   138.00000
     282.34595    28.83099   152.14200
     282.34595    24.04201   166.91901
     282.34595    16.33200   179.94299
     282.34595    13.20600   194.35699
     282.34595     0.00000   201.38699
&BPNODE  TNODE=      3, TNPC=      0, TINTC=      0,                          &END
&SECT1   STX=   0.0000, STY=   0.0000, STZ=   0.0000, SCALE=   1.0000,
     ALF=      0.0, THETA=    0.0,
     INMODE=     4, TNODS=      3, TNPS=       0, TINTS=        0,           &END
     328.00000     0.00000   121.00000
     328.00000    14.86000   121.00000
     328.00000    28.51601   125.18899
     328.00000    30.58900   139.50000
     328.00000    29.24100   154.28600
     328.00000    25.38100   168.91600
     328.00000    17.39000   181.56599
     328.00000    12.95200   195.45200
     328.00000     0.00000   202.50000
&BPNODE  TNODE=      3, TNPC=      0, TINTC=      0,                          &END

&PATCH1  IREV=0,  IDPAT= 2,  MAKE= 0,  KCOMP= 2,  KASS=   3,      &END
  F14 INLET REGION FORWARD #15
&SECT1   STX=   0.0000, STY=   0.0000, STZ=   0.0000, SCALE=   1.0000,
     ALF=      0.0, THETA=    0.0,
     INMODE=     4, TNODS=      0, TNPS=       0, TINTS=        0,           &END
     328.00000     0.00000   121.00000
     328.00000    14.86000   121.00000
     328.00000    28.51601   125.18899
     328.00000    30.58900   139.50000
     328.00000    29.24100   154.28600
     328.00000    37.00000   154.70000
     328.00000    66.20000   159.70000
     328.00000    66.20000   159.70000
     328.00000    66.20000   159.70000
```

```
      328.00000    51.61000   157.39999
      328.00000    37.00000   154.70000
      328.00000    29.24100   154.28600
      328.00000    25.38100   168.91600
      328.00000    17.39000   181.56599
      328.00000    12.95200   195.45200
      328.00000     0.00000   202.50000
 &BPNODE TNODE=     3, TNPC=      0, TINTC=     0,                  &END
 &SECT1  STX=   0.0000, STY=   0.0000, STZ=   0.0000, SCALE=   1.0000,
      ALF=      0.0, THETA=    0.0,
      INMODE=     4, TNODS=      0, TNPS=      0, TINTS=      0,    &END
      357.08691     0.00000   122.01800
      357.08691    14.14000   122.01800
      357.08691    27.86501   124.20000
      357.08691    31.13400   137.08099
      357.08691    30.26401   151.18201
      357.08691    37.00000   152.22800
      357.08691    67.61800   157.86400
      357.08691    69.50101   158.76900
      357.08691    70.54401   160.34000
      357.08691    54.00101   161.64700
      357.08691    35.98199   159.46300
      357.08691    28.72700   158.54500
      357.08691    24.83299   171.10201
      357.08691    17.64301   182.00000
      357.08691    11.81700   193.49899
      357.08691     0.00000   198.79100
 &BPNODE TNODE=     3, TNPC=      0, TINTC=     0,                  &END
 &SECT1  STX=   0.0000, STY=   0.0000, STZ=   0.0000, SCALE=   1.0000,
      ALF=      0.0, THETA=    0.0,
      INMODE=     4, TNODS=      0, TNPS=      0, TINTS=      0,    &END
      386.17505     0.00000   123.24699
      386.17505    12.78800   123.24699
      386.17505    25.44200   123.75900
      386.17505    30.56300   133.70799
      386.17505    30.07500   146.43800
      386.17505    37.04900   147.28700
      386.17505    68.82201   154.23399
      386.17505    75.02901   156.59399
      386.17505    80.02100   160.00200
      386.17505    58.87100   165.02200
      386.17505    34.87601   162.34599
      386.17505    27.45100   161.24699
      386.17505    24.01199   171.91400
      386.17505    17.36400   180.76601
      386.17505    10.32100   189.32600
      386.17505     0.00000   193.44000
 &BPNODE TNODE=     3, TNPC=      0, TINTC=     0,                  &END
 &SECT1  STX=   0.0000, STY=   0.0000, STZ=   0.0000, SCALE=   1.0000,
      ALF=      0.0, THETA=    0.0,
      INMODE=     4, TNODS=      0, TNPS=      0, TINTS=      0,    &END
      415.26294     0.00000   124.44099
      415.26294    11.16300   124.44099
      415.26294    22.29300   124.55701
```

```
      415.26294   29.54201   130.31599
      415.26294   29.44800   141.43401
      415.26294   37.09000   142.61800
      415.26294   69.68401   150.79601
      415.26294   81.52000   154.37601
      415.26294   91.67900   159.97301
      415.26294   65.19400   167.75000
      415.26294   34.42599   163.95200
      415.26294   26.56400   162.25700
      415.26294   22.86800   171.35600
      415.26294   16.87900   178.78200
      415.26294    9.18000   184.71300
      415.26294    0.00000   187.72400
&BPNODE  TNODE=     3, TNPC=      0, TINTC=      0,                     &END
&SECT1   STX=    0.0000, STY=   0.0000, STZ=   0.0000, SCALE=   1.0000,
      ALF=      0.0, THETA=    0.0,
      INMODE=    4, TNODS=     3, TNPS=      0, TINTS=      0,          &END
      444.35107    0.00000   125.88400
      444.35107    8.36100   125.88400
      444.35107   16.71700   125.90199
      444.35107   24.23399   127.19800
      444.35107   27.81599   132.70300
      444.35107   37.41299   134.37399
      444.35107   70.11400   147.76100
      444.35107   87.96400   152.57401
      444.35107  103.00700   160.05800
      444.35107   71.23000   170.03200
      444.35107   34.35699   165.24200
      444.35107   24.38800   162.92799
      444.35107   20.74600   170.36200
      444.35107   15.17400   176.36000
      444.35107    7.97000   180.43201
      444.35107    0.00000   182.50600
&BPNODE  TNODE=     3, TNPC=      0, TINTC=      0,                     &END

&PATCH1  IREV= 0,  IDPAT=  2,  MAKE=  0,  KCOMP=  2,  KASS=    3,      &END
  F14 INLET SIDE OUT #16
&SECT1   STX=    0.0000, STY=   0.0000, STZ=   0.0000, SCALE=   1.0000,
      ALF=      0.0, THETA=    0.0,
      INMODE=    4, TNODS=     0, TNPS=      0, TINTS=      0,          &END
      328.00000   66.20000   159.70000
      328.00000   66.20000   159.70000
      328.00000   66.20000   159.70000
      328.00000   66.20000   159.70000
      328.00000   66.20000   159.70000
      328.00000   66.20000   159.70000
&BPNODE  TNODE=     3, TNPC=      0, TINTC=      0,                     &END
&SECT1   STX=    0.0000, STY=   0.0000, STZ=   0.0000, SCALE=   1.0000,
      ALF=      0.0, THETA=    0.0,
      INMODE=    4, TNODS=     0, TNPS=      0, TINTS=      0,          &END
      357.08691   66.61800   157.86400
      357.08691   66.82899   153.14799
      357.08691   67.16499   148.43700
      357.08691   68.16499   148.43700
```

```
      357.08691   67.82899   153.14799
      357.08691   67.61800   157.86400
&BPNODE  TNODE=     3, TNPC=      0, TINTC=     0,                    &END
&SECT1   STX=   0.0000, STY=   0.0000, STZ=   0.0000, SCALE=   1.0000,
      ALF=      0.0, THETA=    0.0,
      INMODE=     4, TNODS=      0, TNPS=       0, TINTS=       0,    &END
      386.17505   67.82201   154.23399
      386.17505   68.60899   145.74001
      386.17505   69.13699   137.22099
      386.17505   70.13699   137.22099
      386.17505   69.60899   145.74001
      386.17505   68.82201   154.23399
&BPNODE  TNODE=     3, TNPC=      0, TINTC=     0,                    &END
&SECT1   STX=   0.0000, STY=   0.0000, STZ=   0.0000, SCALE=   1.0000,
      ALF=      0.0, THETA=    0.0,
      INMODE=     4, TNODS=      0, TNPS=       0, TINTS=       0,    &END
      415.26294   68.68401   150.79601
      415.26294   70.55299   138.46600
      415.26294   71.10500   126.01199
      415.26294   72.10500   126.01199
      415.26294   71.55299   138.46600
      415.26294   69.68401   150.79601
&BPNODE  TNODE=     3, TNPC=      0, TINTC=     0,                    &END
&SECT1   STX=   0.0000, STY=   0.0000, STZ=   0.0000, SCALE=   1.0000,
      ALF=      0.0, THETA=    0.0,
      INMODE=     4, TNODS=      3, TNPS=       0, TINTS=       0,    &END
      444.35107   69.11400   147.76100
      444.35107   71.67500   131.95000
      444.35107   70.13499   117.03900
      444.35107   71.13499   117.03900
      444.35107   72.67500   131.95000
      444.35107   70.11400   147.76100
&BPNODE  TNODE=     3, TNPC=      0, TINTC=     0,                    &END

&PATCH1  IREV= 0,  IDPAT= 2,  MAKE= 0,  KCOMP= 2,  KASS= 3,           &END
F14 INLET FACE #17
&SECT1   STX=   0.0000, STY=   0.0000, STZ=   0.0000, SCALE=   1.0000,
      ALF=      0.0, THETA=    0.0,
      INMODE=     4, TNODS=      0, TNPS=       0, TINTS=       0,    &END
      444.35107   45.38000   112.40401
      444.35107   39.77499   122.21201
      444.35107   37.41299   134.37399
&BPNODE  TNODE=     3, TNPC=      0, TINTC=     0,                    &END
&SECT1   STX=   0.0000, STY=   0.0000, STZ=   0.0000, SCALE=   1.0000,
      ALF=      0.0, THETA=    0.0,
      INMODE=     4, TNODS=      0, TNPS=       0, TINTS=       0,    &END
      444.35107   58.25800   114.72200
      444.35107   56.22500   127.08101
      444.35107   53.76349   141.06750
&BPNODE  TNODE=     3, TNPC=      0, TINTC=     0,                    &END
&SECT1   STX=   0.0000, STY=   0.0000, STZ=   0.0000, SCALE=   1.0000,
      ALF=      0.0, THETA=    0.0,
      INMODE=     4, TNODS=      3, TNPS=       0, TINTS=       0,    &END
      444.35107   71.13499   117.03900
```

```
     444.35107    72.67500   131.95000
     444.35107    70.11400   147.76100
&BPNODE  TNODE=      3, TNPC=       0, TINTC=      0,                        &END

&PATCH1  IREV= 0,  IDPAT= 2,  MAKE=  0,   KCOMP= 2,  KASS= 4,      &END
  F14 INLET REGION AFT #18
&SECT1   STX=    0.0000, STY=    0.0000, STZ=    0.0000, SCALE=    1.0000,
     ALF=       0.0, THETA=     0.0,
     INMODE=     4, TNODS=       0, TNPS=        0, TINTS=        0,             &END
     444.35107     0.00000   125.88400
     444.35107     8.36100   125.88400
     444.35107    16.71700   125.90199
     444.35107    24.23399   127.19800
     444.35107    27.81599   132.70300
     444.35107    37.41299   134.37399
     444.35107    39.77499   122.21201
     444.35107    45.38000   112.40401
     444.35107    58.25800   114.72200
     444.35107    71.13499   117.03900
     444.35107    72.67500   131.95000
     444.35107    70.11400   147.76100
     444.35107    87.96400   152.57401
     444.35107   103.00700   160.05800
     444.35107    71.23000   170.03200
     444.35107    34.35699   165.24200
     444.35107    24.38800   162.92799
     444.35107    20.74600   170.36200
     444.35107    15.17400   176.36000
     444.35107     7.97000   180.43201
     444.35107     0.00000   182.50600
&BPNODE  TNODE=      3, TNPC=       0, TINTC=      0,                        &END
&SECT1   STX=    0.0000, STY=    0.0000, STZ=    0.0000, SCALE=    1.0000,
     ALF=       0.0, THETA=     0.0,
     INMODE=     4, TNODS=       0, TNPS=        0, TINTS=        0,             &END
     473.43799     0.00000   127.17400
     473.43799     6.60500   127.17400
     473.43799    13.21100   127.17400
     473.43799    19.81500   127.17400
     473.43799    26.34599   127.86700
     473.43799    38.01900   128.03999
     473.43799    40.06000   116.52699
     473.43799    47.74100   109.59900
     473.43799    58.27699   111.42300
     473.43799    68.81300   113.24600
     473.43799    73.53500   127.91299
     473.43799    70.76700   144.75900
     473.43799    94.41499   151.69299
     473.43799   114.50301   159.95900
     473.43799    77.30400   171.36800
     473.43799    34.08701   166.06700
     473.43799    22.09900   163.22701
     473.43799    18.43300   169.16000
     473.43799    13.36900   173.84801
     473.43799     6.88200   176.34300
```

```
        473.43799    0.00000   177.56500
&BPNODE TNODE=      3, TNPC=       0, TINTC=      0,                    &END
&SECT1  STX=   0.0000, STY=   0.0000, STZ=   0.0000, SCALE=   1.0000,
        ALF=      0.0, THETA=    0.0,
        INMODE=     4, TNODS=      3, TNPS=       0, TINTS=       0,    &END
        502.52588    0.00000   128.58400
        502.52588    6.71300   128.58400
        502.52588   13.42700   128.58400
        502.52588   20.14000   128.58400
        502.52588   26.85300   128.58400
        502.52588   35.79401   128.58400
        502.52588   38.81200   114.92200
        502.52588   49.58400   108.03599
        502.52588   58.37900   109.60500
        502.52588   67.17300   111.17300
        502.52588   73.88800   125.70500
        502.52588   71.30099   142.89500
        502.52588  100.27901   151.67700
        502.52588  124.46500   161.01900
        502.52588   82.08000   171.69000
        502.52588   34.00000   166.54100
        502.52588   18.95100   163.46100
        502.52588   15.44200   167.86800
        502.52588   10.95000   171.23801
        502.52588    5.61800   173.00200
        502.52588    0.00000   173.55099
&BPNODE TNODE=      3, TNPC=       0, TINTC=      0,                    &END

&PATCH1 IREV= 0, IDPAT= 2, MAKE= 0, KCOMP= 2, KASS= 3,   &END
F14 UPPER WING ROOT REGION #19
&SECT1  STX=   0.0000, STY=   0.0000, STZ=   0.0000, SCALE=   1.0000,
        ALF=      0.0, THETA=    0.0,
        INMODE=     4, TNODS=      0, TNPS=       0, TINTS=       0,    &END
        502.52588  124.46500   161.01900
        502.52588   82.08000   171.69000
        502.52588   34.00000   166.54100
        502.52588   18.95100   163.46100
        502.52588   15.44200   167.86800
        502.52588   10.95000   171.23801
        502.52588    5.61800   173.00200
        502.52588    0.00000   173.55099
&BPNODE TNODE=      3, TNPC=       0, TINTC=      0,                    &END
&SECT1  STX=   0.0000, STY=   0.0000, STZ=   0.0000, SCALE=   1.0000,
        ALF=      0.0, THETA=    0.0,
        INMODE=     4, TNODS=      0, TNPS=       0, TINTS=       0,    &END
        506.24194  125.32700   163.75900
        506.24194   81.28200   171.63800
        506.24194   34.00000   166.56799
        506.24194   18.58299   163.50200
        506.24194   15.08500   167.72501
        506.24194   10.66200   170.94000
        506.24194    5.46700   172.64600
        506.24194    0.00000   173.18201
&BPNODE TNODE=      3, TNPC=       0, TINTC=      0,                    &END
```

```
&SECT1  STX=   0.0000, STY=   0.0000, STZ=   0.0000, SCALE=   1.0000,
       ALF=     0.0, THETA=   0.0,
       INMODE=    4, TNODS=      0, TNPS=       0, TINTS=       0,          &END
       511.12305  126.10500  165.30200
       511.12305   80.66299  171.57500
       511.12305   34.00000  166.60400
       511.12305   18.09801  163.55600
       511.12305   14.61600  167.53500
       511.12305   10.28500  170.54800
       511.12305    5.27000  172.17799
       511.12305    0.00000  172.69800
&BPNODE  TNODE=     3, TNPC=      0, TINTC=     0,                          &END
&SECT1  STX=   0.0000, STY=   0.0000, STZ=   0.0000, SCALE=   1.0000,
       ALF=     0.0, THETA=   0.0,
       INMODE=    4, TNODS=      0, TNPS=       0, TINTS=       0,          &END
       517.27002  125.32400  166.69701
       517.27002   79.91299  171.49200
       517.27002   34.00000  166.64900
       517.27002   17.48801  163.62300
       517.27002   14.02900  167.29401
       517.27002    9.81600  170.05200
       517.27002    5.02500  171.58800
       517.27002    0.00000  172.08800
&BPNODE  TNODE=     3, TNPC=      0, TINTC=     0,                          &END
&SECT1  STX=   0.0000, STY=   0.0000, STZ=   0.0000, SCALE=   1.0000,
       ALF=     0.0, THETA=   0.0,
       INMODE=    4, TNODS=      0, TNPS=       0, TINTS=       0,          &END
       524.79297  124.90900  167.69901
       524.79297   79.59300  171.37601
       524.79297   34.00000  166.70000
       524.79297   16.80499  163.73300
       524.79297   13.33400  166.98900
       524.79297    9.26200  169.44200
       524.79297    4.73600  170.86900
       524.79297    0.00000  171.35400
&BPNODE  TNODE=     3, TNPC=      0, TINTC=     0,                          &END
&SECT1  STX=   0.0000, STY=   0.0000, STZ=   0.0000, SCALE=   1.0000,
       ALF=     0.0, THETA=   0.0,
       INMODE=    4, TNODS=      0, TNPS=       0, TINTS=       0,          &END
       533.80591  119.49400  168.57700
       533.80591   76.75900  170.82401
       533.80591   34.00000  166.70000
       533.80591   16.88800  164.22900
       533.80591   12.89000  166.42300
       533.80591    8.89900  168.67799
       533.80591    4.54500  170.05299
       533.80591    0.00000  170.65100
&BPNODE  TNODE=     3, TNPC=      0, TINTC=     0,                          &END
&SECT1  STX=   0.0000, STY=   0.0000, STZ=   0.0000, SCALE=   1.0000,
       ALF=     0.0, THETA=   0.0,
       INMODE=    4, TNODS=      0, TNPS=       0, TINTS=       0,          &END
       544.42896  112.61700  168.84599
       544.42896   73.29201  170.20599
       544.42896   34.00000  166.70000
```

```
        544.42896   16.98599  164.81300
        544.42896   12.76300  165.47501
        544.42896    8.76700  167.63000
        544.42896    4.48000  169.06100
        544.42896    0.00000  169.82201
&BPNODE TNODE=     3, TNPC=     0, TINTC=     0,                    &END
&SECT1  STX=  0.0000, STY=  0.0000, STZ=  0.0000, SCALE=  1.0000,
        ALF=     0.0, THETA=   0.0,
        INMODE=     4, TNODS=     0, TNPS=      0, TINTS=      0,       &END
        556.78906  103.03000  168.47600
        556.78906   68.48599  169.35800
        556.78906   34.00000  166.50700
        556.78906   17.53900  164.55299
        556.78906   13.06700  164.62100
        556.78906    8.87000  166.45799
        556.78906    4.53400  167.91400
        556.78906    0.00000  168.62100
&BPNODE TNODE=     3, TNPC=     0, TINTC=     0,                    &END
&SECT1  STX=  0.0000, STY=  0.0000, STZ=  0.0000, SCALE=  1.0000,
        ALF=     0.0, THETA=   0.0,
        INMODE=     4, TNODS=     0, TNPS=      0, TINTS=      0,       &END
        571.02002   98.51700  167.31900
        571.02002   66.23199  168.46899
        571.02002   34.00000  166.25301
        571.02002   18.25101  164.09599
        571.02002   13.56100  163.64900
        571.02002    9.12400  165.07001
        571.02002    4.66700  166.58400
        571.02002    0.00000  167.19800
&BPNODE TNODE=     3, TNPC=     0, TINTC=     0,                    &END
&SECT1  STX=  0.0000, STY=  0.0000, STZ=  0.0000, SCALE=  1.0000,
        ALF=     0.0, THETA=   0.0,
        INMODE=     4, TNODS=     0, TNPS=      0, TINTS=      0,       &END
        587.26099   90.91499  165.54300
        587.26099   62.46899  166.91200
        587.26099   34.00000  165.23100
        587.26099   18.91000  163.79601
        587.26099   14.11600  163.38200
        587.26099    9.40000  164.08900
        587.26099    4.77400  165.39900
        587.26099    0.00000  165.93100
&BPNODE TNODE=     3, TNPC=     0, TINTC=     0,                    &END
&SECT1  STX=  0.0000, STY=  0.0000, STZ=  0.0000, SCALE=  1.0000,
        ALF=     0.0, THETA=   0.0,
        INMODE=     4, TNODS=     0, TNPS=      0, TINTS=      0,       &END
        605.66089   85.64600  163.09500
        605.66089   60.12300  165.03700
        605.66089   34.40401  163.97600
        605.66089   19.48100  163.31700
        605.66089   14.57800  163.09000
        605.66089    9.70100  163.18401
        605.66089    4.88800  164.12300
        605.66089    0.00000  164.51500
&BPNODE TNODE=     3, TNPC=     0, TINTC=     0,                    &END
```

```
&SECT1  STX=   0.0000, STY=   0.0000, STZ=   0.0000, SCALE=   1.0000,
     ALF=      0.0, THETA=   0.0,
     INMODE=    4, TNODS=     3, TNPS=      0, TINTS=      0,        &END
     626.37207    85.03799  159.84200
     626.37207    61.09300  162.53000
     626.37207    35.88400  162.79300
     626.37207    19.77699  162.28101
     626.37207    14.82800  162.26500
     626.37207     9.88100  162.31300
     626.37207     4.94700  162.65100
     626.37207     0.00000  162.73900
&BPNODE  TNODE=     3, TNPC=      0, TINTC=      0,                     &END

&PATCH1  IREV= 0, IDPAT=  2,  MAKE=  0,  KCOMP=  2,  KASS=  3,          &END
F14 LOWER WING ROOT REGION #20
&SECT1  STX=   0.0000, STY=   0.0000, STZ=   0.0000, SCALE=   1.0000,
     ALF=      0.0, THETA=   0.0,
     INMODE=    4, TNODS=     0, TNPS=      0, TINTS=      0,        &END
     502.52588     0.00000  128.58400
     502.52588     6.71300  128.58400
     502.52588    13.42700  128.58400
     502.52588    20.14000  128.58400
     502.52588    26.85300  128.58400
     502.52588    35.79401  128.58400
     502.52588    38.81200  114.92200
     502.52588    49.58400  108.03599
     502.52588    58.37900  109.60500
     502.52588    67.17300  111.17300
     502.52588    73.88800  125.70500
     502.52588    71.30099  142.89500
     502.52588   100.27901  151.67700
     502.52588   124.46500  161.01900
&BPNODE  TNODE=     3, TNPC=      0, TINTC=      0,                     &END
&SECT1  STX=   0.0000, STY=   0.0000, STZ=   0.0000, SCALE=   1.0000,
     ALF=      0.0, THETA=   0.0,
     INMODE=    4, TNODS=     0, TNPS=      0, TINTS=      0,        &END
     506.24194     0.00000  128.77600
     506.24194     6.85700  128.77499
     506.24194    13.71400  128.77600
     506.24194    20.57001  128.77499
     506.24194    27.42700  128.77600
     506.24194    35.52000  128.77600
     506.24194    38.66901  114.88300
     506.24194    49.77600  107.85800
     506.24194    58.33099  109.37199
     506.24194    66.88600  110.88600
     506.24194    73.89600  125.42999
     506.24194    71.37000  142.69000
     506.24194    99.88100  151.27299
     506.24194   124.81900  158.46100
&BPNODE  TNODE=     3, TNPC=      0, TINTC=      0,                     &END
&SECT1  STX=   0.0000, STY=   0.0000, STZ=   0.0000, SCALE=   1.0000,
     ALF=      0.0, THETA=   0.0,
     INMODE=    4, TNODS=     0, TNPS=      0, TINTS=      0,        &END
```

```
     511.12305      0.00000    129.02699
     511.12305      7.04500    129.02699
     511.12305     14.09000    129.02699
     511.12305     21.13499    129.02699
     511.12305     28.18100    129.02699
     511.12305     35.16200    129.02699
     511.12305     38.48100    114.82600
     511.12305     50.02699    107.62500
     511.12305     58.26801    109.06700
     511.12305     66.50999    110.50999
     511.12305     73.90700    125.06500
     511.12305     71.46001    142.42101
     511.12305    100.25700    151.17101
     511.12305    125.66400    157.50500
&BPNODE TNODE=     3, TNPC=     0, TINTC=     0,                    &END
&SECT1  STX=   0.0000, STY=   0.0000, STZ=   0.0000, SCALE=   1.0000,
     ALF=     0.0, THETA=   0.0,
     INMODE=    4, TNODS=     0, TNPS=     0, TINTS=     0,         &END
     517.27002      0.00000    129.34300
     517.27002      7.28200    129.34300
     517.27002     14.56500    129.34300
     517.27002     21.84700    129.34300
     517.27002     29.13000    129.34300
     517.27002     34.70900    129.34300
     517.27002     38.24600    114.74300
     517.27002     50.34300    107.33099
     517.27002     58.18900    108.68300
     517.27002     66.03500    110.03500
     517.27002     73.92101    124.59801
     517.27002     71.57300    142.08200
     517.27002    100.91600    151.13200
     517.27002    126.83701    156.89799
&BPNODE TNODE=     3, TNPC=     0, TINTC=     0,                    &END
&SECT1  STX=   0.0000, STY=   0.0000, STZ=   0.0000, SCALE=   1.0000,
     ALF=     0.0, THETA=   0.0,
     INMODE=    4, TNODS=     0, TNPS=     0, TINTS=     0,         &END
     524.79297      0.00000    129.73000
     524.79297      7.53800    129.73000
     524.79297     15.07700    129.73000
     524.79297     22.61501    129.73000
     524.79297     30.15401    129.73000
     524.79297     34.15401    129.73000
     524.79297     37.97600    114.60400
     524.79297     50.78200    106.96700
     524.79297     58.10699    108.20799
     524.79297     65.43201    109.44800
     524.79297     73.92799    123.99100
     524.79297     71.73300    141.64799
     524.79297     99.69501    150.14700
     524.79297    127.78599    156.44701
&BPNODE TNODE=     3, TNPC=     0, TINTC=     0,                    &END
&SECT1  STX=   0.0000, STY=   0.0000, STZ=   0.0000, SCALE=   1.0000,
     ALF=     0.0, THETA=   0.0,
     INMODE=    4, TNODS=     0, TNPS=     0, TINTS=     0,         &END
```

```
          533.80591     0.00000   130.18500
          533.80591     7.36300   130.18500
          533.80591    14.72500   130.18500
          533.80591    22.08800   130.18500
          533.80591    29.45100   130.18500
          533.80591    33.45100   130.18500
          533.80591    37.89000   114.10400
          533.80591    52.02200   106.47099
          533.80591    58.21001   107.56700
          533.80591    64.39800   108.66299
          533.80591    73.77800   122.91701
          533.80591    72.22900   140.86301
          533.80591    97.58800   149.31599
          533.80591   123.47000   156.09300
 &BPNODE TNODE=     3, TNPC=      0, TINTC=     0,                    &END
 &SECT1  STX=   0.0000, STY=   0.0000, STZ=   0.0000, SCALE=   1.0000,
         ALF=     0.0, THETA=   0.0,
         INMODE=    4, TNODS=     0, TNPS=      0, TINTS=       0,    &END
          544.42896     0.00000   130.72099
          544.42896     7.15600   130.72099
          544.42896    14.31100   130.72099
          544.42896    21.46700   130.72099
          544.42896    28.62300   130.72099
          544.42896    32.62199   130.72099
          544.42896    37.80200   113.51100
          544.42896    53.48399   105.88600
          544.42896    58.33200   106.81200
          544.42896    63.17999   107.73700
          544.42896    73.59801   121.63600
          544.42896    72.81300   139.93700
          544.42896    96.19501   148.75200
          544.42896   119.92999   155.97301
 &BPNODE TNODE=     3, TNPC=      0, TINTC=     0,                    &END
 &SECT1  STX=   0.0000, STY=   0.0000, STZ=   0.0000, SCALE=   1.0000,
         ALF=     0.0, THETA=   0.0,
         INMODE=    4, TNODS=     0, TNPS=      0, TINTS=       0,    &END
          556.78906     0.00000   131.26199
          556.78906     6.98000   131.26199
          556.78906    13.96100   131.26199
          556.78906    20.94099   131.26199
          556.78906    27.92200   131.26199
          556.78906    31.92200   131.26199
          556.78906    37.06799   114.24300
          556.78906    51.88901   105.68401
          556.78906    56.86600   106.33400
          556.78906    61.84399   106.98300
          556.78906    73.58701   120.44900
          556.78906    73.59399   139.18300
          556.78906    92.73500   147.60600
          556.78906   111.56599   156.15401
 &BPNODE TNODE=     3, TNPC=      0, TINTC=     0,                    &END
 &SECT1  STX=   0.0000, STY=   0.0000, STZ=   0.0000, SCALE=   1.0000,
         ALF=     0.0, THETA=   0.0,
         INMODE=    4, TNODS=     0, TNPS=      0, TINTS=       0,    &END
```

```
    571.02002     0.00000   131.87199
    571.02002     6.79000   131.87199
    571.02002    13.58000   131.87199
    571.02002    20.37000   131.87199
    571.02002    27.16000   131.87199
    571.02002    31.16000   131.87199
    571.02002    36.14500   115.22900
    571.02002    49.50000   105.53200
    571.02002    54.91000   105.85100
    571.02002    60.31900   106.17000
    571.02002    73.61099   119.09300
    571.02002    74.50800   138.37000
    571.02002    89.76401   146.58200
    571.02002   103.62601   156.68201
&BPNODE TNODE=    3, TNPC=     0, TINTC=     0,                  &END
&SECT1  STX=   0.0000, STY=   0.0000, STZ=   0.0000, SCALE=   1.0000,
    ALF=     0.0, THETA=   0.0,
    INMODE=    4, TNODS=     0, TNPS=     0, TINTS=     0,        &END
    587.26099     0.00000   132.66299
    587.26099     6.62200   132.66299
    587.26099    13.24500   132.66299
    587.26099    19.86700   132.66299
    587.26099    26.49001   132.66299
    587.26099    30.59200   132.66299
    587.26099    35.68700   115.52299
    587.26099    49.50999   104.99001
    587.26099    54.75500   105.11200
    587.26099    60.00000   105.23500
    587.26099    74.04100   117.84700
    587.26099    75.72000   137.17999
    587.26099    88.18300   144.52100
    587.26099    95.70599   157.50301
&BPNODE TNODE=    3, TNPC=     0, TINTC=     0,                  &END
&SECT1  STX=   0.0000, STY=   0.0000, STZ=   0.0000, SCALE=   1.0000,
    ALF=     0.0, THETA=   0.0,
    INMODE=    4, TNODS=     0, TNPS=     0, TINTS=     0,        &END
    605.66089     0.00000   133.58299
    605.66089     6.48500   133.58299
    605.66089    12.97000   133.58299
    605.66089    19.45399   133.58299
    605.66089    25.93900   133.58299
    605.66089    30.09900   133.58299
    605.66089    35.38600   115.67400
    605.66089    50.00000   104.39900
    605.66089    55.00000   104.39900
    605.66089    60.00000   104.39900
    605.66089    74.45799   116.80099
    605.66089    76.94299   135.99800
    605.66089    87.76500   144.20599
    605.66089    88.13400   158.54201
&BPNODE TNODE=    3, TNPC=     0, TINTC=     0,                  &END
&SECT1  STX=   0.0000, STY=   0.0000, STZ=   0.0000, SCALE=   1.0000,
    ALF=     0.0, THETA=   0.0,
    INMODE=    4, TNODS=     3, TNPS=     0, TINTS=     0,        &END
```

```
        626.37207     0.00000   134.61800
        626.37207     6.42900   134.61800
        626.37207    12.85900   134.61800
        626.37207    19.28799   134.61800
        626.37207    25.71700   134.61900
        626.37207    29.72900   134.61900
        626.37207    35.17200   116.06100
        626.37207    50.00000   104.02901
        626.37207    55.00000   104.02901
        626.37207    60.00000   104.02901
        626.37207    74.50000   116.35699
        626.37207    77.83000   135.25800
        626.37207    86.06300   145.53000
        626.37207    85.03799   159.84200
&BPNODE  TNODE=      3, TNPC=       0, TINTC=      0,                    &END

&PATCH1  IREV= 0,   IDPAT= 2,  MAKE= 0,  KCOMP= 2,  KASS= 3,    &END
  F14 FUSELAGE AFT OF WING TE #21
&SECT1   STX=   0.0000, STY=   0.0000, STZ=   0.0000, SCALE=   1.0000,
        ALF=      0.0, THETA=    0.0,
        INMODE=     4, TNODS=       0, TNPS=       0, TINTS=       0,        &END
        626.37207     0.00000   134.61800
        626.37207     6.42900   134.61800
        626.37207    12.85900   134.61800
        626.37207    19.28799   134.61800
        626.37207    25.71700   134.61900
        626.37207    29.72900   134.61900
        626.37207    35.17200   116.06100
        626.37207    50.00000   104.02901
        626.37207    55.00000   104.02901
        626.37207    60.00000   104.02901
        626.37207    74.50000   116.35699
        626.37207    77.83000   135.25800
        626.37207    86.06300   145.53000
        626.37207    85.03799   159.84200
        626.37207    61.09300   162.53000
        626.37207    35.88400   162.79300
        626.37207    19.77699   162.28101
        626.37207    14.82800   162.26500
        626.37207     9.88100   162.31300
        626.37207     4.94700   162.65100
        626.37207     0.00000   162.73900
&BPNODE  TNODE=      3, TNPC=       0, TINTC=      0,                    &END
&SECT1   STX=   0.0000, STY=   0.0000, STZ=   0.0000, SCALE=   1.0000,
        ALF=      0.0, THETA=    0.0,
        INMODE=     4, TNODS=       0, TNPS=       0, TINTS=       0,        &END
        654.75000     0.00000   136.39200
        654.75000     6.42500   136.39200
        654.75000    12.85000   136.39200
        654.75000    19.27499   136.39200
        654.75000    25.70000   136.39200
        654.75000    29.11800   136.39200
        654.75000    35.95200   115.55800
        654.75000    54.14500   104.38400
```

```
          654.75000   58.86800   105.27000
          654.75000   63.59000   106.15601
          654.75000   75.65900   117.25400
          654.75000   79.38300   133.42599
          654.75000   87.54800   148.95900
          654.75000   77.73300   160.97400
          654.75000   61.18800   162.54401
          654.75000   44.56500   162.40100
          654.75000   30.76700   159.88000
          654.75000   23.07500   159.88000
          654.75000   15.38400   159.88000
          654.75000    7.69200   159.88000
          654.75000    0.00000   159.88000
 &BPNODE  TNODE=     3, TNPC=      0, TINTC=     0,                      &END
 &SECT1   STX=   0.0000, STY=   0.0000, STZ=   0.0000, SCALE=   1.0000,
          ALF=      0.0, THETA=    0.0,
          INMODE=     4, TNODS=      0, TNPS=      0, TINTS=      0,       &END
          681.50000    0.00000   137.90900
          681.50000    6.42500   137.90900
          681.50000   12.85000   137.90900
          681.50000   19.27499   137.90900
          681.50000   25.70000   137.90900
          681.50000   29.20000   137.90900
          681.50000   35.71001   117.27800
          681.50000   53.95200   106.51900
          681.50000   58.47400   107.08000
          681.50000   62.99500   107.64000
          681.50000   75.26300   117.16200
          681.50000   80.33099   131.93800
          681.50000   90.13100   146.81900
          681.50000   81.01500   160.26199
          681.50000   63.71100   163.72200
          681.50000   46.12100   163.43100
          681.50000   34.17400   157.39799
          681.50000   25.63000   157.39799
          681.50000   17.08701   157.39799
          681.50000    8.54300   157.39799
          681.50000    0.00000   157.39799
 &BPNODE  TNODE=     3, TNPC=      0, TINTC=     0,                      &END
 &SECT1   STX=   0.0000, STY=   0.0000, STZ=   0.0000, SCALE=   1.0000,
          ALF=      0.0, THETA=    0.0,
          INMODE=     4, TNODS=      0, TNPS=      0, TINTS=      0,       &END
          708.25000    0.00000   139.06200
          708.25000    6.42500   139.06200
          708.25000   12.85000   139.06200
          708.25000   19.27499   139.06200
          708.25000   25.70000   139.06200
          708.25000   29.26601   139.06200
          708.25000   35.69501   118.71001
          708.25000   54.06700   108.46100
          708.25000   58.26801   108.92799
          708.25000   62.46800   109.39400
          708.25000   74.49001   117.63400
          708.25000   80.79900   130.96800
```

```
     708.25000   90.33501  145.56000
     708.25000   80.97400  158.83400
     708.25000   63.68401  164.15700
     708.25000   45.76801  163.93201
     708.25000   34.06700  154.70700
     708.25000   25.55000  154.70700
     708.25000   17.03300  154.70700
     708.25000    8.51700  154.70700
     708.25000    0.00000  154.70700
&BPNODE TNODE=    3, TNPC=     0, TINTC=    0,                 &END
&SECT1  STX=   0.0000, STY=   0.0000, STZ=   0.0000, SCALE=   1.0000,
     ALF=      0.0, THETA=    0.0,
     INMODE=    4, TNODS=     0, TNPS=      0, TINTS=      0,           &END
     735.00000    0.00000  140.36000
     735.00000    6.45400  140.36000
     735.00000   12.90700  140.36000
     735.00000   19.36099  140.36000
     735.00000   25.81400  140.36000
     735.00000   29.58299  140.36000
     735.00000   36.01500  120.47501
     735.00000   54.13699  110.34300
     735.00000   58.08000  110.83099
     735.00000   62.02300  111.32001
     735.00000   73.89600  118.48900
     735.00000   80.95399  130.47701
     735.00000   89.65700  145.00101
     735.00000   79.34300  157.84599
     735.00000   62.82700  164.46300
     735.00000   45.31700  163.97099
     735.00000   34.00000  152.56300
     735.00000   25.50000  152.56300
     735.00000   17.00000  152.56300
     735.00000    8.50000  152.56300
     735.00000    0.00000  152.56300
&BPNODE TNODE=    3, TNPC=     0, TINTC=    0,                 &END
&SECT1  STX=   0.0000, STY=   0.0000, STZ=   0.0000, SCALE=   1.0000,
     ALF=      0.0, THETA=    0.0,
     INMODE=    4, TNODS=     0, TNPS=      0, TINTS=      0,           &END
     761.75000    0.00000  142.78600
     761.75000    6.75600  142.79800
     761.75000   13.51100  142.81000
     761.75000   20.26801  142.81200
     761.75000   27.02400  142.81100
     761.75000   31.02400  142.83000
     761.75000   37.15500  122.34599
     761.75000   56.11900  113.10899
     761.75000   59.46800  113.41299
     761.75000   62.81599  113.71600
     761.75000   73.71600  119.99499
     761.75000   80.60100  130.53500
     761.75000   86.92300  144.64999
     761.75000   75.72800  157.15300
     761.75000   60.27200  164.18500
     761.75000   43.89200  161.66600
```

```
     761.75000   34.00000  150.97701
     761.75000   25.49899  150.98100
     761.75000   16.99699  150.98399
     761.75000    8.50100  151.01100
     761.75000    0.00000  151.01300
&BPNODE  TNODE=      3, TNPC=      0, TINTC=     0,                    &END
&SECT1   STX=   0.0000, STY=   0.0000, STZ=   0.0000, SCALE=   1.0000,
     ALF=      0.0, THETA=    0.0,
     INMODE=     4, TNODS=      3, TNPS=      0, TINTS=      0,        &END
     788.50000    0.00000  142.32100
     788.50000    8.00600  142.88200
     788.50000   15.95800  143.92400
     788.50000   23.88600  145.17599
     788.50000   31.81400  146.42799
     788.50000   34.59599  149.06599
     788.50000   37.10200  125.63800
     788.50000   57.66400  114.92500
     788.50000   60.67500  115.44900
     788.50000   63.68700  115.97301
     788.50000   74.24100  122.92000
     788.50000   80.74300  133.89400
     788.50000   80.03300  146.55701
     788.50000   72.40300  156.48100
     788.50000   58.70100  162.17999
     788.50000   44.10600  158.66901
     788.50000   34.59599  149.06599
     788.50000   26.10899  150.95200
     788.50000   17.36700  151.13800
     788.50000    8.74800  152.44600
     788.50000    0.00000  152.16499
&BPNODE  TNODE=      3, TNPC=      0, TINTC=     0,                    &END

&PATCH1  IREV= 0,  IDPAT= 2,  MAKE= 0,  KCOMP= 2,  KASS= 3,            &END
  F14 EXHAUST CONE #22
&SECT1   STX=   0.0000, STY=   0.0000, STZ=   0.0000, SCALE=   1.0000,
     ALF=      0.0, THETA=    0.0,
     INMODE=     4, TNODS=      0, TNPS=      0, TINTS=      0,        &END
     788.50000   34.59599  149.06599
     788.50000   37.10200  125.63800
     788.50000   57.66400  114.92500
     788.50000   60.67500  115.44900
     788.50000   63.68700  115.97301
     788.50000   74.24100  122.92000
     788.50000   80.74300  133.89400
     788.50000   80.03300  146.55701
     788.50000   72.40300  156.48100
     788.50000   58.70100  162.17999
     788.50000   44.10600  158.66901
     788.50000   34.59599  149.06599
&BPNODE  TNODE=      3, TNPC=      0, TINTC=     0,                    &END
&SECT1   STX=   0.0000, STY=   0.0000, STZ=   0.0000, SCALE=   1.0000,
     ALF=      0.0, THETA=    0.0,
     INMODE=     4, TNODS=      3, TNPS=      0, TINTS=      0,        &END
     813.00000   45.48801  144.40100
```

```
        813.00000   45.73599  131.46500
        813.00000   57.16100  125.38600
        813.00000   58.82700  125.66600
        813.00000   60.49300  125.94701
        813.00000   66.12399  129.47099
        813.00000   69.17999  135.35300
        813.00000   68.91200  142.06400
        813.00000   65.01801  147.42999
        813.00000   57.82100  150.74899
        813.00000   49.94901  149.25301
        813.00000   45.48801  144.40100
&BPNODE  TNODE=     3, TNPC=       0, TINTC=      0,                    &END

&PATCH1  IREV= 0,   IDPAT=  2,  MAKE=  0,  KCOMP=  2,  KASS=  3,      &END
  F14 FUSELAGE TIP #23
&SECT1   STX=    0.0000, STY=    0.0000, STZ=    0.0000, SCALE=   1.0000,
        ALF=       0.0, THETA=    0.0,
        INMODE=     4, TNODS=      0, TNPS=       0, TINTS=       0,      &END
        788.50000    0.00000  142.32100
        788.50000    8.00600  142.88200
        788.50000   15.95800  143.92400
        788.50000   23.88600  145.17599
        788.50000   31.81400  146.42799
        788.50000   34.59599  149.06599
        788.50000   26.10899  150.95200
        788.50000   17.36700  151.13800
        788.50000    8.74800  152.44600
        788.50000    0.00000  152.16499
&BPNODE  TNODE=     3, TNPC=       0, TINTC=      0,                    &END
&SECT1   STX=    0.0000, STY=    0.0000, STZ=    0.0000, SCALE=   1.0000,
        ALF=       0.0, THETA=    0.0,
        INMODE=     4, TNODS=      0, TNPS=       0, TINTS=       0,      &END
        813.00000    0.00000  145.46100
        813.00000    5.13400  145.23100
        813.00000   10.26700  144.99899
        813.00000   15.35800  144.29700
        813.00000   22.44901  146.59500
        813.00000   24.42900  149.31200
        813.00000   21.57300  152.52100
        813.00000   14.38900  152.59100
        813.00000    7.20500  152.03600
        813.00000    0.00000  151.85500
&BPNODE  TNODE=     3, TNPC=       0, TINTC=      0,                    &END
&SECT1   STX=    0.0000, STY=    0.0000, STZ=    0.0000, SCALE=   1.0000,
        ALF=       0.0, THETA=    0.0,
        INMODE=     4, TNODS=      3, TNPS=       0, TINTS=       0,      &END
        834.00000    0.00000  147.53500
        834.00000    5.20300  147.53500
        834.00000   10.40600  147.53500
        834.00000   15.60900  147.53500
        834.00000   20.81200  147.53500
        834.00000   20.81200  149.53500
        834.00000   15.60900  149.53500
        834.00000   10.40600  149.53500
```

```
      834.00000     5.20300   149.53500
      834.00000     0.00000   149.53500
&BPNODE TNODE=      3, TNPC=      0, TINTC=      0,                    &END

&PATCH1 IREV= 0,  IDPAT= 2,  MAKE= 0,  KCOMP= 2,  KASS= 4,      &END
F14 FUSELAGE TIP COVER #24
&SECT1   STX=   0.0000, STY=   0.0000, STZ=   0.0000, SCALE=   1.0000,
      ALF=      0.0, THETA=    0.0,
      INMODE=    4, TNODS=     0, TNPS=       0, TINTS=       0,         &END
      834.00000    0.00000   148.53500
      834.00000    0.00000   148.53500
      834.00000    0.00000   148.53500
      834.00000    0.00000   148.53500
      834.00000    0.00000   148.53500
      834.00000    0.00000   148.53500
      834.00000    0.00000   148.53500
      834.00000    0.00000   148.53500
      834.00000    0.00000   148.53500
      834.00000    0.00000   148.53500
&BPNODE TNODE=      3, TNPC=      0, TINTC=      0,                    &END
&SECT1   STX=   0.0000, STY=   0.0000, STZ=   0.0000, SCALE=   1.0000,
      ALF=      0.0, THETA=    0.0,
      INMODE=    4, TNODS=     3, TNPS=       0, TINTS=       0,         &END
      834.00000     0.00000   149.53500
      834.00000     5.20300   149.53500
      834.00000    10.40600   149.53500
      834.00000    15.60900   149.53500
      834.00000    20.81200   149.53500
      834.00000    20.81200   147.53500
      834.00000    15.60900   147.53500
      834.00000    10.40600   147.53500
      834.00000     5.20300   147.53500
      834.00000     0.00000   147.53500
&BPNODE TNODE=      3, TNPC=      0, TINTC=      0,                    &END

&PATCH1 IREV= 0,  IDPAT= 2,  MAKE= 0,  KCOMP= 2,  KASS= 4,      &END
 F14 EXHAUST COVER #25
&SECT1   STX=   0.0000, STY=   0.0000, STZ=   0.0000, SCALE=   1.0000,
      ALF=      0.0, THETA=    0.0,
      INMODE=    4, TNODS=     0, TNPS=       0, TINTS=       0,         &END
      813.00000    57.33299   138.00000
      813.00000    57.33299   138.00000
      813.00000    57.33299   138.00000
      813.00000    57.33299   138.00000
      813.00000    57.33299   138.00000
      813.00000    57.33299   138.00000
      813.00000    57.33299   138.00000
      813.00000    57.33299   138.00000
      813.00000    57.33299   138.00000
      813.00000    57.33299   138.00000
      813.00000    57.33299   138.00000
      813.00000    57.33299   138.00000
&BPNODE TNODE=      3, TNPC=      0, TINTC=      0,                    &END
&SECT1   STX=   0.0000, STY=   0.0000, STZ=   0.0000, SCALE=   1.0000,
```

```
      ALF=     0.0, THETA=    0.0,
      INMODE=    4, TNODS=     3, TNPS=      0, TINTS=      0,          &END
      813.00000   45.48801   144.40100
      813.00000   49.94901   149.25301
      813.00000   57.82100   150.74899
      813.00000   65.01801   147.42999
      813.00000   68.91200   142.06400
      813.00000   69.17999   135.35300
      813.00000   66.12399   129.47099
      813.00000   60.49300   125.94701
      813.00000   58.82700   125.66600
      813.00000   57.16100   125.38600
      813.00000   45.73599   131.46500
      813.00000   45.48801   144.40100
&BPNODE  TNODE=     3, TNPC=      0, TINTC=     0,                        &END

&PATCH1  IREV= 0,   IDPAT= 1,  MAKE= 0,  KCOMP= 2,  KASS= 3,              &END
  F14 WING #26
&SECT1   STX=   0.0000, STY=   0.0000, STZ=   0.0000, SCALE=   1.0000,
      ALF=     0.0, THETA=    0.0,
      INMODE=    4, TNODS=     0, TNPS=      0, TINTS=      0,          &END
      626.37207    85.03799   159.84200
      605.66089    88.13400   158.54201
      587.26099    95.70599   157.50301
      571.02002   103.62601   156.68201
      556.78906   111.56599   156.15401
      544.42896   119.92999   155.97301
      533.80591   123.47000   156.09300
      524.79297   127.78599   156.44701
      517.27002   126.83701   156.89799
      511.12305   125.66400   157.50500
      506.24194   124.81900   158.46100
      502.52588   124.46500   161.01900
      506.24194   125.32700   163.75900
      511.12305   126.10500   165.30200
      517.27002   125.32400   166.69701
      524.79297   124.90900   167.69901
      533.80591   119.49400   168.57700
      544.42896   112.61700   168.84599
      556.78906   103.03000   168.47600
      571.02002    98.51700   167.31900
      587.26099    90.91499   165.54300
      605.66089    85.64600   163.09500
      626.37207    85.03799   159.84200
&BPNODE  TNODE=     3, TNPC=      0, TINTC=     0,                        &END
&SECT1   STX=   0.0000, STY=   0.0000, STZ=   0.0000, SCALE=   1.0000,
      ALF=     0.0, THETA=    0.0,
      INMODE=    4, TNODS=     0, TNPS=      0, TINTS=      0,          &END
      622.3692     92.0181     142.7208
      604.7296     95.1021     153.6552
      587.26099   102.70599   157.50301
      571.02002   110.62601   156.68201
      556.78906   118.56599   156.15401
      544.42896   126.92999   155.97301
```

```
     533.80591   130.47000   156.09300
     524.79297   134.78599   156.44701
     517.27002   133.83701   156.89799
     511.12305   132.66400   157.50500
     506.24194   131.81900   158.46100
     502.52588   131.46500   161.01900
     506.24194   132.32700   163.75900
     511.12305   133.10500   165.30200
     517.27002   132.32400   166.69701
     524.79297   131.90900   167.69901
     533.80591   126.49400   168.57700
     544.42896   119.61700   168.84599
     556.78906   110.03000   168.47600
     571.02002   105.51700   167.31900
     587.26099    97.91499   165.54300
     607.2193     92.2753    157.2231
     622.3692     92.0181    142.7208
&BPNODE  TNODE=      3, TNPC=       0, TINTC=      0,                  &END
&SECT1   STX=    0.0000, STY=    0.0000, STZ=    0.0000, SCALE=    1.0000,
     ALF=       0.0, THETA=    0.0,
     INMODE=     4, TNODS=      0, TNPS=       0, TINTS=       0,       &END
     631.606     169.4923    142.01
     615.33      169.4796    151.994
     598.78296   169.58299   156.26801
     583.83203   169.58299   155.82899
     570.73193   169.58299   155.67200
     559.35498   169.58299   155.73100
     549.57593   169.58299   155.92799
     541.28003   169.58299   156.20799
     534.35498   169.58299   156.56599
     528.69604   169.58299   157.05499
     524.20313   169.58299   157.80901
     520.78296   169.58299   159.97400
     524.20313   169.58299   162.53000
     528.69604   169.58299   163.84399
     534.35498   169.58299   164.90700
     541.28003   169.58299   165.73300
     549.57593   169.58299   166.25101
     559.35498   169.58299   166.36600
     570.73193   169.58299   165.95799
     583.83203   169.58299   164.92900
     598.78296   169.58299   163.23801
     617.5477    169.1831    155.1908
     631.606    169.4923    142.01
&BPNODE  TNODE=      3, TNPC=       0, TINTC=      0,                  &END
&SECT1   STX=    0.0000, STY=    0.0000, STZ=    0.0000, SCALE=    1.0000,
     ALF=       0.0, THETA=    0.0,
     INMODE=     4, TNODS=      0, TNPS=       0, TINTS=       0,       &END
     634.9622    211.0303    142.0361
     620.5685    211.0325    150.6627
     606.11182   211.13400   154.95799
     592.97974   211.13400   154.50200
     581.47485   211.13400   154.33400
     571.48169   211.13400   154.38200
```

```
     562.89380   211.13400   154.55400
     555.60669   211.13400   154.79401
     549.52466   211.13400   155.09399
     544.55469   211.13400   155.49500
     540.60864   211.13400   156.11200
     537.60474   211.13400   157.96201
     540.60864   211.13400   160.18401
     544.55469   211.13400   161.32001
     549.52466   211.13400   162.25800
     555.60669   211.13400   163.02499
     562.89380   211.13400   163.55499
     571.48169   211.13400   163.75200
     581.47485   211.13400   163.49300
     592.97974   211.13400   162.67700
     606.11182   211.13400   161.26100
     622.5768    210.7639    153.5582
     634.9622    211.0303    142.0361
&BPNODE TNODE=    3, TNPC=     0, TINTC=    0,                  &END
&SECT1  STX=  0.0000, STY=  0.0000, STZ=  0.0000, SCALE=  1.0000,
     ALF=     0.0, THETA=   0.0,
     INMODE=   4, TNODS=    0, TNPS=     0, TINTS=      0,        &END
     638.2167    252.5822    141.9295
     625.6762    252.6031    149.1553
     613.43481   252.68600   153.38300
     602.12476   252.68600   152.84801
     592.21387   252.68600   152.60500
     583.60571   252.68600   152.58099
     576.20874   252.68600   152.68900
     569.93164   252.68600   152.86700
     564.69287   252.68600   153.09900
     560.41187   252.68600   153.41701
     557.01270   252.68600   153.92101
     554.42578   252.68600   155.49300
     557.01270   252.68600   157.43500
     560.41187   252.68600   158.43401
     564.69287   252.68600   159.27200
     569.93164   252.68600   159.98300
     576.20874   252.68600   160.52000
     583.60571   252.68600   160.80000
     592.21387   252.68600   160.71100
     602.12476   252.68600   160.14999
     613.43481   252.68600   159.06599
     627.5032    252.3588    151.7894
     638.2167    252.5822    141.9295
&BPNODE TNODE=    3, TNPC=     0, TINTC=    0,                  &END
&SECT1  STX=  0.0000, STY=  0.0000, STZ=  0.0000, SCALE=  1.0000,
     ALF=     0.0, THETA=   0.0,
     INMODE=   4, TNODS=    0, TNPS=     0, TINTS=      0,        &END
     641.4686    294.1341    141.81
     630.7969    294.1714    147.6581
     620.76270   294.23706   151.84200
     611.27271   294.23706   151.23700
     602.95679   294.23706   150.91499
     595.73462   294.23706   150.80600
```

```
      589.52686   294.23706   150.83600
      584.26074   294.23706   150.94299
      579.86475   294.23706   151.10201
      576.27173   294.23706   151.33000
      573.41968   294.23706   151.71500
      571.24976   294.23706   153.00600
      573.41968   294.23706   154.66901
      576.27173   294.23706   155.53101
      579.86475   294.23706   156.26500
      584.26074   294.23706   156.91100
      589.52686   294.23706   157.43900
      595.73462   294.23706   157.78600
      602.95679   294.23706   157.85500
      611.27271   294.23706   157.55000
      620.76270   294.23706   156.80901
      632.4114    293.9556    149.9858
      641.4686    294.1341    141.81
&BPNODE  TNODE=     3, TNPC=     0, TINTC=     0,                    &END
&SECT1   STX=   0.0000, STY=   0.0000, STZ=   0.0000, SCALE=   1.0000,
      ALF=     0.0, THETA=    0.0,
      INMODE=    4, TNODS=     0, TNPS=     0, TINTS=     0,          &END
      644.7274    335.6856    141.7054
      635.9524    335.736     146.2158
      628.08862   335.78906   150.39900
      620.41870   335.78906   149.74001
      613.69873   335.78906   149.34000
      607.86182   335.78906   149.13600
      602.84473   335.78906   149.06500
      598.58862   335.78906   149.07700
      595.03564   335.78906   149.14500
      592.13281   335.78906   149.27200
      589.82764   335.78906   149.52699
      588.07373   335.78906   150.54601
      589.82764   335.78906   151.91701
      592.13281   335.78906   152.64101
      595.03564   335.78906   153.26401
      598.58862   335.78906   153.83000
      602.84473   335.78906   154.32899
      607.86182   335.78906   154.71899
      613.69873   335.78906   154.92500
      620.41870   335.78906   154.86700
      628.08862   335.78906   154.48000
      637.2959    335.5563    148.1527
      644.7274    335.6856    141.7054
&BPNODE  TNODE=     3, TNPC=     0, TINTC=     0,                    &END
&SECT1   STX=   0.0000, STY=   0.0000, STZ=   0.0000, SCALE=   1.0000,
      ALF=     0.0, THETA=    0.0,
      INMODE=    4, TNODS=     3, TNPS=     0, TINTS=     0,          &END
      648.0172    372.5153    141.08
      641.1824    372.5725    144.3174
      635.71191   372.60010   149.03300
      629.86084   372.60010   148.35500
      624.73486   372.60010   147.90900
      620.28296   372.60010   147.64000
```

```
      616.45703   372.60010   147.48500
      613.20996   372.60010   147.39600
      610.50098   372.60010   147.34000
      608.28589   372.60010   147.30499
      606.52783   372.60010   147.36200
      605.18994   372.60010   148.07100
      606.52783   372.60010   149.15700
      608.28589   372.60010   149.74100
      610.50098   372.60010   150.24899
      613.20996   372.60010   150.72400
      616.45703   372.60010   151.17000
      620.28296   372.60010   151.56700
      624.73486   372.60010   151.87199
      629.86084   372.60010   152.02699
      635.71191   372.60010   151.98399
      642.1627    372.4414    145.7307
      648.0172    372.5153    141.08
&BPNODE  TNODE=     3, TNPC=      0, TINTC=      0,                    &END

&PATCH1  IREV=0, IDPAT=1,  MAKE=26,  KCOMP=2, KASS=4,                  &END
  F14 WING TIP #27
&PATCH2  ITYP=1,  TNODS=3,  TNPS=3,  TINTS=3, NPTTIP=0,                &END

&PATCH1  IREV=0,  IDPAT=1,  MAKE=0, KCOMP=2,  KASS=3,                  &END
  HORIZONTAL TAIL #28
&SECT1  STX=   684.6,  STY=   92.0,   STZ=   145.5,  SCALE=   0.96000,
      ALF=     -4.9, THETA=    0.0,
      INMODE=    4, TNODS=     0, TNPS=      0, TINTS=       0,        &END
      148.600     0.0       0.0
      141.170     0.0      -0.549
      133.74      0.0      -1.080
      126.31      0.0      -1.609
      118.88      0.0      -2.135
      111.45      0.0      -2.637
      104.02      0.0      -3.101
       96.59      0.0      -3.512
       89.16      0.0      -3.866
       81.73      0.0      -4.15
       74.3       0.0      -4.346
       66.87      0.0      -4.446
       59.44      0.0      -4.452
       52.01      0.0      -4.376
       44.58      0.0      -4.223
       37.15      0.0      -3.992
       29.72      0.0      -3.676
       22.29      0.0      -3.26
       14.86      0.0      -2.71
       11.145     0.0      -2.364
        7.43      0.0      -1.951
        3.715     0.0      -1.457
        1.857     0.0      -1.066
        1.114     0.0      -0.836
        0.743     0.0      -0.689
        0.0       0.0       0.0
```

```
&BPNODE  TNODE=      2, TNPC=        15, TINTC=      0,                        &END
         0.0          0.0        0.0
         0.743        0.0        0.689
         1.114        0.0        0.836
         1.857        0.0        1.066
         3.715        0.0        1.457
         7.43         0.0        1.951
         11.145       0.0        2.364
         14.86        0.0        2.71
         22.29        0.0        3.26
         29.72        0.0        3.676
         37.15        0.0        3.992
         44.58        0.0        4.223
         52.01        0.0        4.376
         59.44        0.0        4.452
         66.87        0.0        4.446
         74.3         0.0        4.346
         81.73        0.0        4.15
         89.16        0.0        3.866
         96.59        0.0        3.512
         104.02       0.0        3.101
         111.45       0.0        2.633
         118.88       0.0        2.135
         126.31       0.0        1.609
         133.74       0.0        1.080
         141.17       0.0        0.549
         148.6        0.0        0.0
&BPNODE  TNODE=      3, TNPC=        15, TINTC=      0,                        &END
&SECT1  STX=   808.0,  STY=   202.7,  STZ=   138.7,  SCALE=  0.2133,
        ALF=     0.0, THETA=    0.0,
        INMODE=    0, TNODS=      3, TNPS=       5, TINTS=       0,            &END

&PATCH1  IREV=0,  IDPAT=1, MAKE=28, KCOMP=2, KASS=4,                           &END
  HORIZONTAL TAIL TIP #29
&PATCH2  ITYP=1,  TNODS=3,  TNPS=2,  TINTS=3, NPTTIP=0,                        &END

&PATCH1  IREV=0,  IDPAT=1, MAKE=-28, KCOMP=2, KASS=4,                          &END
  HORIZONTAL TAIL TIP #30
&PATCH2  ITYP=1,  TNODS=3,  TNPS=3,  TINTS=3, NPTTIP=0,                        &END

&PATCH1  IREV=0, IDPAT=2,  MAKE=0,  KCOMP=2, KASS=3,                           &END
 VERTICAL TAIL  #31
&SECT1  STX=   680.0,  STY=   56.5,   STZ=   166.0,  SCALE=   1.0000,
        ALF=     0.0, THETA=    0.0,
        INMODE=    4, TNODS=      0, TNPS=       0, TINTS=       0,            &END
        123.0         0.0        0.0
        116.85        0.455      0.0
        110.7         0.894      0.0
        104.550       1.332      0.0
        98.4          1.762      0.0
        92.25         2.183      0.0
        86.1          2.567      0.0
        79.95         2.907      0.0
        73.8          3.2        0.0
```

```
      67.65       3.435     0.0
      61.5        3.597     0.0
      55.350      3.68      0.0
      49.2        3.685     0.0
      43.05       3.622     0.0
      36.9        3.495     0.0
      30.75       3.305     0.0
      24.6        3.043     0.0
      18.45       2.698     0.0
      12.3        2.243     0.0
       9.225      1.956     0.0
       6.15       1.614     0.0
       3.075       1.206    0.0
       1.537       0.883    0.0
       0.922       0.692    0.0
       0.615       0.57     0.0
       0.0         0.0      0.0
&BPNODE  TNODE=     2, TNPC=     12, TINTC=      0,              &END
       0.0         0.0       0.0
       0.615      -0.57      0.0
       0.922      -0.692     0.0
       1.537      -0.883     0.0
       3.075      -1.206     0.0
       6.15       -1.614     0.0
       9.225      -1.956     0.0
      12.3        -2.243     0.0
      18.45       -2.698     0.0
      24.6        -3.043     0.0
      30.75       -3.305     0.0
      36.9        -3.495     0.0
      43.05       -3.622     0.0
      49.2        -3.685     0.0
      55.350      -3.68      0.0
      61.5        -3.597     0.0
      67.65       -3.435     0.0
      73.8        -3.2       0.0
      79.95       -2.907     0.0
      86.1        -2.567     0.0
      92.25       -2.183     0.0
      98.4        -1.762     0.0
     104.550      -1.332     0.0
     110.7        -0.894     0.0
     116.85       -0.455     0.0
     123.0         0.0       0.0
&BPNODE  TNODE=     3, TNPC=     12, TINTC=      0,              &END
&SECT1  STX=   787.0,  STY=   65.4,  STZ=   266.0,  SCALE=   0.35772,
     ALF=     0.0, THETA=    0.0,
     INMODE=    0, TNODS=     3, TNPS=     5, TINTS=     0,      &END

&PATCH1  IREV=0,  IDPAT=1, MAKE=31, KCOMP=2, KASS=4,             &END
  VERTICAL TAIL TIP #32
&PATCH2  ITYP=1,  TNODS=5,  TNPS=3,  TINTS=3, NPTTIP=0,          &END
```

```
&WAKE1   IDWAK=1,  IFLXW=0,                                              &END
 T34 WING WAKE
&WAKE2   KWPACH=9,  KWSIDE=4,  KWLINE=2,  KWPAN1=0,
         KWPAN2=0,  NODEW=0,   INITIAL=1,                                &END
&WAKE2   KWPACH=6,  KWSIDE=4,  KWLINE=4,  KWPAN1=0,
         KWPAN2=0,  NODEW=0,   INITIAL=1,                                &END
&WAKE2   KWPACH=2,  KWSIDE=2,  KWLINE=0,  KWPAN1=0,
         KWPAN2=0,  NODEW=3,   INITIAL=1,                                &END
&SECT1   STX=1900.0, STY=0.0,   STZ=0.0,   SCALE=1.0,
         ALF=0.0,   THETA=0.0,
         INMODE=-1, TNODS=3,   TNPS=15,   TINTS=1,                       &END
&WAKE1   IDWAK=1,  IFLXW=0,                                              &END
 T34 TAIL WAKE
&WAKE2   KWPACH=7,  KWSIDE=2,  KWLINE=0,  KWPAN1=0,
         KWPAN2=0,  NODEW=3,   INITIAL=1,                                &END
&SECT1   STX=1500.0, STY=0.0,   STZ=0.0,   SCALE=1.0,
         ALF=0.0,   THETA=0.0,
         INMODE=-1, TNODS=3,   TNPS=15,  TINTS=1,                        &END

&WAKE1  IDWAK=1,      IFLXW=0,                                           &END
 F14 HORIZONTAL TAIL WAKE
&WAKE2  KWPACH=28,     KWSIDE=4,     KWLINE=0,     KWPAN1=0,
        KWPAN2=0,      NODEW=3,      INITIAL=1,                          &END
&SECT1  STX=1800.0,    STY=0.0,  STZ=0.0,    SCALE=1.0,
        ALF=0.0,  THETA=0.0,
        INMODE=-1,   TNODS=3,   TNPS=15,  TINTS=0,                       &END

&WAKE1  IDWAK=1,      IFLXW=0,                                           &END
 F14 VERTICAL TAIL WAKE
&WAKE2  KWPACH=31,     KWSIDE=2,     KWLINE=0,     KWPAN1=0,
        KWPAN2=0,      NODEW=3,      INITIAL=1,                          &END
&SECT1  STX=1800.0,    STY=0.0,  STZ=0.0,    SCALE=1.0,
        ALF=0.0,  THETA=0.0,
        INMODE=-1,   TNODS=3,   TNPS=15,  TINTS=0,                       &END


&WAKE1  IDWAK=1,      IFLXW=0,                                           &END
 F14 WING WAKE
&WAKE2  KWPACH=26,     KWSIDE=4,     KWLINE=0,     KWPAN1=0,
        KWPAN2=0,      NODEW=0,      INITIAL=1,                          &END
&WAKE2  KWPACH=21,     KWSIDE=2,     KWLINE=13,    KWPAN1=1,
        KWPAN2=1,      NODEW=0,      INITIAL=1,                          &END
&WAKE2  KWPACH=21,     KWSIDE=3,     KWLINE=1,     KWPAN1=8,
        KWPAN2=8,      NODEW=0,      INITIAL=1,                          &END
&WAKE2  KWPACH=21,     KWSIDE=2,     KWLINE=12,    KWPAN1=2,
        KWPAN2=2,      NODEW=0,      INITIAL=1,                          &END
&WAKE2  KWPACH=21,     KWSIDE=3,     KWLINE=2,     KWPAN1=9,
        KWPAN2=10,     NODEW=0,      INITIAL=1,                          &END
&WAKE2  KWPACH=21,     KWSIDE=2,     KWLINE=10,    KWPAN1=3,
        KWPAN2=0,      NODEW=0,      INITIAL=1,                          &END
&WAKE2  KWPACH=22,     KWSIDE=2,     KWLINE=5,     KWPAN1=0,
        KWPAN2=0,      NODEW=0,      INITIAL=1,                          &END
&WAKE2  KWPACH=25,     KWSIDE=4,     KWLINE=7,     KWPAN1=0,
        KWPAN2=0,      NODEW=0,      INITIAL=1,                          &END
```

```
&WAKE2  KWPACH=25,    KWSIDE=2,    KWLINE=11,    KWPAN1=0,
        KWPAN2=0,     NODEW=0,     INITIAL=1,              &END
&WAKE2  KWPACH=22,    KWSIDE=4,    KWLINE=1,     KWPAN1=0,
        KWPAN2=0,     NODEW=0,     INITIAL=1,              &END
&WAKE2  KWPACH=23,    KWSIDE=2,    KWLINE=5,     KWPAN1=0,
        KWPAN2=0,     NODEW=0,     INITIAL=1,              &END
&WAKE2  KWPACH=24,    KWSIDE=4,    KWLINE=5,     KWPAN1=0,
        KWPAN2=0,     NODEW=5,     INITIAL=1,              &END
&SECT1  STX=-511.0,  STY=0.0,  STZ=2004.0,  SCALE=1.0,
    ALF=11.0,  THETA=0.0,
    INMODE=4,  TNODS=2,  TNPS=0,  TINTS=0,                 &END
    651.0   372.5153   140.0
    651.0   335.686    140.57
    650.0   294.134    141.04
    645.0   252.5822   139.54
    643.9   211.0303   138.02
    643.0   169.4923   136.313
    640.0   120.0      133.91
    635.0    95.0      133.0
    656.0    82.0      148.0
    656.0    88.5      142.0
    683.0    92.0      141.0
    683.0    83.0      129.0
    684.0    77.0      116.0
    711.0    77.0      116.5
    739.0    76.0      117.0
    764.0    76.2      118.3
    789.5    75.0      121.4
    817.0    66.5      128.0
    817.0    57.333    136.5
    817.0    45.5      143.0
    792.0    34.596    148.0
    817.0    26.0      148.0
    838.0    20.812    148.5
    838.0     0.0      148.5
&BPNODE  TNODE=3,  TNPC=0,  TINTC=0,                       &END
&SECT1  STX=-511.0,  STY=0.0,  STZ=2004.0,  SCALE=1.0,
    ALF=11.0,  THETA=0.0,
    INMODE=4,  TNODS=2,  TNPS=0,  TINTS=0,                 &END
    656.0   372.515    137.0
    656.0   335.7      136.0
    654.0   294.1      135.5
    653.0   252.582    135.0
    653.0   211.0      134.0
    653.0   169.5      132.0
    645.0   130.0      131.5
    645.0   125.0      130.0
    660.0   105.0      130.0
    665.0    98.0      131.0
    687.0    94.0      135.0
    687.0    85.0      127.0
    687.0    79.0      115.5
    715.0    78.0      116.0
    743.0    77.0      116.0
```

```
        768.0    76.5      117.5
        794.0    75.5      120.5
        821.0    66.5      127.5
        821.0    57.4      135.5
        821.0    45.5      142.0
        798.0    34.6      147.0
        821.0    26.0      147.0
        842.0    20.8      147.5
        842.0     0.0      147.5
&BPNODE TNODE=3, TNPC=0, TINTC=0,                                &END
&SECT1  STX=-511.0,  STY=0.0, STZ=2004.0,  SCALE=1.0,
         ALF=11.0, THETA=0.0,
        INMODE=4, TNODS=2, TNPS=0, TINTS=0,                      &END
        666.0   372.5      133.0
        666.0   335.7      132.0
        666.0   294.1      131.5
        663.0   252.6      132.0
        663.0   211.0      131.5
        663.0   169.5      130.0
        660.0   130.0      127.0
        660.0   125.0      125.0
        668.0   110.0      125.0
        668.0   107.0      125.0
        691.0    96.0      130.0
        691.0    88.0      125.0
        691.0    80.0      115.0
        720.0    78.5      115.5
        748.0    77.5      115.5
        773.0    77.0      115.0
        799.0    75.6      120.0
        826.0    66.6      127.0
        826.0    57.4      135.0
        826.0    45.5      141.5
        815.0    34.6      146.5
        826.0    26.0      146.5
        848.0    20.8      147.0
        848.0     0.0      147.0
&BPNODE TNODE=3, TNPC=0, TINTC=0,                                &END
&SECT1  STX=-511.0,  STY=0.0, STZ=2004.0,  SCALE=1.0,
         ALF=11.0, THETA=0.0,
        INMODE=4, TNODS=2, TNPS=0, TINTS=0,                      &END
        695.0   372.5      121.0
        695.0   335.7      121.0
        695.0   294.1      121.0
        695.0   252.6      121.0
        695.0   211.0      121.0
        695.0   169.5      121.0
        695.0   130.0      121.0
        695.0   125.0      115.0
        695.0   120.0      115.0
        695.0   115.0      115.0
        695.0   100.0      125.0
        695.0    90.0      115.0
        695.0    85.0      110.0
```

```
     728.0      80.0         115.0
     756.0      81.0         112.0
     781.0      80.0         114.0
     806.0      75.6         120.0
     834.0      66.6         127.0
     834.0      57.4         135.0
     834.0      45.5         141.5
     834.0      34.6         146.5
     834.0      26.0         146.5
     856.0      20.8         147.0
     856.0       0.0         147.0
&BPNODE TNODE=3, TNPC=0, TINTC=0,                                  &END
&SECT1  STX=-511.0,  STY=0.0, STZ=2004.0,  SCALE=1.0,
     ALF=11.0, THETA=0.0,
     INMODE=4, TNODS=2, TNPS=0, TINTS=0,                           &END
     760.0     372.5         105.0
     760.0     335.7         105.0
     760.0     294.1         105.0
     760.0     252.6         105.0
     760.0     211.0         105.0
     760.0     169.5         105.0
     760.0     130.0         105.0
     760.0     125.0         105.0
     760.0     120.0         105.0
     760.0     115.0         105.0
     760.0     105.0         110.0
     760.0     100.0         110.0
     760.0      95.0         105.0
     760.0      85.0         110.0
     760.0      82.0         110.0
     791.0      80.0         110.0
     816.0      75.6         120.0
     844.0      66.6         126.5
     844.0      57.4         134.5
     844.0      45.5         141.0
     844.0      34.6         146.0
     844.0      26.0         146.0
     865.0      20.8         146.5
     865.0       0.0         146.5
&BPNODE TNODE=3, TNPC=0, TINTC=0,                                  &END
&SECT1  STX=-511.0,  STY=0.0, STZ=2004.0,  SCALE=1.0,
     ALF=11.0, THETA=0.0,
     INMODE=4, TNODS=2, TNPS=0, TINTS=0,                           &END
     870.0     372.5          95.0
     870.0     335.7          95.0
     870.0     294.1          95.0
     870.0     252.6          95.0
     870.0     211.0          95.0
     870.0     169.5          95.0
     870.0     130.0          95.0
     870.0     125.0          95.0
     870.0     120.0          95.0
     870.0     115.0          95.0
     870.0     105.0         100.0
```

```
         870.0     100.0        100.0
         870.0      95.0        100.0
         870.0      90.0        100.0
         870.0      85.0        105.0
         870.0      80.0        105.0
         870.0      75.6        120.0
         870.0      66.6        126.5
         870.0      57.4        134.5
         870.0      45.5        141.0
         870.0      34.6        146.0
         870.0      26.0        146.0
         870.0      20.8        146.0
         870.0       0.0        146.0
&BPNODE  TNODE=3, TNPC=0, TINTC=0,                                  &END
&SECT1   STX=1000.0,  STY=0.0,  STZ=0.0,  SCALE=1.0,
         ALF=11.0, THETA=0.0,
         INMODE=-1, TNODS=3, TNPS=20, TINTS=3,                      &END


&VS1     NVOLR= 0,      NVOLC= 0,                                   &END
&VS2     X0=   -2.0000, Y0=    0.0000, Z0=   -2.0000,               &END
&VS3     X1=    2.0000, Y1=    0.0000, Z1=   -2.0000, NPT1= 20,     &END
&VS4     X2=   -2.0000, Y2=    0.0000, Z2=   -2.0000, NPT2=  0,     &END
&VS5     X3=   -2.0000, Y3=    0.0000, Z3=    2.0000, NPT3= 40,     &END

&VS6     XR0=   0.0000, YR0=   0.0000, ZR0=   0.0000,               &END
&VS7     XR1=   0.0000, YR1=  10.0000, ZR1=   0.0000,
         XR2=   0.0000, YR2=   0.0000, ZR2=   1.0000,               &END
&VS8     R1=    0.5000, R2=    5.0000, PHI1=  0.0,   PHI2=330.0,    &END
&VS9     NRAD=  10,     NPHI=  12,     NLEN=  5,                    &END

&SLIN1   NSTLIN=16,                                                 &END
&SLIN2    SX0=-110.0,  SY0=40.0,  SZ0=5.0,
          SU=50.0,     SD=450.0,  DS=5.0,                           &END
&SLIN2    SX0=-110.0,  SY0=40.0,  SZ0=15.0,
          SU=50.0,     SD=450.0,  DS=5.0,                           &END
&SLIN2    SX0=-110.0,  SY0=40.0,  SZ0=25.0,
          SU=50.0,     SD=450.0,  DS=5.0,                           &END
&SLIN2    SX0=-110.0,  SY0=40.0,  SZ0=35.0,
          SU=50.0,     SD=450.0,  DS=5.0,                           &END
&SLIN2    SX0=-110.0,  SY0=40.0,  SZ0=45.0,
          SU=50.0,     SD=450.0,  DS=5.0,                           &END
&SLIN2    SX0=-110.0,  SY0=40.0,  SZ0=55.0,
          SU=50.0,     SD=450.0,  DS=5.0,                           &END
&SLIN2    SX0=-110.0,  SY0=40.0,  SZ0=65.0,
          SU=50.0,     SD=450.0,  DS=5.0,                           &END
&SLIN2    SX0=-110.0,  SY0=40.0,  SZ0=75.0,
          SU=50.0,     SD=450.0,  DS=5.0,                           &END
&SLIN2    SX0=-110.0,  SY0=40.0,  SZ0=85.0,
          SU=50.0,     SD=450.0,  DS=5.0,                           &END
&SLIN2    SX0=-110.0,  SY0=40.0,  SZ0=95.0,
          SU=50.0,     SD=450.0,  DS=5.0,                           &END
&SLIN2    SX0=-110.0,  SY0=40.0,  SZ0=-5.0,
          SU=50.0,     SD=450.0,  DS=5.0,                           &END
```

```
&SLIN2   SX0=-110.0,  SY0=40.0,  SZ0=-15.0,
         SU=50.0,     SD=450.0,  DS=5.0,                 &END
&SLIN2   SX0=-110.0,  SY0=40.0,  SZ0=-25.0,
         SU=50.0,     SD=450.0,  DS=5.0,                 &END
&SLIN2   SX0=-110.0,  SY0=40.0,  SZ0=-35.0,
         SU=50.0,     SD=450.0,  DS=5.0,                 &END
&SLIN2   SX0=-110.0,  SY0=40.0,  SZ0=-45.0,
         SU=50.0,     SD=450.0,  DS=5.0,                 &END
&SLIN2   SX0=-110.0,  SY0=40.0,  SZ0=-55.0,
         SU=50.0,     SD=450.0,  DS=5.0,                 &END
```

LIST OF REFERENCES

1. Naval Safety Center, *Summary of Mid-Air Collisions During Formation Flight*, Compiled by Mr. C. Byrd, NSC Code 10, February 1993.

2. Headquarters Air Force Safety Agency, HQ AFSA/SERD, *1982 To Date Mid-Air Collision Summary*, Compiled by LtCol. J. R. Perkins, USAF, Director of Reports and Analysis, February 1993.

3. Chief of Naval Air Training, *T-34C Formation Flight Training Instruction*, CNAT P-357 (Rev. 05-93) PAT, 23 April 1993.

4. Hurt, H. H., *Aerodynamics For Naval Aviators*, pp. 383-385, Aviation Maintenance Publishers, Inc., 1965

5. Air Force Human Resources Lab, AFHRL-TR-74-102, *Transfer of Training with Formation Flight Trainer*, by G. B. Reid, M. L. Cyrus, December 1974.

6. Aircraft Engineering Vol. 43, Num. 7, *Formation Flight Technology*, by T. K. Speer, E. C. Mill, and J. L. Tate, July 1971.

7. National Aeronautics and Space Administration, NASA-TM-4465, *Summary of the Effects of Engine Throttle Response on Airplane Formation-Flying Qualities*, by K. R. Walsh, March 1993.

8. Analytical Methods, Inc., NASA-CR-151974, *Formation Flying Benefits Based on Vortex Lattice Calculations*, by B. Maskew, April 1977.

9. Lyons, D. F., *Aerodynamic Analysis of a U.S. Navy and Marine Corps Unmanned Air Vehicle*, Master's Thesis, Naval Postgraduate School, Monterey, California, June 1989.

10. Rixey, J. W., *A Multi-Faceted Engineering Study of Aerodynamic Errors of the Service Aircraft Instrumentation Package (SAIP)*, Master's Thesis, Naval Postgraduate School, Monterey, California, September 1992.

11. NASA Technical Memorandum 102851, *Potential Flow Theory and Operation Guide for the Panel Code PMARC*, by D. L. Ashby, M. R. Dudley, S. K. Iguchi, L. Browne, and J. Katz, January 1991.

12. Naval Postgraduate School, W. R. Church Computer Center, *Visualization Laboratory User's Guide*, pp. 4-5, 18 June 1993.

13. Naval Air Systems Command, Report Number SD-507-3-2, *Detailed Specification for Model T-34C Airplane Single Engine Turboprop Training Airplane, FY-78 Procurement*, pp. 15-18 and 8-A, 15 February 1978.

14. Grumman Aircraft Corporation, Report Number A51-335-R-70-2, *F-14A Stability and Control, and Flying Qualities Report, Status III, Part II, Aerodynamic Characteristics and Dimensional Data*, pp. 3-3 through 3-13 and 6-35 through 6-37, June 1970.

15. COSMIC, The University of Georgia, *GVS General Visualization System Handbook*, S. R. Keith, p. 1-7, 1993.

16. Smetana, F. O., *Computer Assisted Analysis of Aircraft Performance Stability and Control*, pp. 57-102, McGraw-Hill Book Company, 1984.

17. Perkins, Courtland D., and Hage, Robert E., *Airplane Performance Stability and Control*, p. 224, John Wiley & Sons, Inc., 1950.

18. Abbot, I. H., and Von Doenhoff, A. E., *Theory of Wing Sections*, Dover Publications, Inc., 1959.

19. Roskam, J., *Airplane Flight Dynamics and Automatic Flight Controls*, Part 1, pp. 592-609, Roskam Aviation and Engineering Corporation, 1982.

20. Nelson, Robert C., *Flight Stability and Automatic Control*, p. 252, McGraw-Hill Book Company, 1989.

21. NAVAIRWARCENACDIV, F-14 Six Degree of Freedom Simulator Data, Man Flight Simulator Building, Patuxent River, Maryland., 14 July 1993.

INITIAL DISTRIBUTION LIST

		No. Copies
1.	Defense Technical Information Center Cameron Station Alexandria, Virginia 22304-6145	2
2.	Library, Code 52 Naval Postgraduate School Monterey, California 93943-5002	2
3.	Mr. Jonah Ottensoser Naval Air Systems Command, AIR-53011C Washington, D. C. 20361-5300	2
4.	Chairman, Code AA Department of Aeronautics and Astronautics Naval Postgraduate School Monterey, California 93943-5000	1
5.	Professor Richard M. Howard, Code AA/Ho Department of Aeronautics and Astronautics Naval Postgraduate School Monterey, California 93943-5000	3
6.	Professor Oscar Biblarz, Code AA/Bi Department of Aeronautics and Astronautics Naval Postgraduate School Monterey, California 93943-5000	1
7.	LCdr. David B. Porter, USN 936 Forest Road Lancaster, Pennsylvania 17601	2
8.	Mr. Dale Ashby Full-Scale Aerodynamics Research Division NASA Ames Research Center Moffet Field, California 94035	1
9.	Commanding Officer Training Squadron Six Attn: Lt. Glen B. Freeman, USCG 7700 U.S.S. Enterprise St. Suite 102 Milton, Florida 32570-5100	1

10. LtCol. Steven Grossmeyer 1
Aviation Safety Program, Code 034
Naval Postgraduate School
Monterey, California 93943-5000

11. LtCol. Jerry R. Perkins 1
HQ AFSA/SERD
918 First Ave, Room 330
Norton AFB, California 92409-7001